# Supporting Information

## Synthesis and combined experimental/theoretical structural study of a comprehensive set of Pd/NHC complexes with *o*-, *m*-, and *p*- halogen-substituted aryl groups (X = F, Cl, Br, CF₃)

Roman O. Pankov[§], Darya O. Prima[§], Alexander Yu. Kostyukovich[§], Mikhail E. Minyaev[§], Valentine P. Ananikov[§]*

[§] *Zelinsky Institute of Organic Chemistry, Russian Academy of Sciences, Leninsky prospekt 47, Moscow, 119991, Russia;*

*e-mail: val@ioc.ac.ru; http://AnanikovLab.ru*

**2a, 49%**[b]

**2b, 54%**[b]

**2c, 80%**[a]

**2d, 11%**[c]

**2e, 11%**[a]

**2f, 74%**[a]

**2g, 30%**[b]

**2h, 29%**[b]

**2i, 33%**[b]

**2j, 11%**[d]

**2k, 62%**[a]

**2l, 62%**[a]
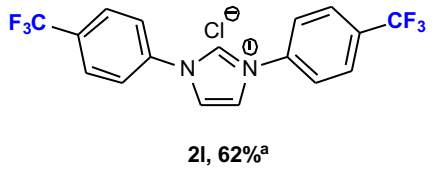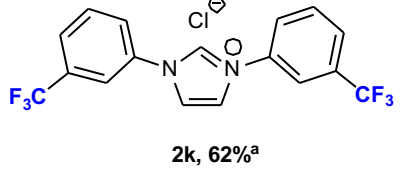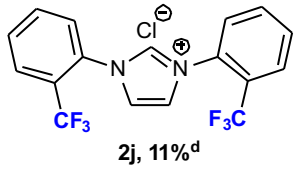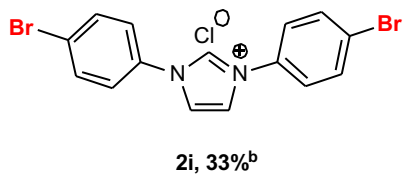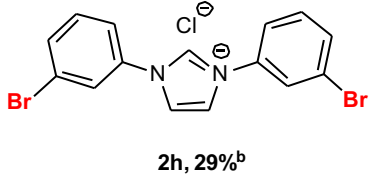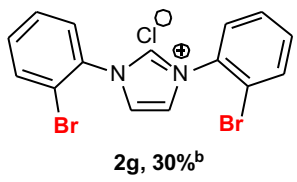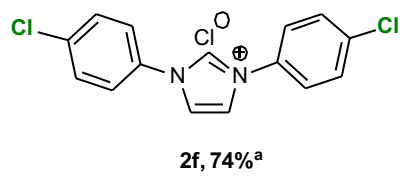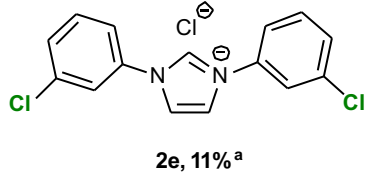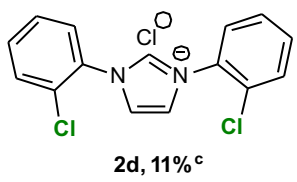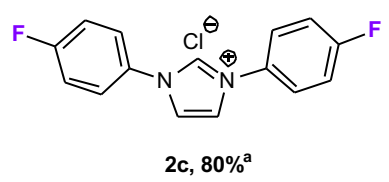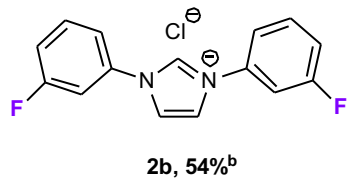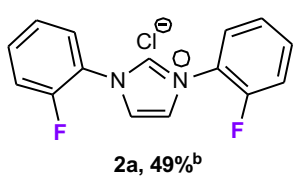
Synthesized imidazolium salts **2 a-l**, and the yields of the isolated products. [a] Method A, [b] Method B, [c] Method C, [d] Method D.

## NMR spectra of the obtained compounds
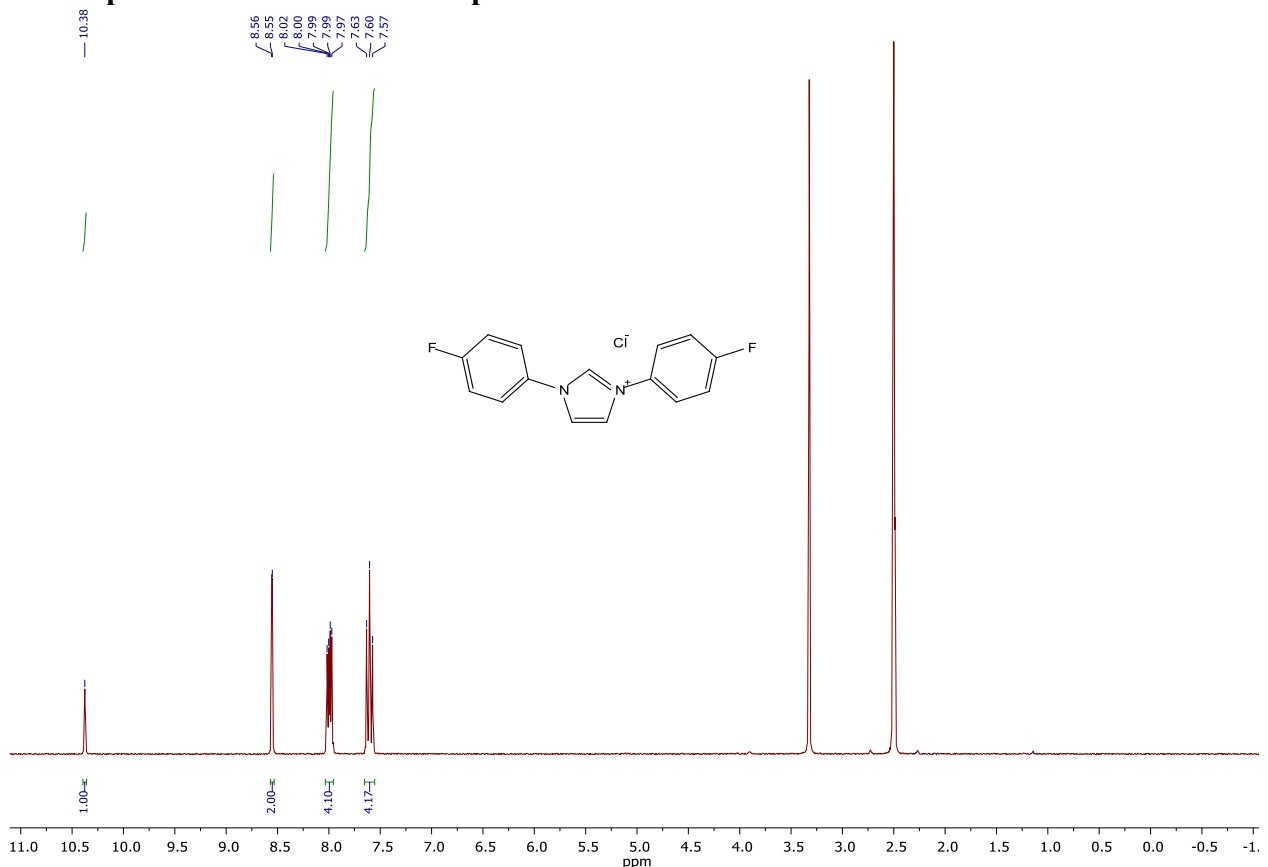


**Figure S1**. $^1$H NMR spectrum of **2c**. Solvent: DMSO-$d_6$, 300 MHz.
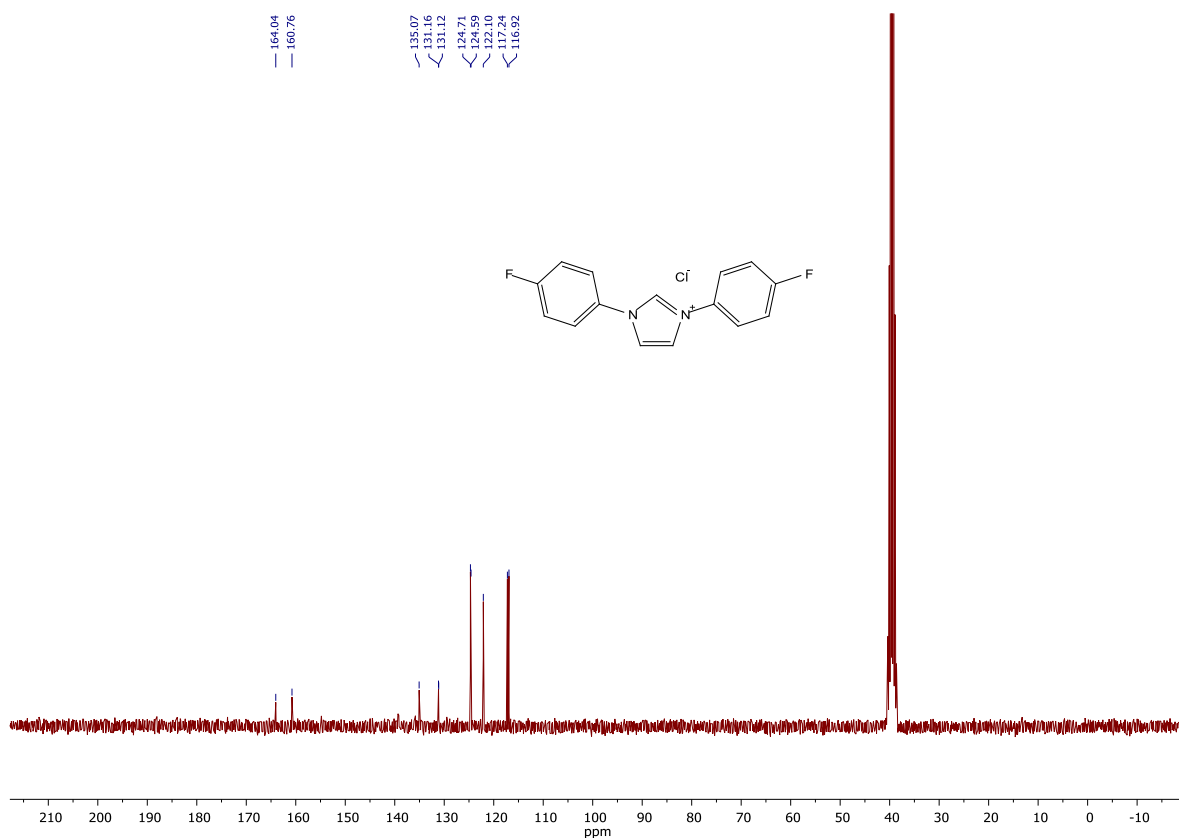


**Figure S2**. $^{13}$C{$^1$H} NMR spectrum of **2c**. Solvent: DMSO-$d_6$, 75 MHz.

4
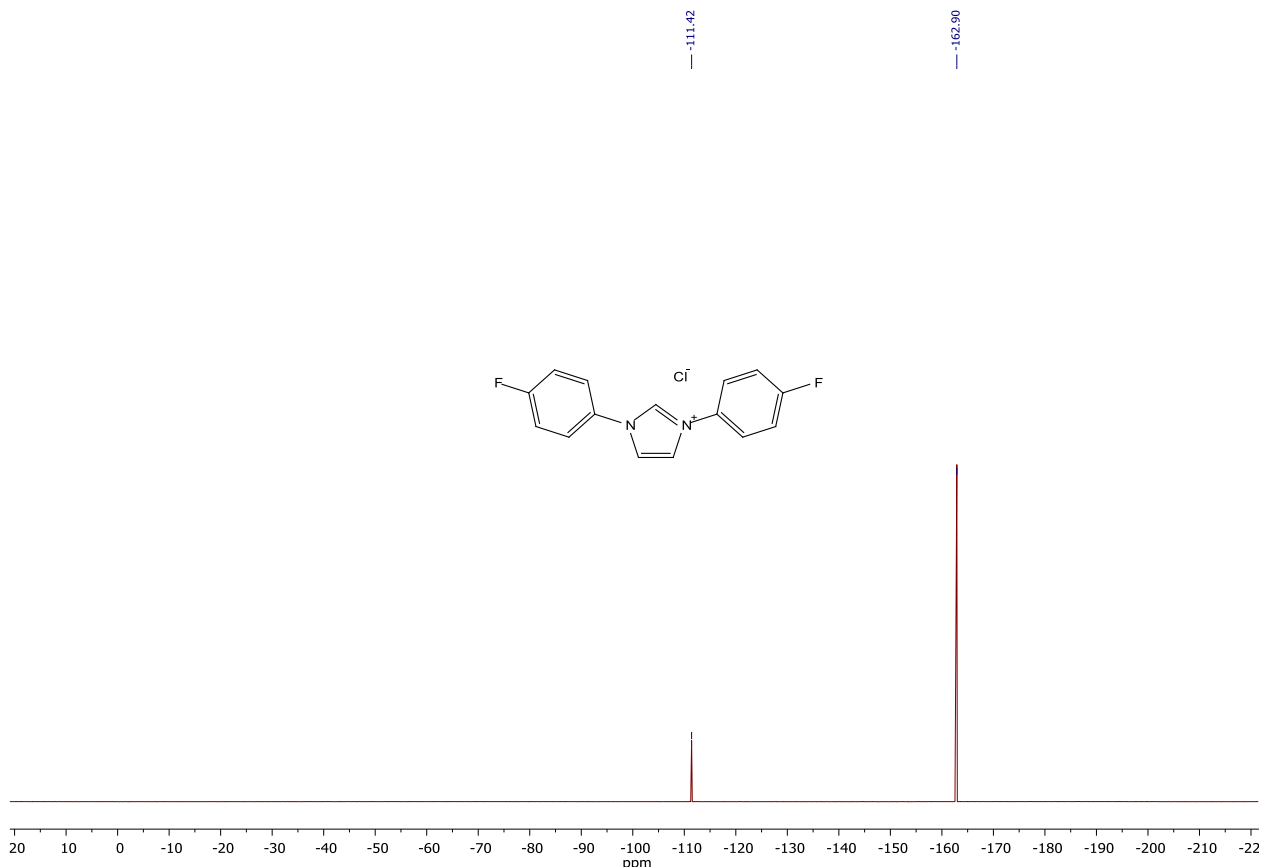
**Figure S3**. $^{19}F\{^1H\}$ NMR spectrum of **2c**. Solvent: DMSO-$d_6$, 282.4 MHz. Standard: $C_6F_6$ with respect to $CFCl_3$.
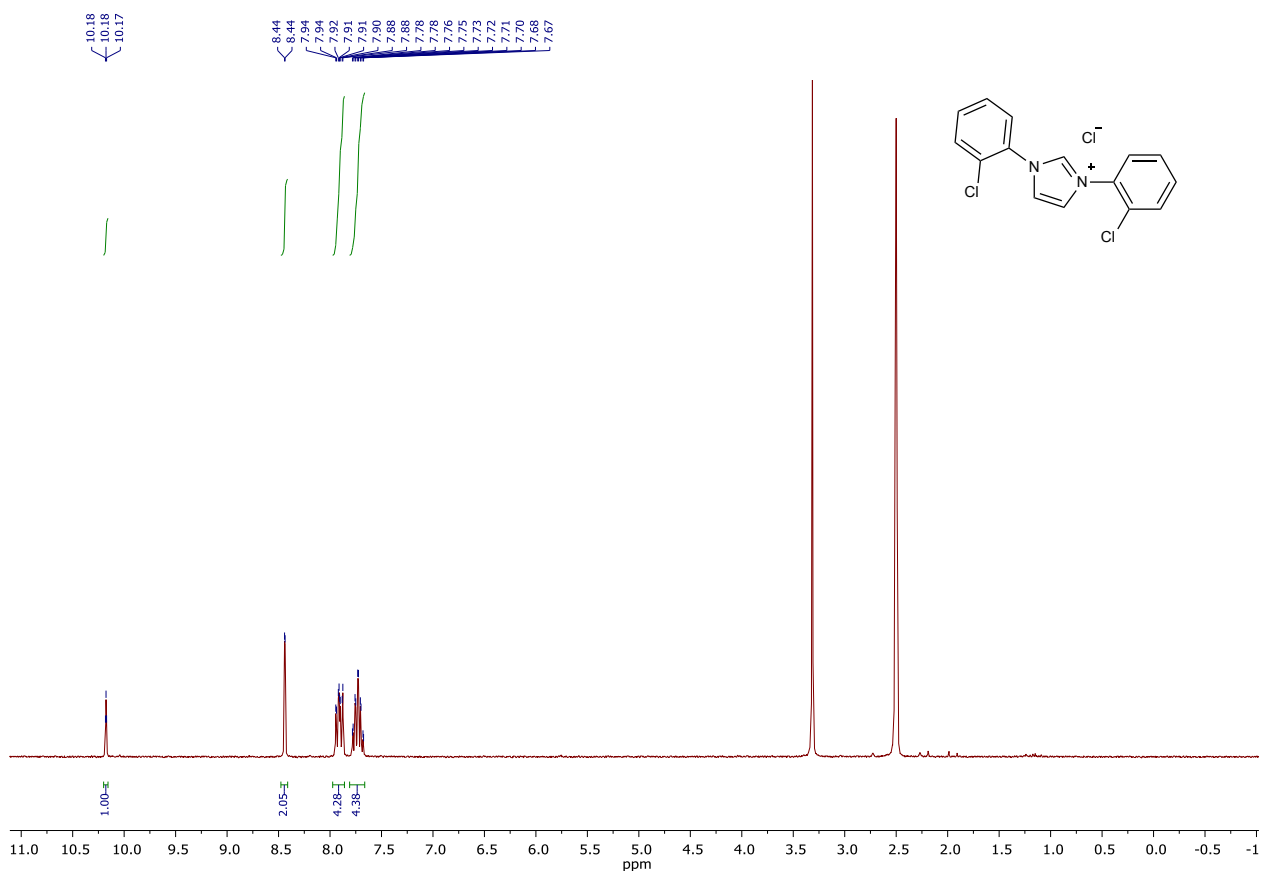


**Figure S4**. $^1H$ NMR spectrum of **2d**. Solvent: DMSO-$d_6$, 300 MHz.
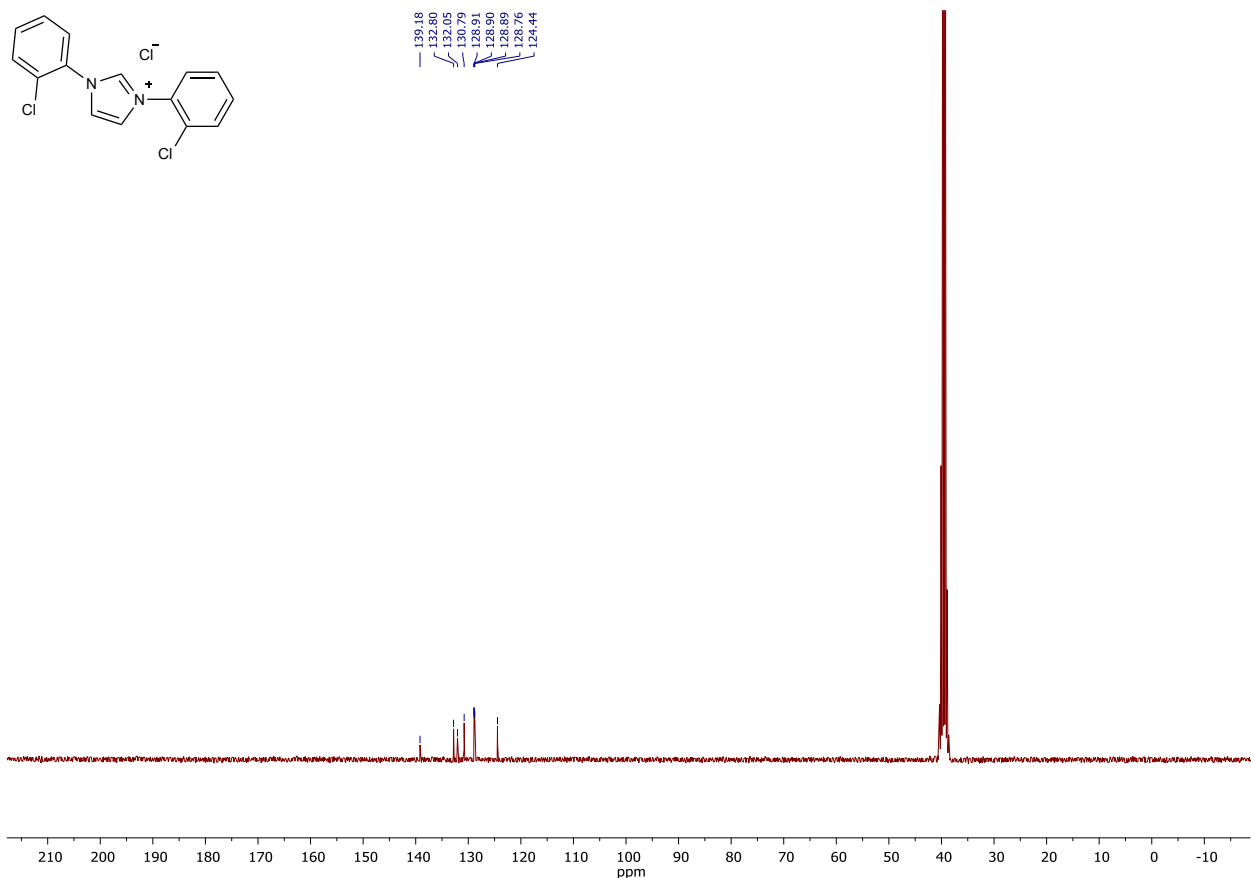
**Figure S5**. $^{13}C\{^1H\}$ NMR spectrum of **2d**. Solvent: DMSO-$d_6$, 75 MHz.
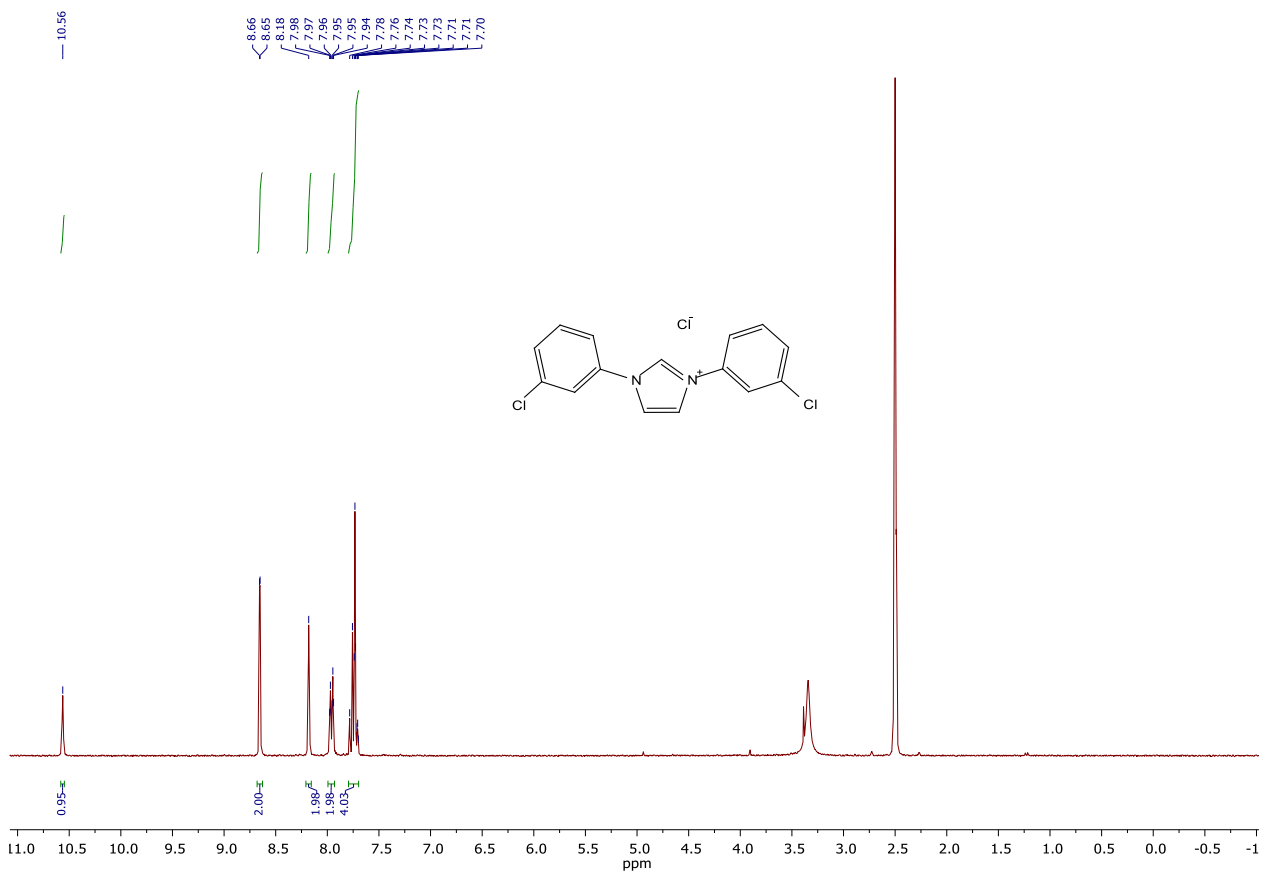


**Figure S6**. $^1H$ NMR spectrum of **2e**. Solvent: DMSO-$d_6$, 300 MHz.
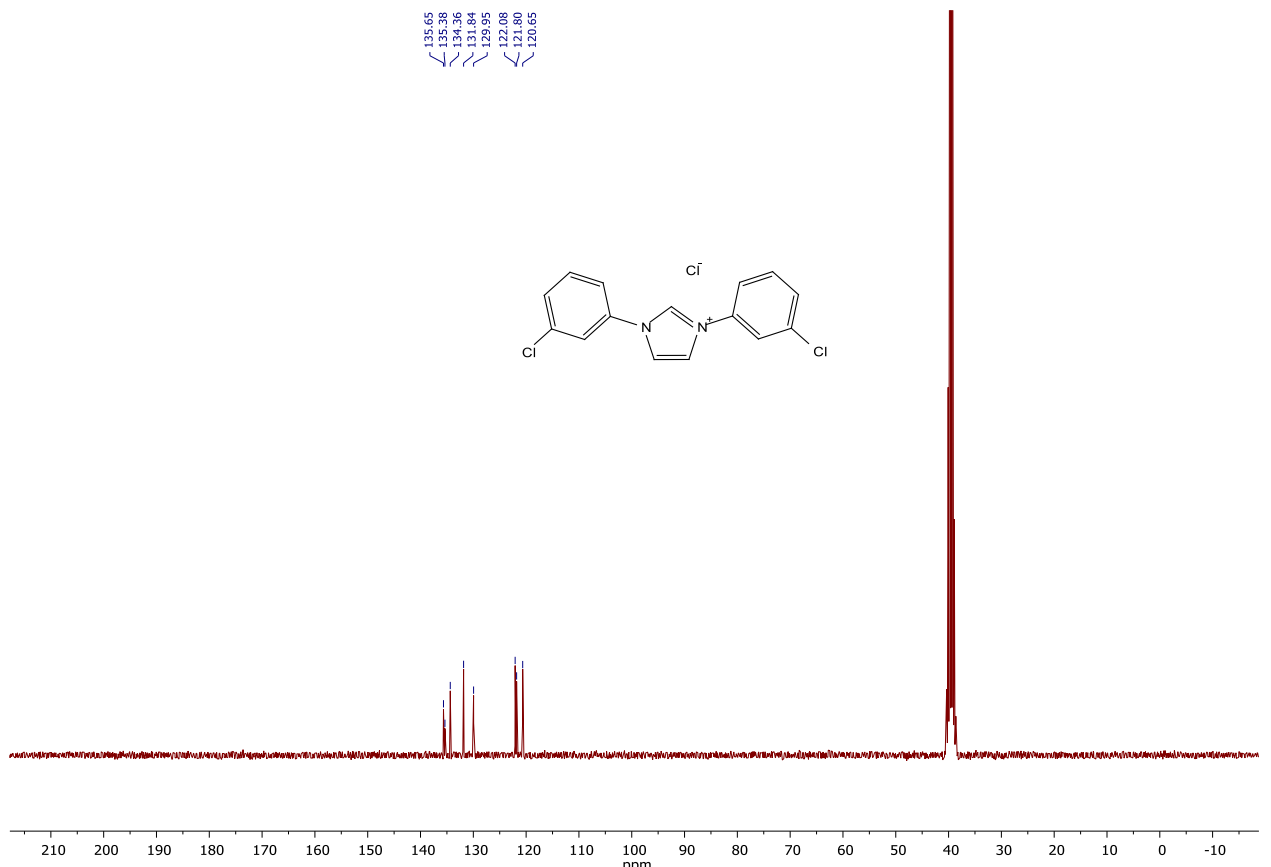
**Figure S7**. $^{13}C\{^{1}H\}$ NMR spectrum of **2e**. Solvent: DMSO-$d_6$, 75 MHz.
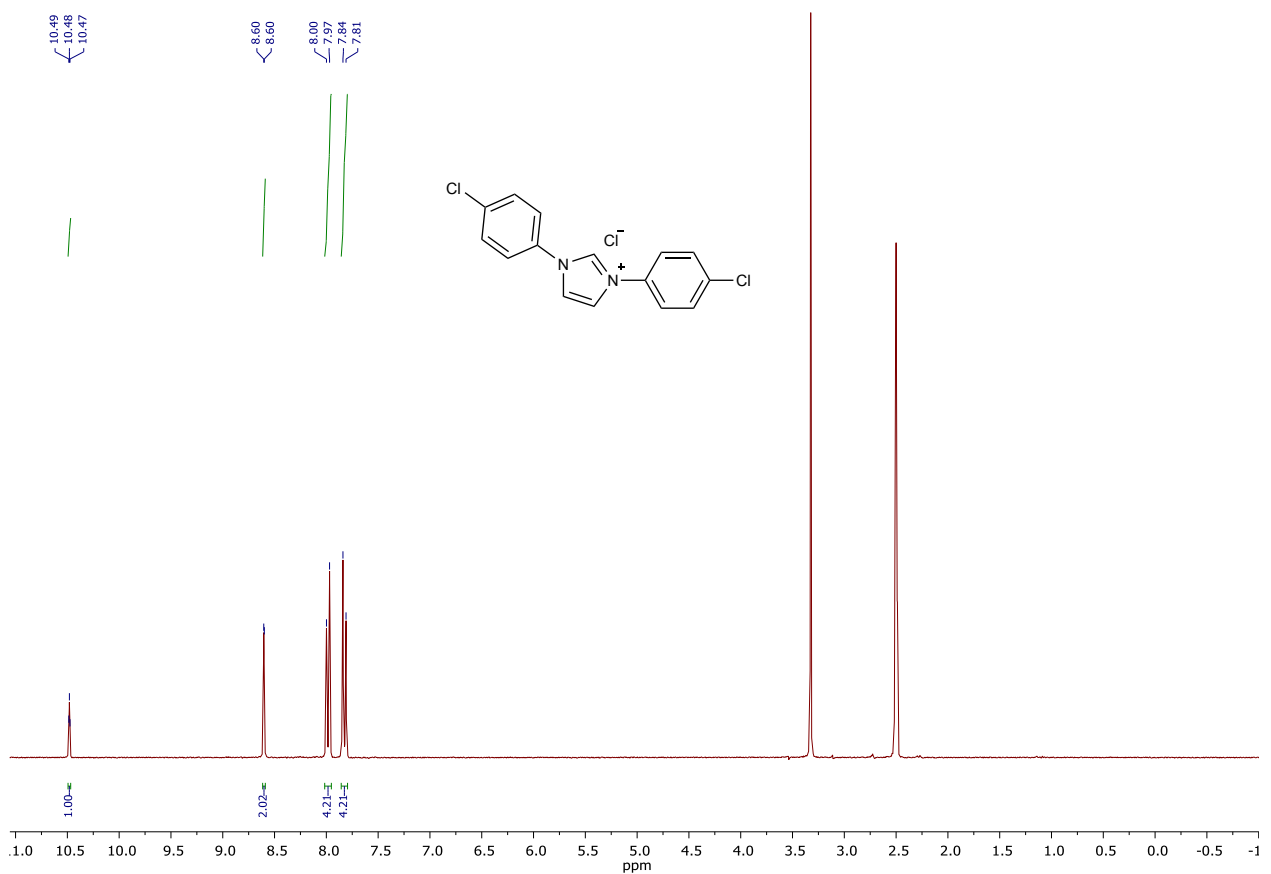


**Figure S8**. $^{1}H$ NMR spectrum of **2f**. Solvent: DMSO-$d_6$, 300 MHz.
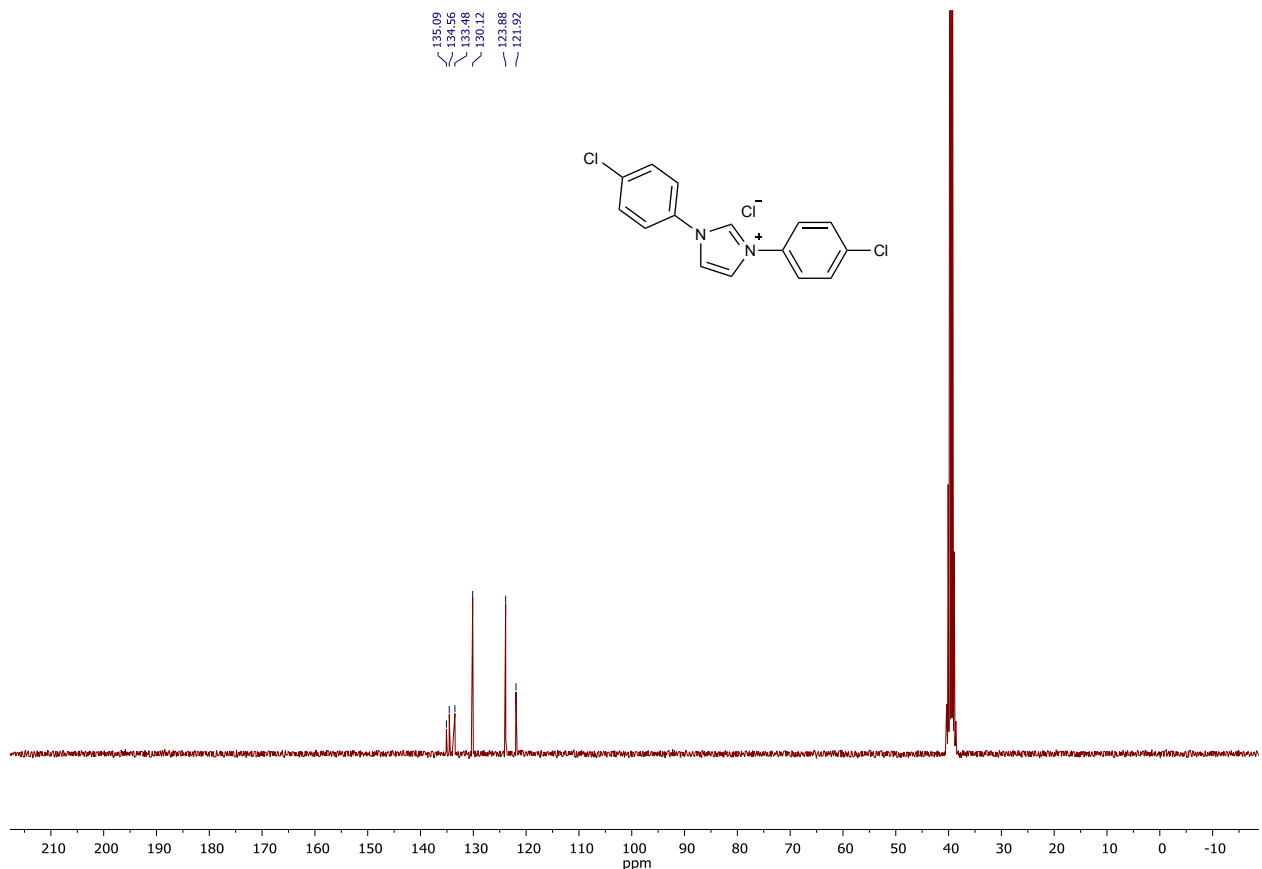
**Figure S9**. $^{13}C\{^1H\}$ NMR spectrum of **2f**. Solvent: DMSO-$d_6$, 75 MHz.
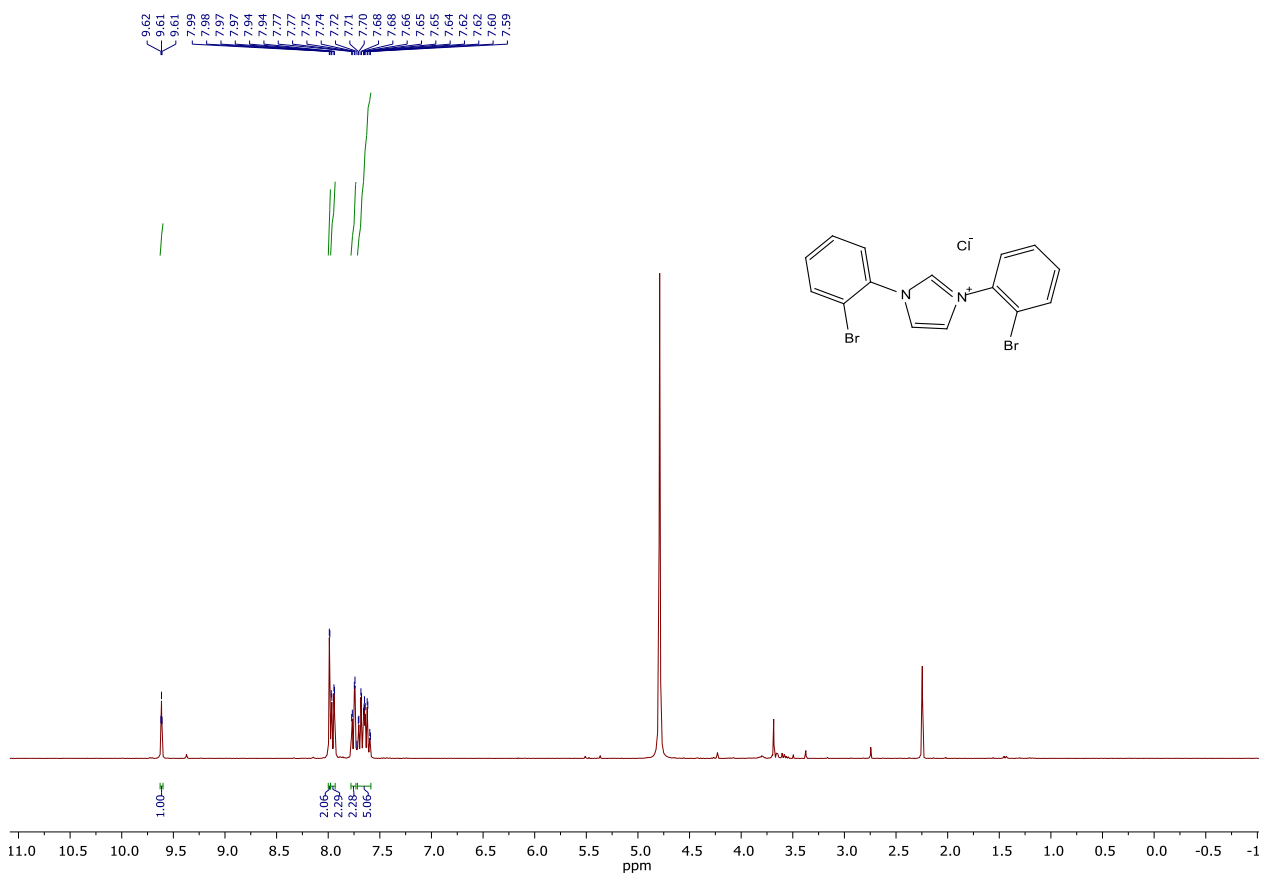


**Figure S10**. $^1H$ NMR spectrum of **2g**. Solvent: D$_2$O, 300 MHz.
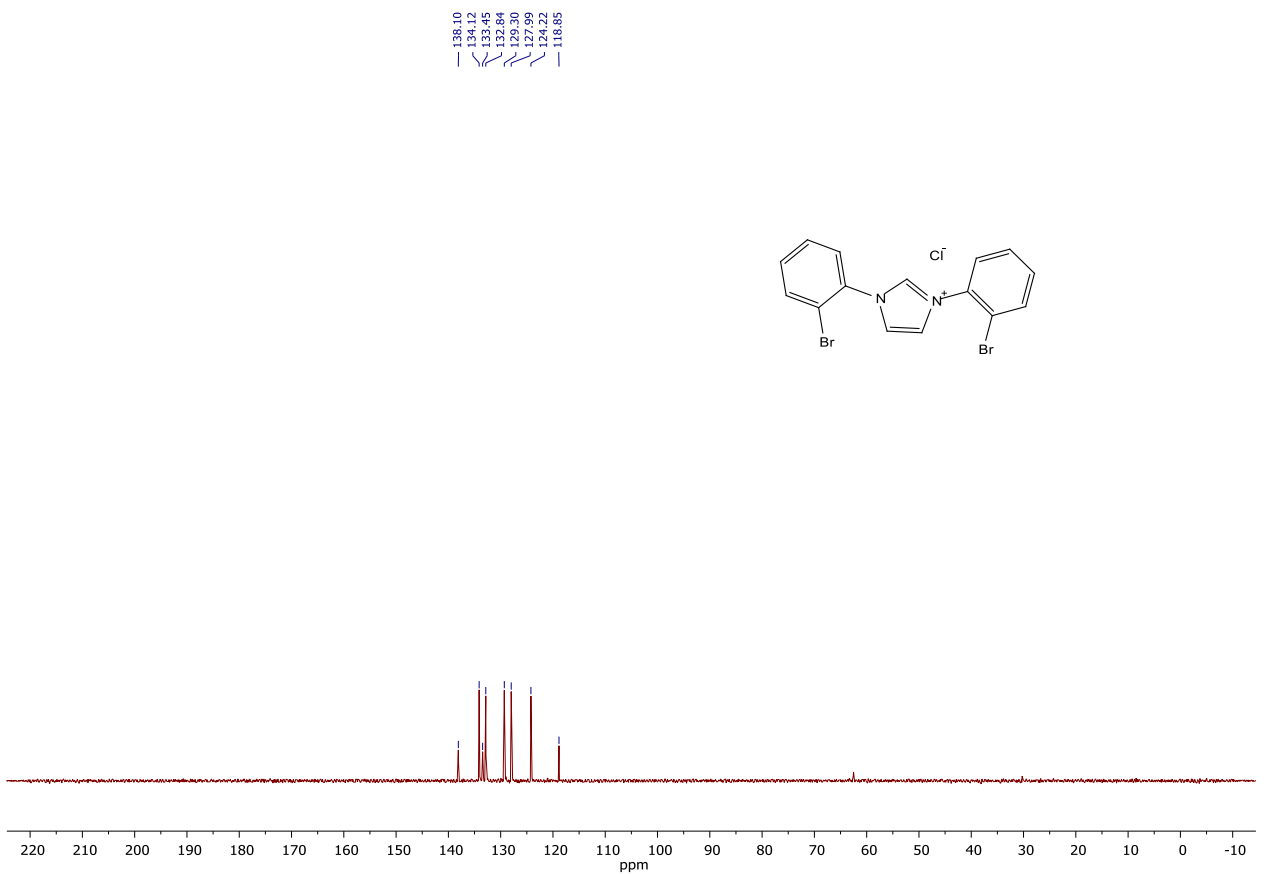
**Figure S11**. $^{13}C\{^1H\}$ NMR spectrum of **2g**. Solvent: D$_2$O, 75 MHz.
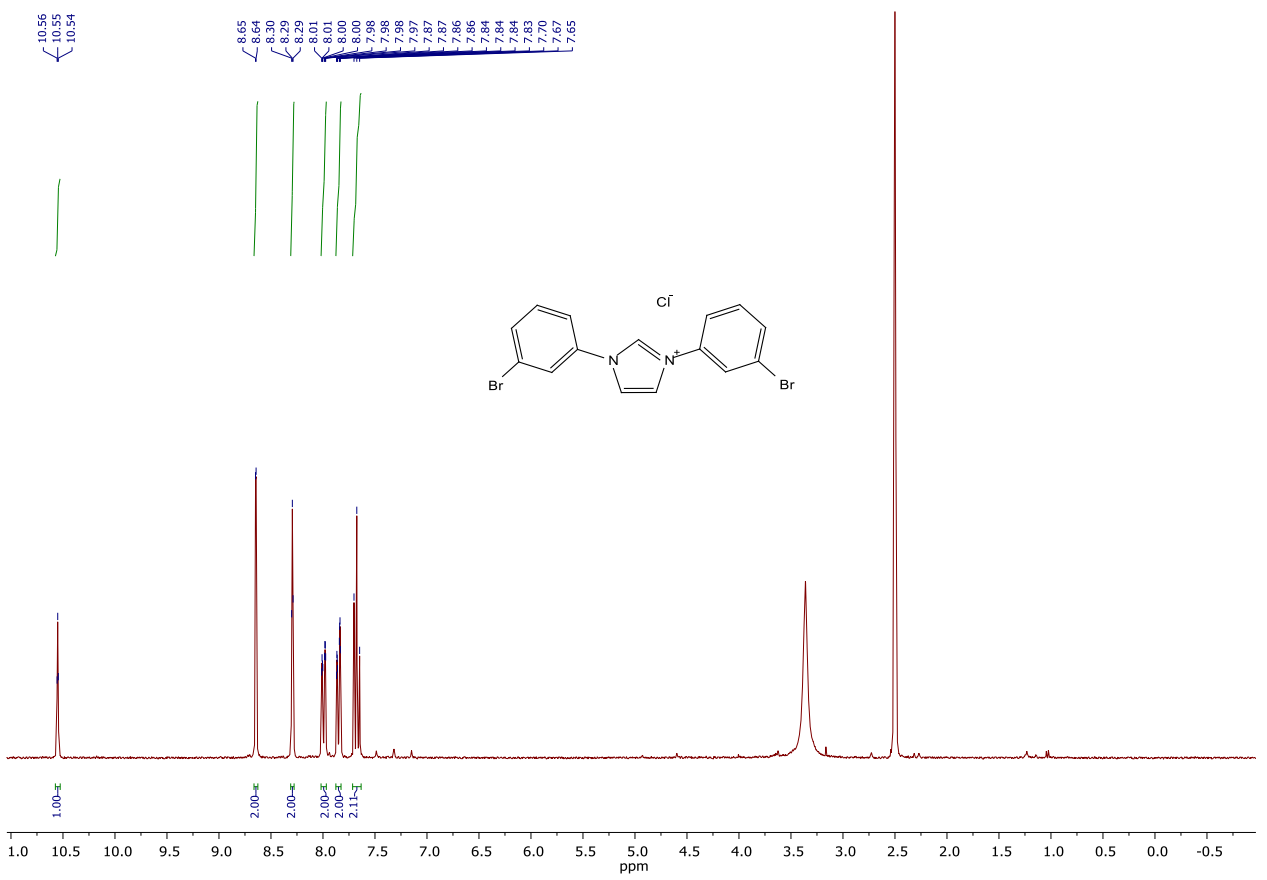


**Figure S12**. $^1H$ NMR spectrum of **2h**. Solvent: DMSO-$d_6$, 300 MHz.
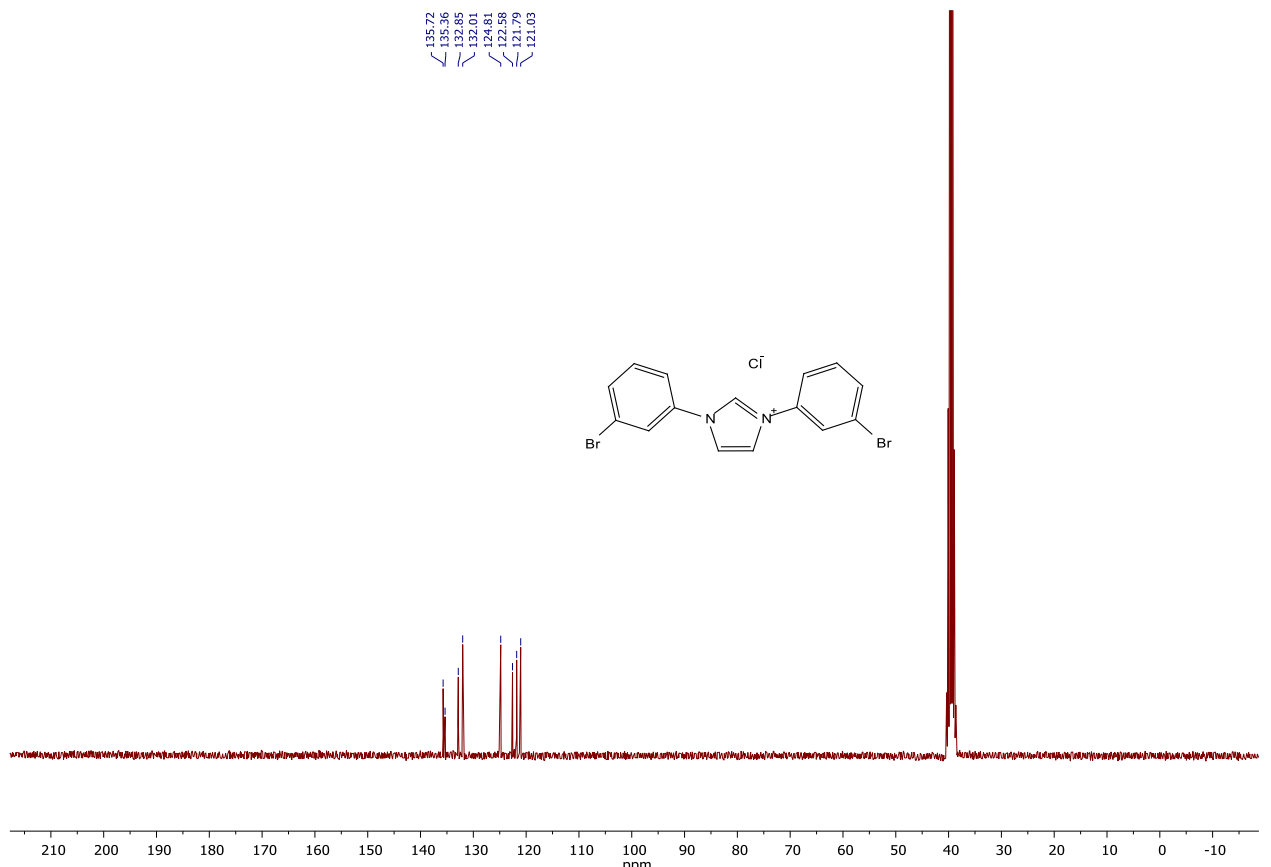
**Figure S13**. $^{13}C\{^1H\}$ NMR spectrum of **2h**. Solvent: DMSO-$d_6$, 75 MHz.
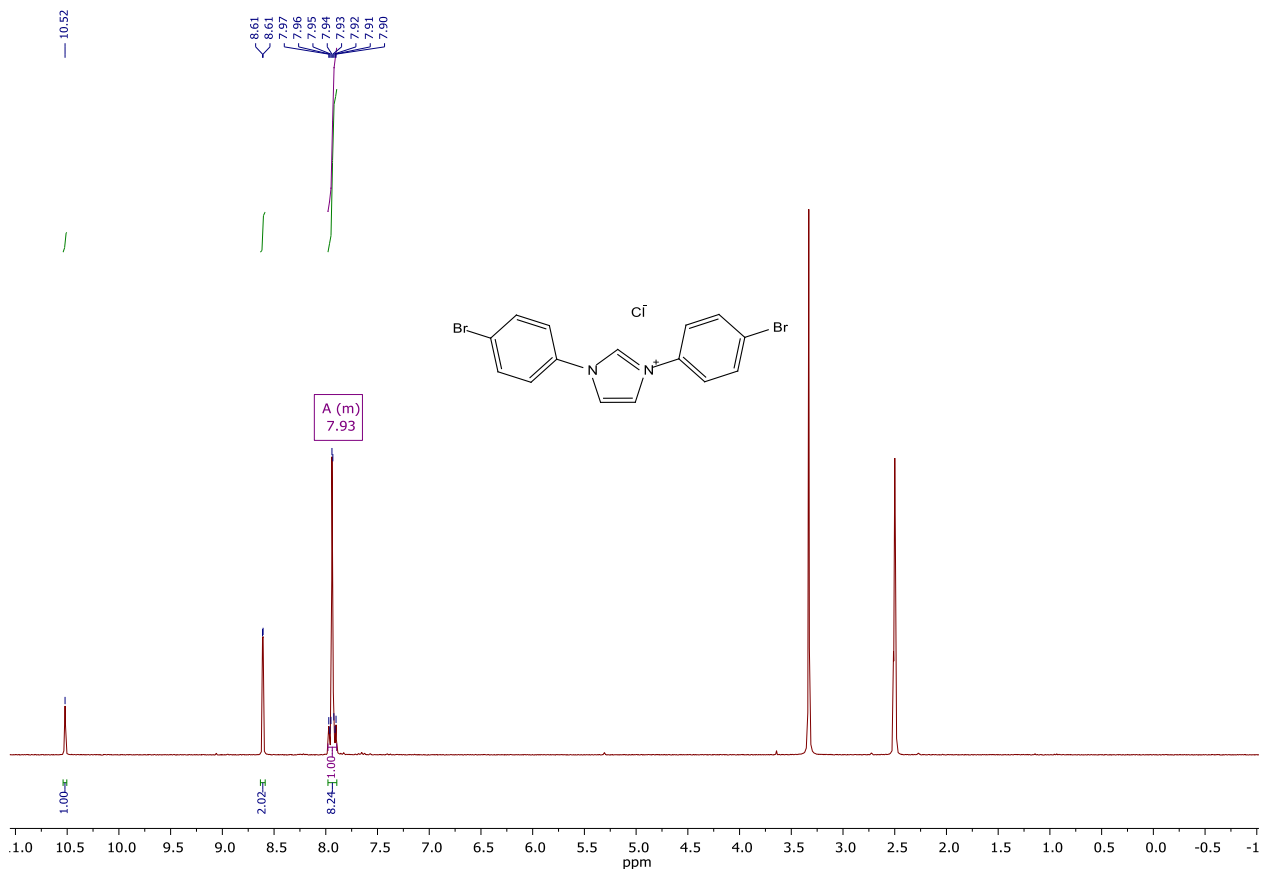


**Figure S14**. $^1H$ NMR spectrum of **2i**. Solvent: DMSO-$d_6$, 300 MHz.
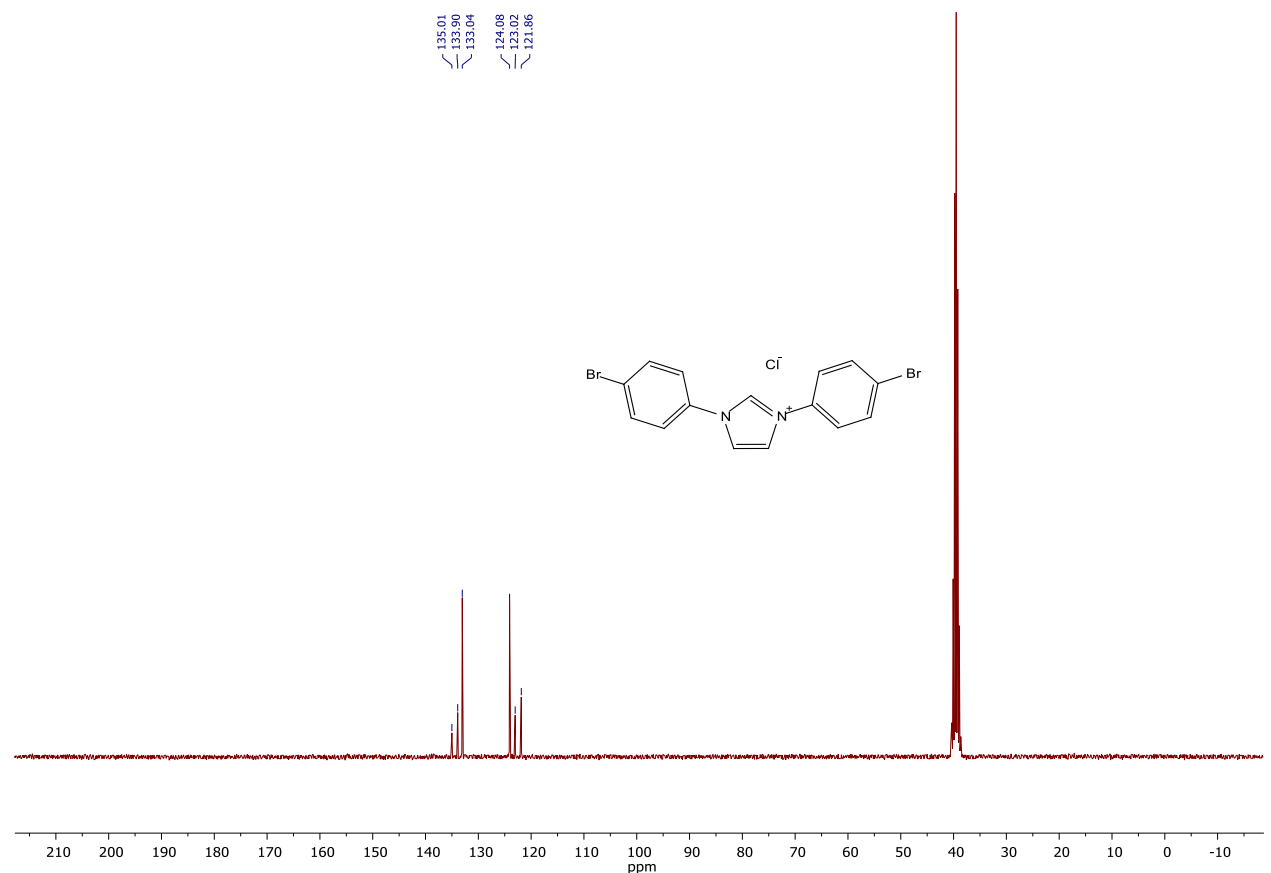
**Figure S15.** $^{13}C\{^1H\}$ NMR spectrum of **2i**. Solvent: DMSO-$d_6$, 75 MHz.
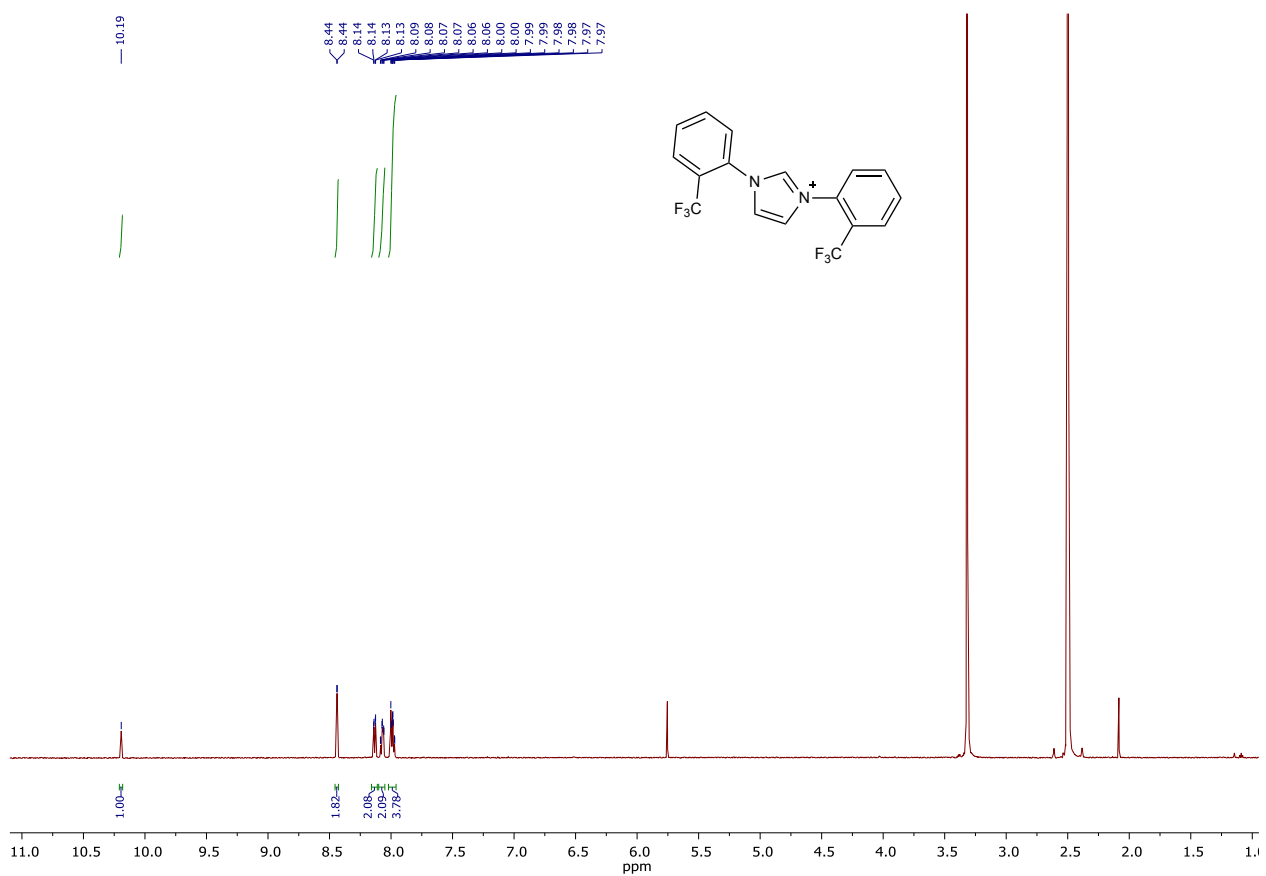


**Figure S16.** $^1H$ NMR spectrum of **2j**. Solvent: DMSO-$d_6$, 600 MHz.

11
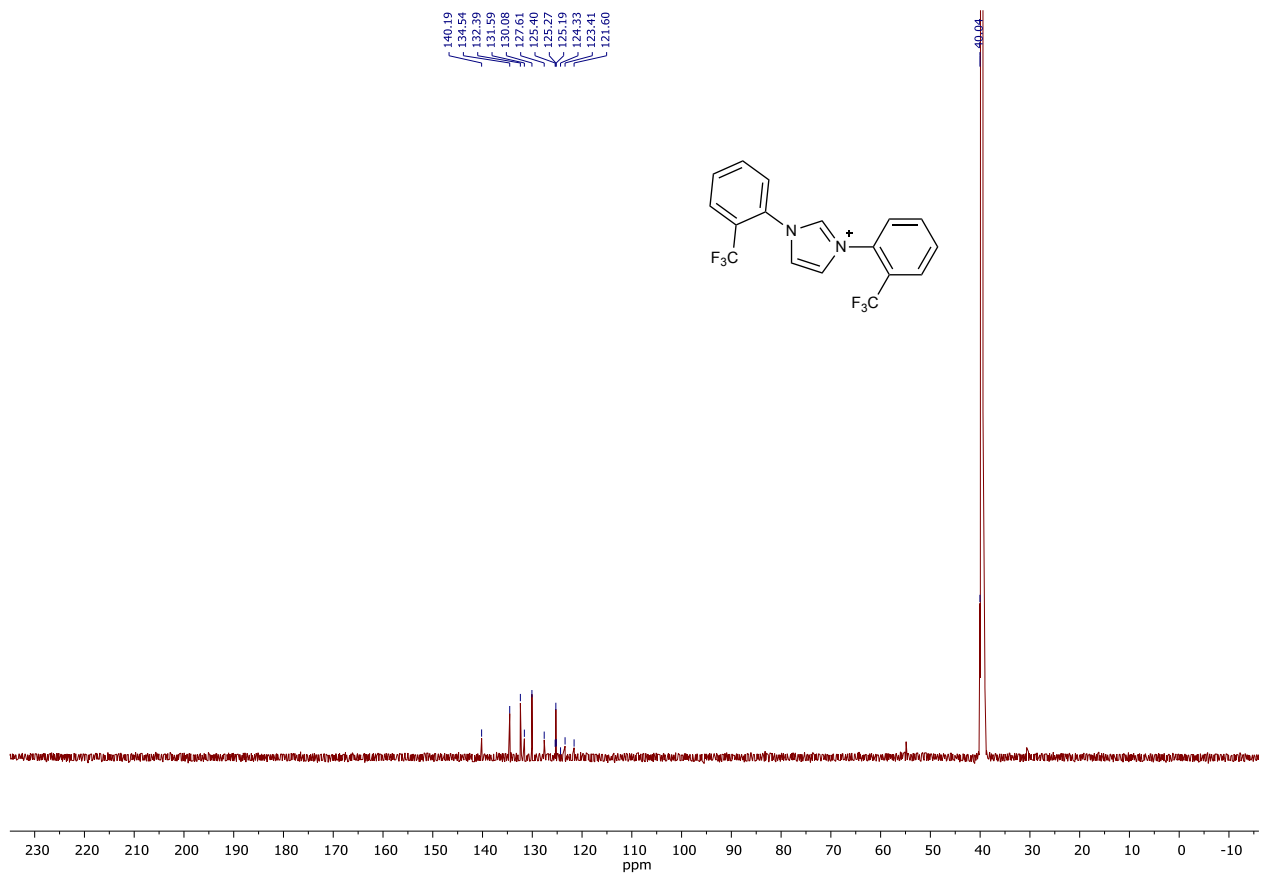
**Figure S17**. $^{13}C\{^1H\}$ NMR spectrum of **2j**. Solvent: DMSO-$d_6$, 151 MHz.
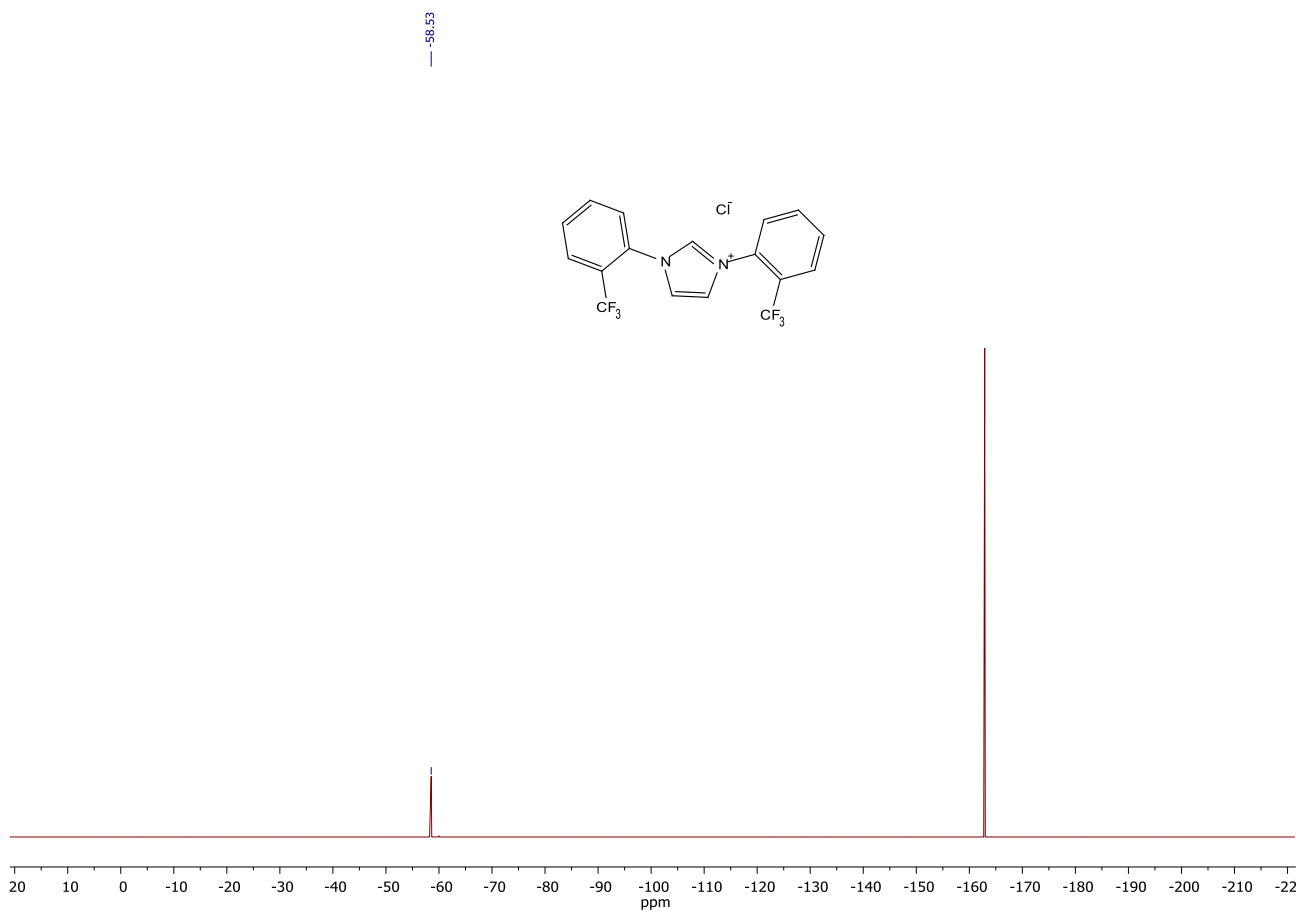
**Figure S18**. $^{19}$F{$^{1}$H} NMR spectrum of **2j**. Solvent: DMSO-$d_6$, 282.4 MHz. Standard: $C_6F_6$ with respect to $CFCl_3$.
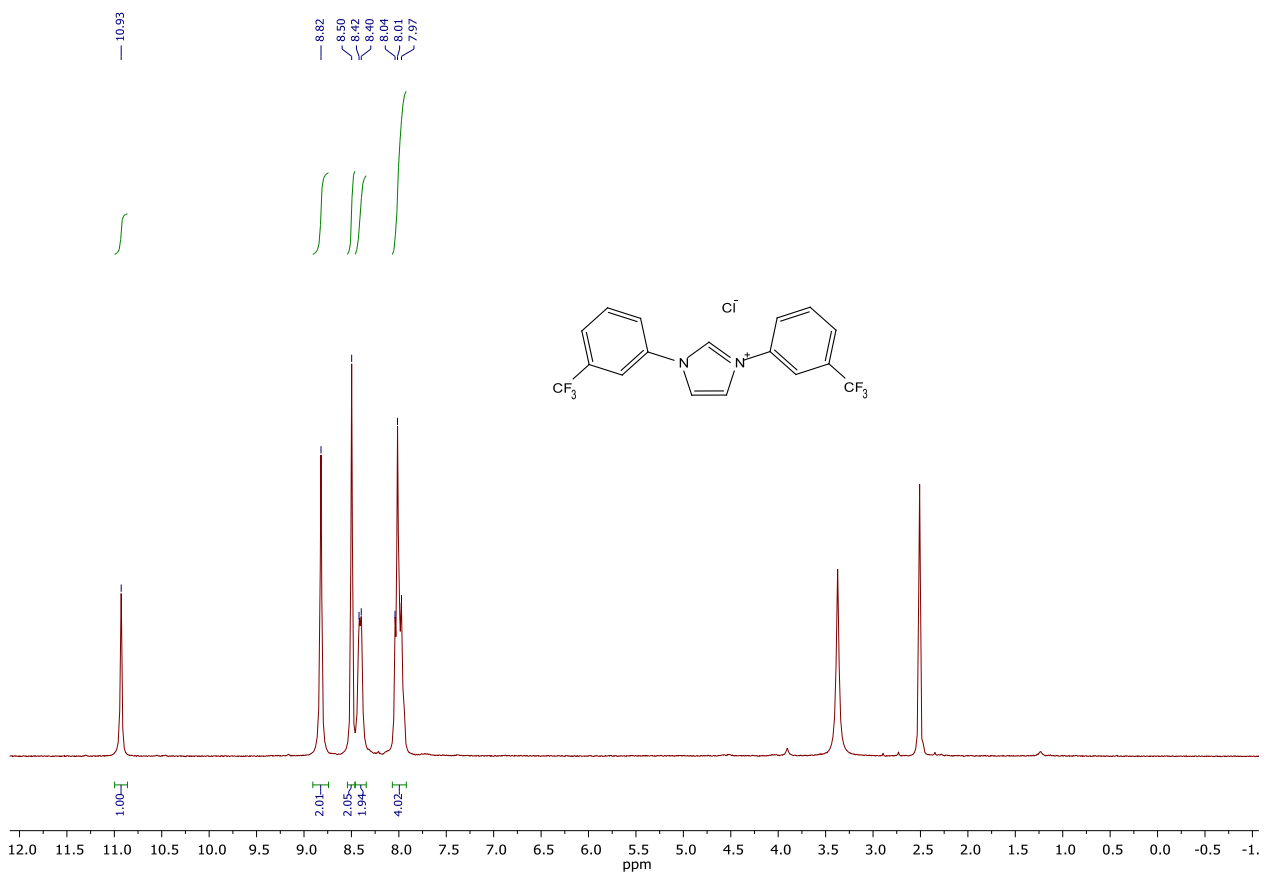


**Figure S19**. $^{1}$H NMR spectrum of **2k**. Solvent: DMSO-$d_6$, 300 MHz.
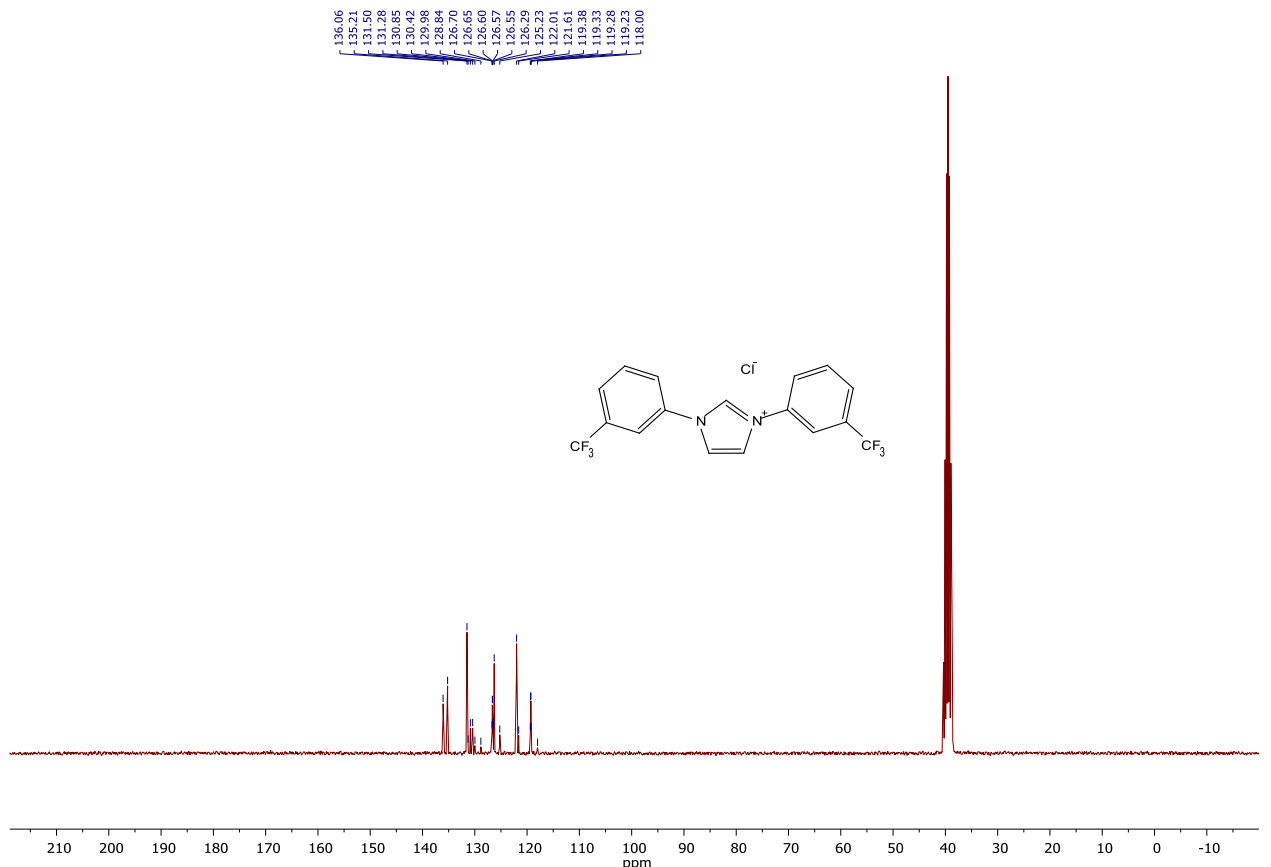
**Figure S20**. $^{13}C\{^1H\}$ NMR spectrum of **2k**. Solvent: DMSO-$d_6$, 75 MHz.
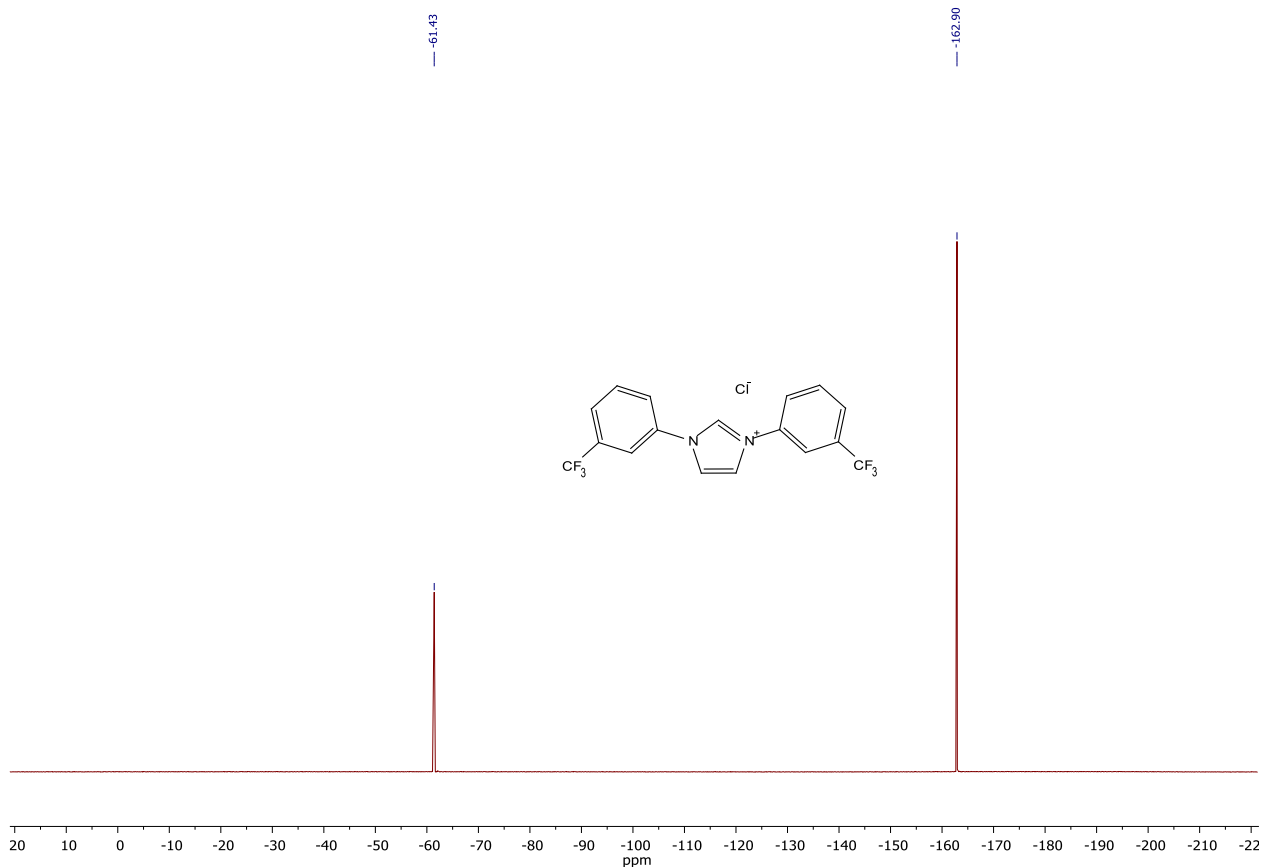


**Figure S21**. $^{19}F\{^1H\}$ NMR spectrum of **2k**. Solvent: DMSO-$d_6$, 282.4 MHz. Standard: $C_6F_6$ with respect to $CFCl_3$.
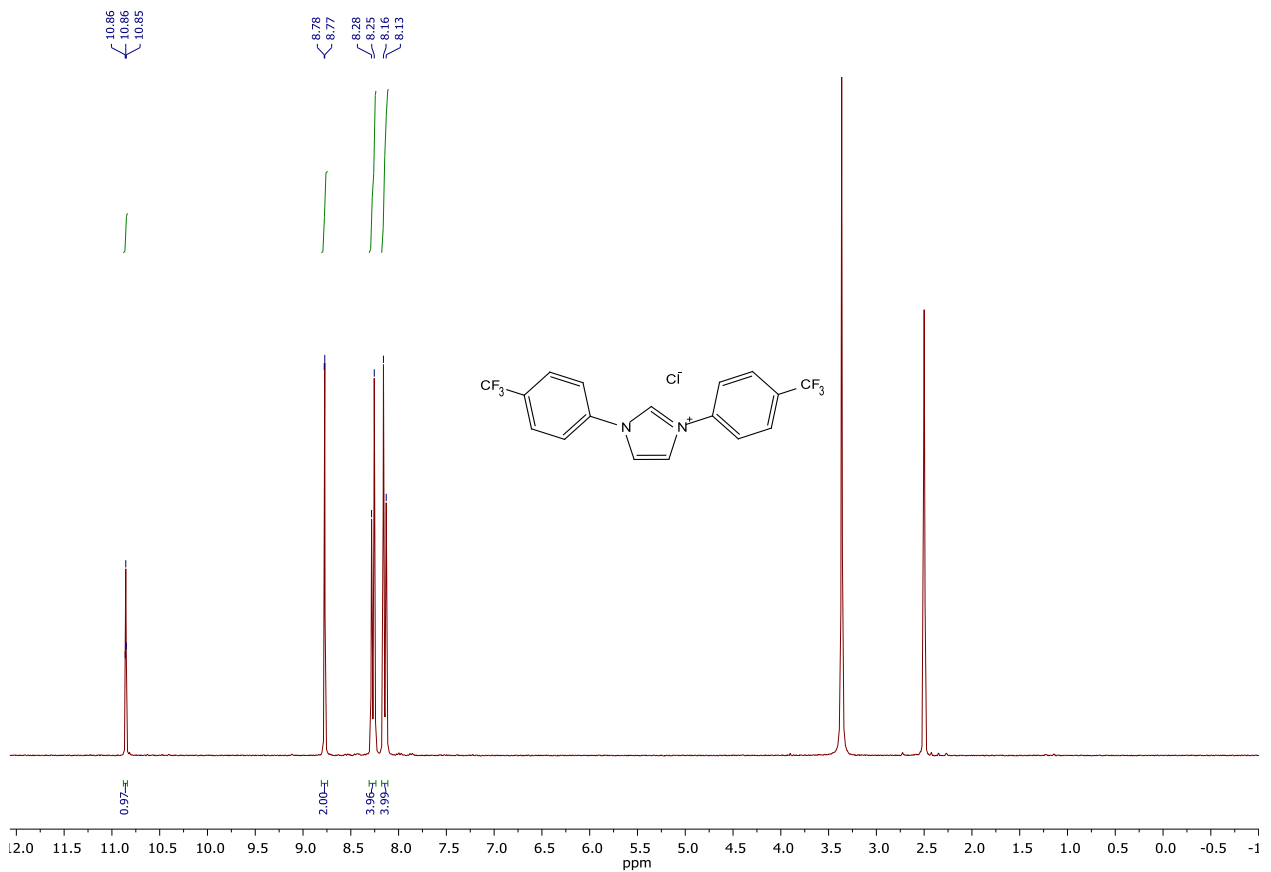
**Figure S22**. $^1$H NMR spectrum of **2l**. Solvent: DMSO-$d_6$, 300 MHz.
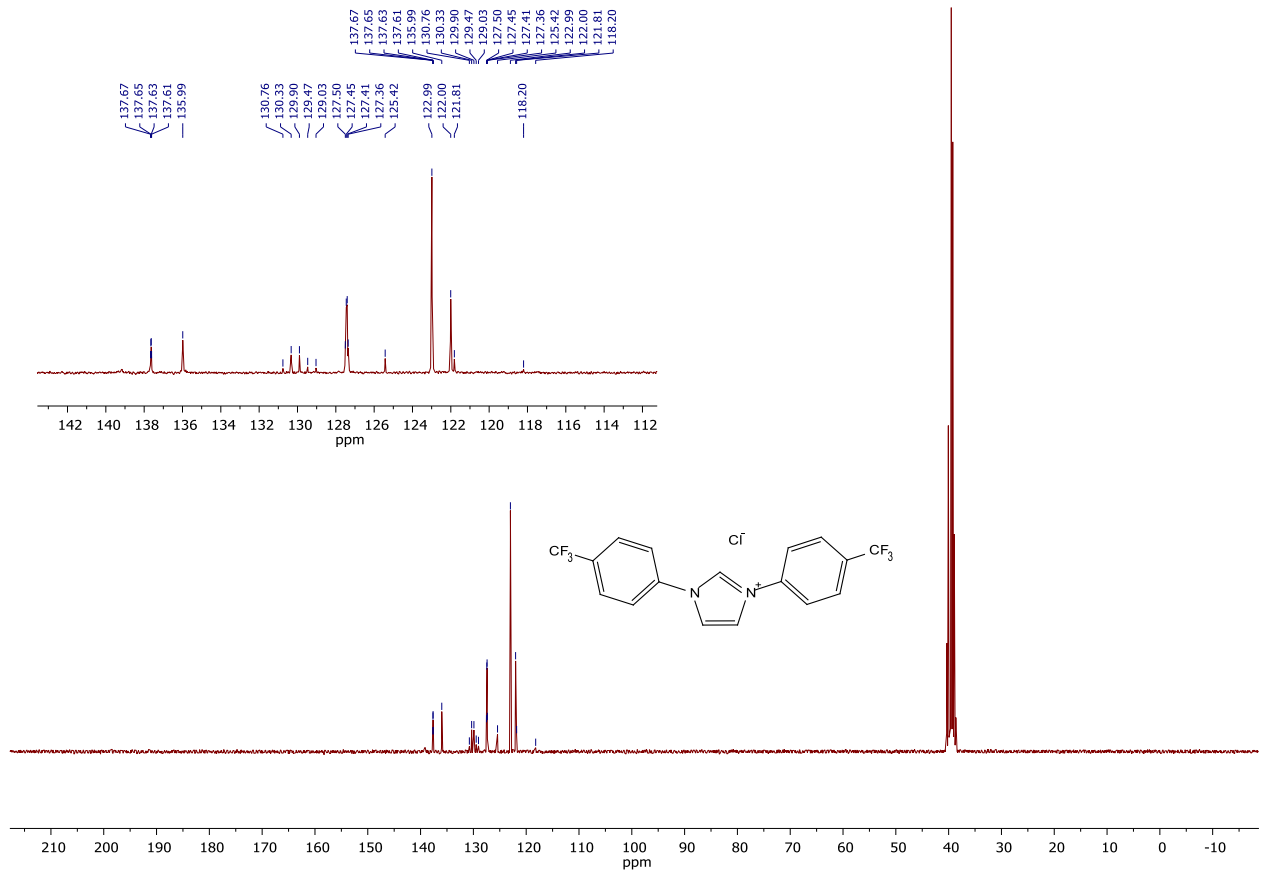


**Figure S23**. $^{13}$C{$^1$H} NMR spectrum of **2l**. Solvent: DMSO-$d_6$, 75 MHz.
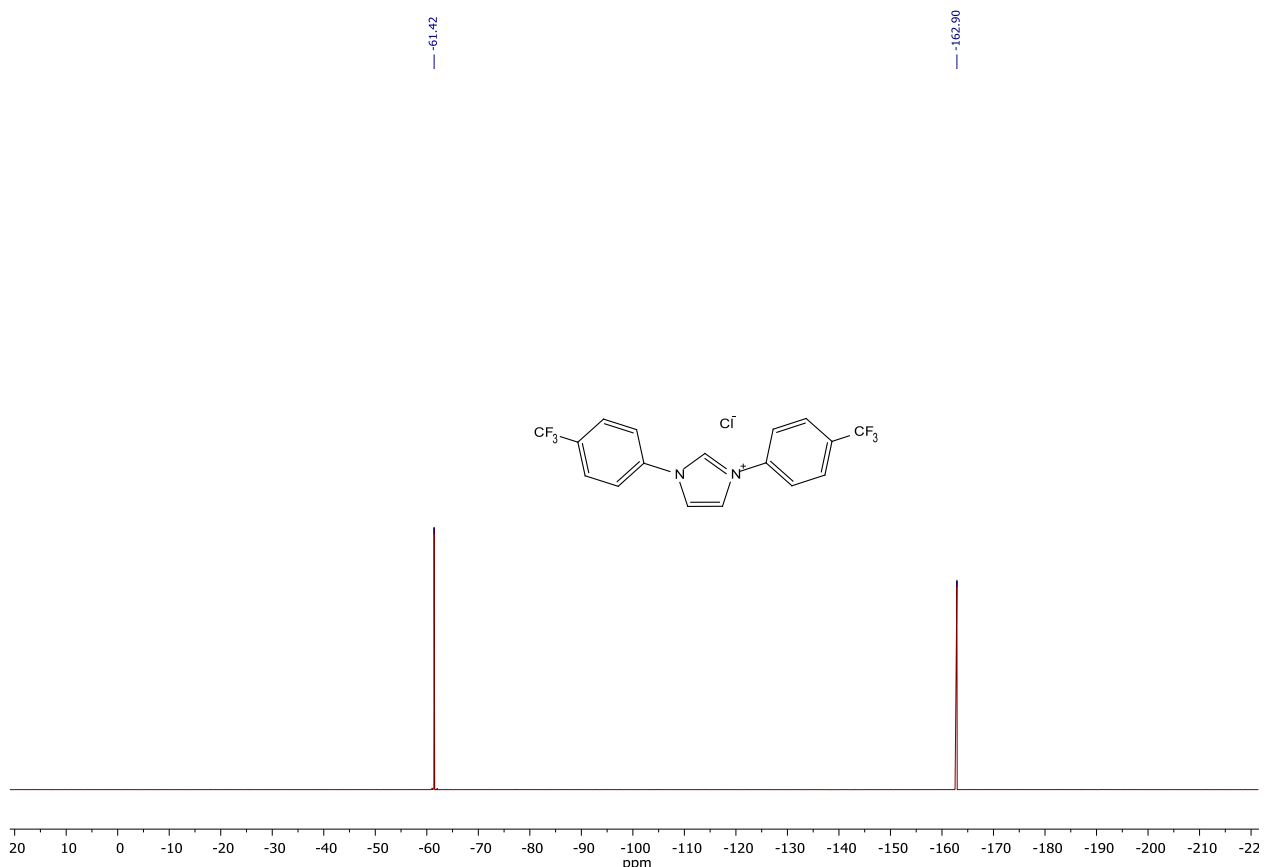
**Figure S24**. $^{19}F\{^{1}H\}$ NMR spectrum of **2l**. Solvent: DMSO-$d_6$, 282.4 MHz. Standard: $C_6F_6$ with respect to $CFCl_3$.



**Figure S25**. $^{1}H$ NMR spectrum of **3**. Solvent: $CDCl_3$, 300 MHz.
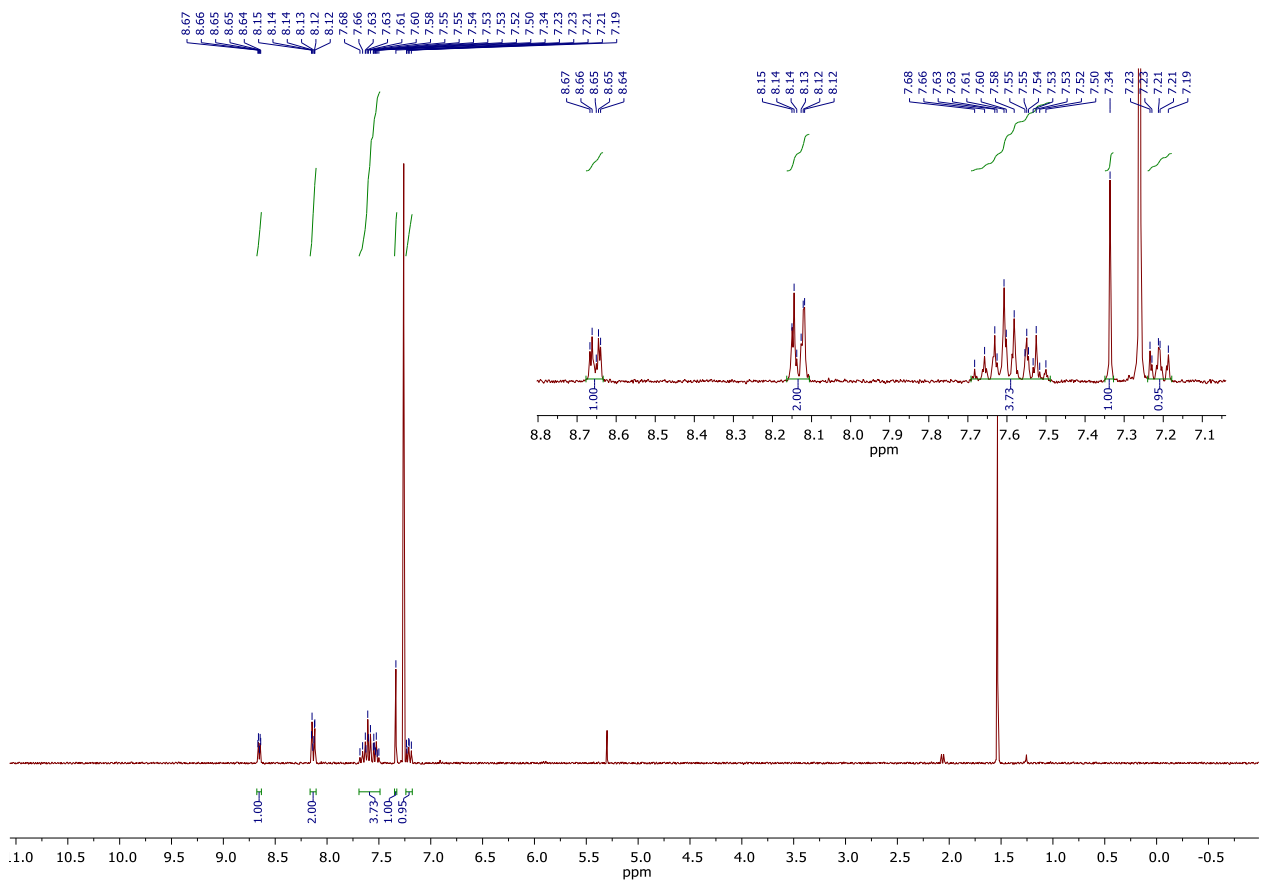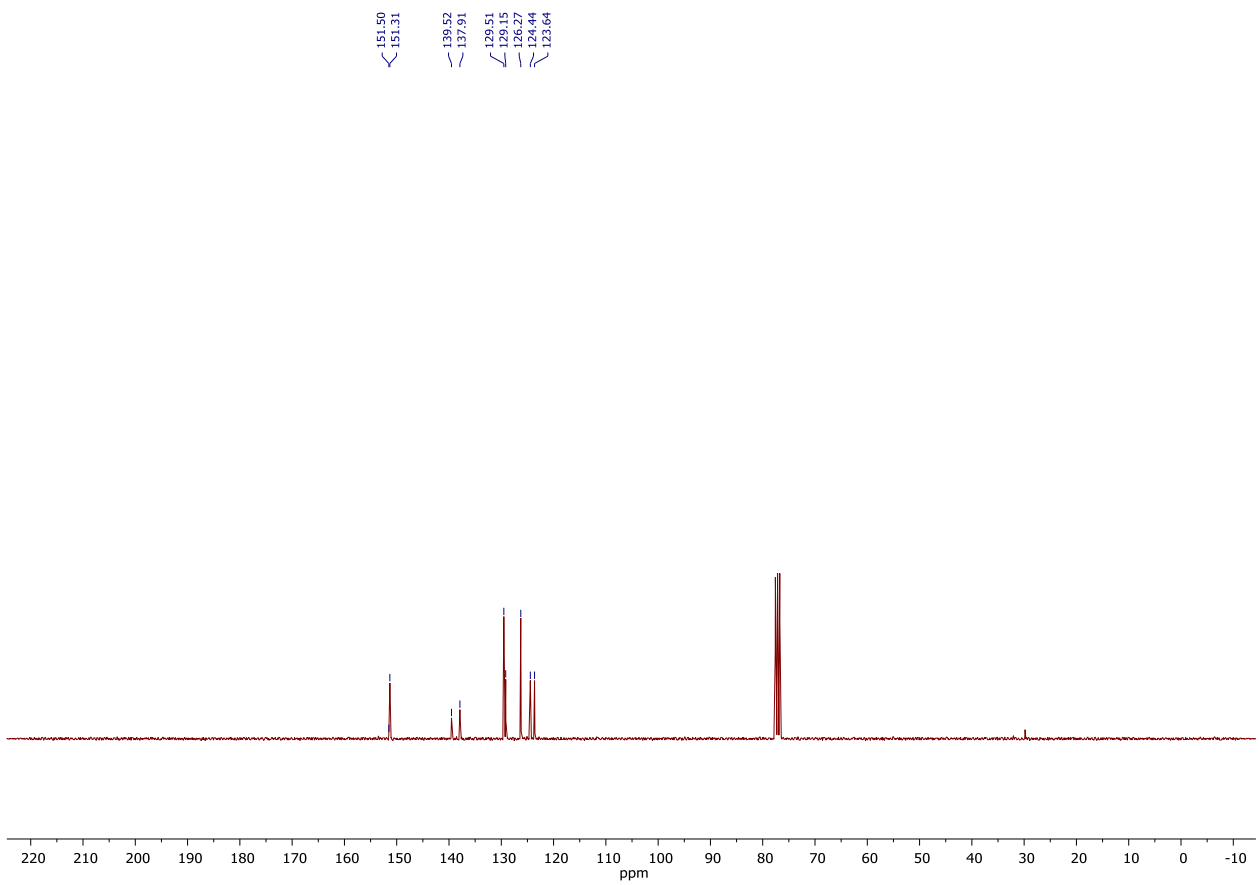
**Figure S26**. $^{13}C\{^1H\}$ NMR spectrum of **3**. Solvent: $CDCl_3$, 75 MHz.
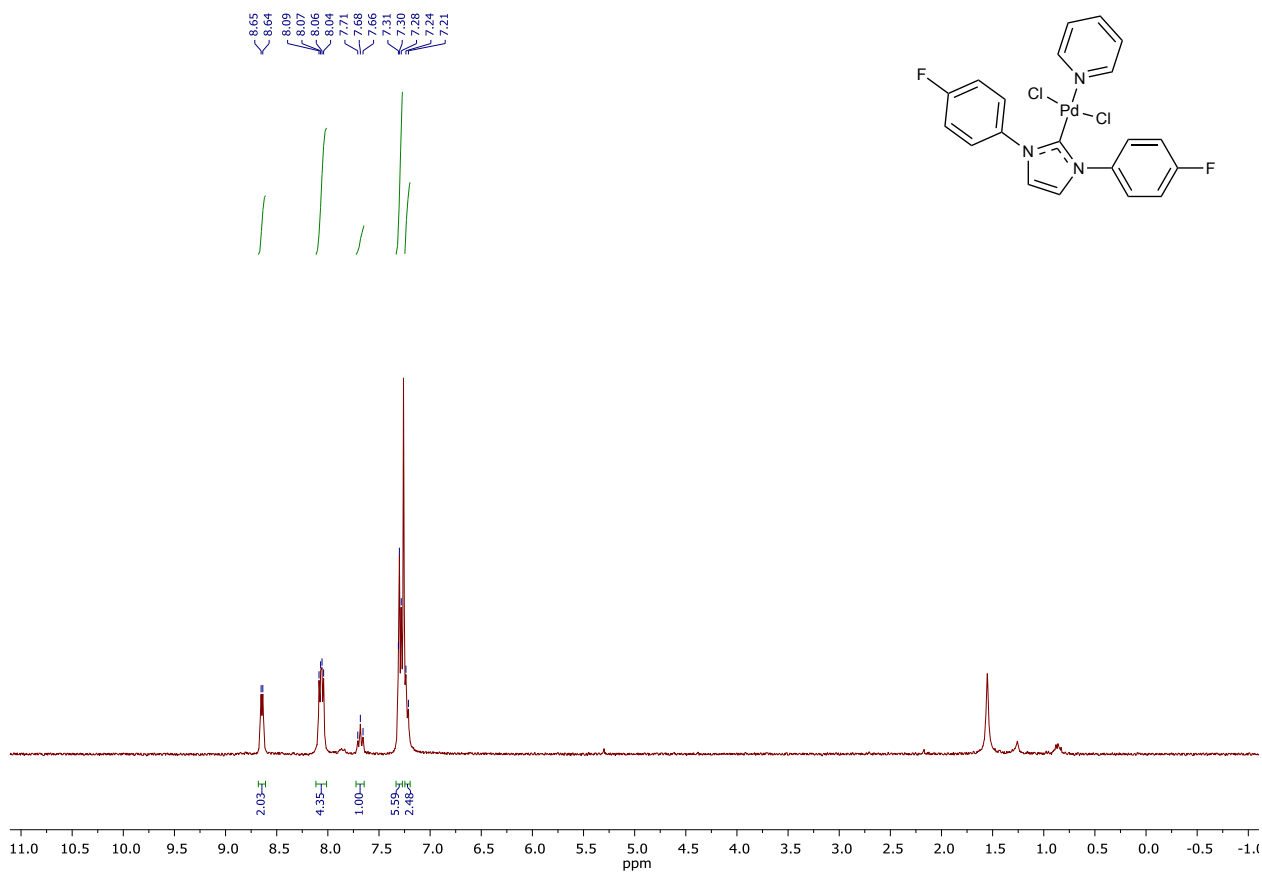


**Figure S27**. $^1H$ NMR spectrum of **3c**. Solvent: $CDCl_3$, 300 MHz.

164.53
161.23
152.56
151.26
138.10
135.44
135.40
128.41
128.29
124.57
123.80
116.70
116.39

210 200 190 180 170 160 150 140 130 120 110 100 90 80 70 60 50 40 30 20 10 0 -10
ppm
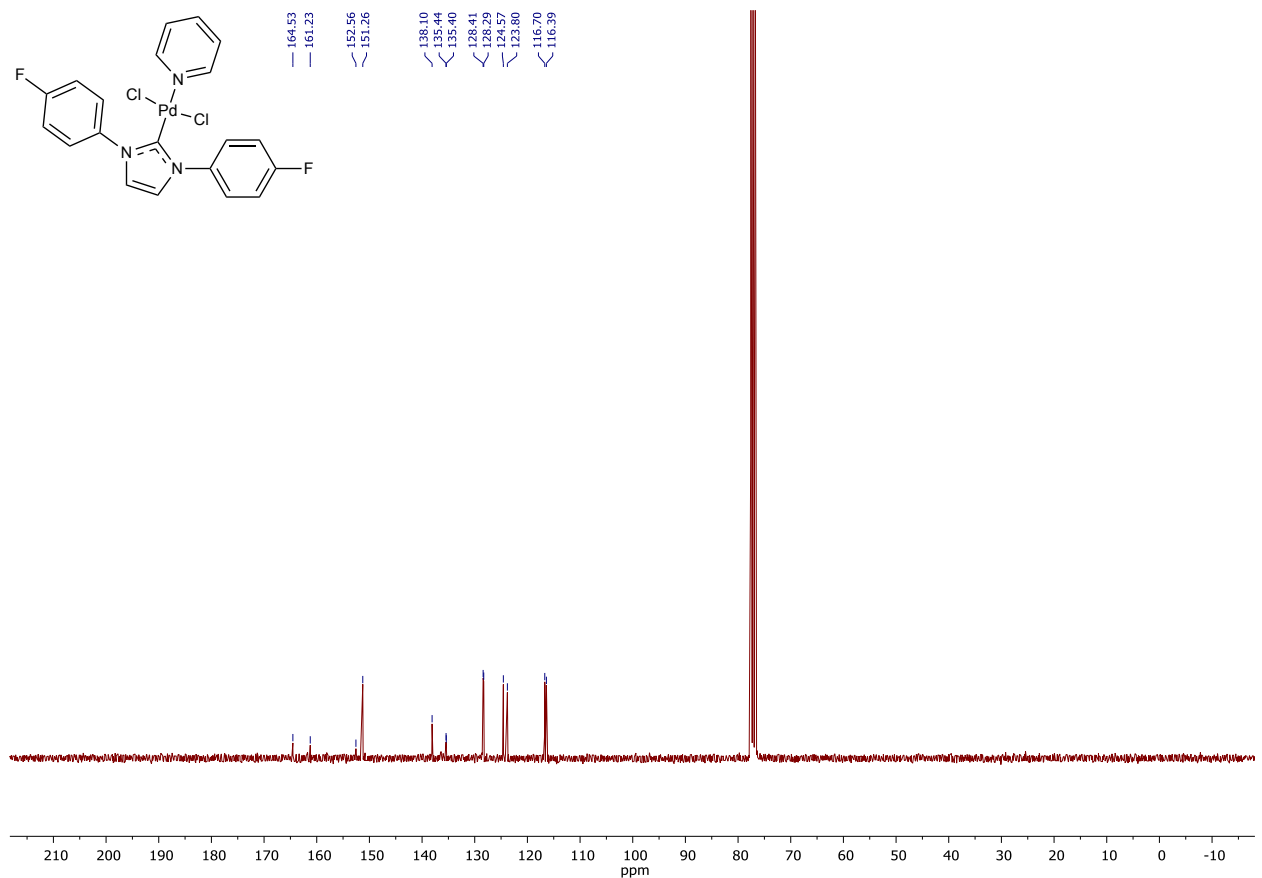
**Figure S28**. $^{13}C\{^1H\}$ NMR spectrum of **3c**. Solvent: CDCl$_3$, 75 MHz.



-112.93

-162.90

20 10 0 -10 -20 -30 -40 -50 -60 -70 -80 -90 -100 -110 -120 -130 -140 -150 -160 -170 -180 -190 -200 -210 -220
ppm
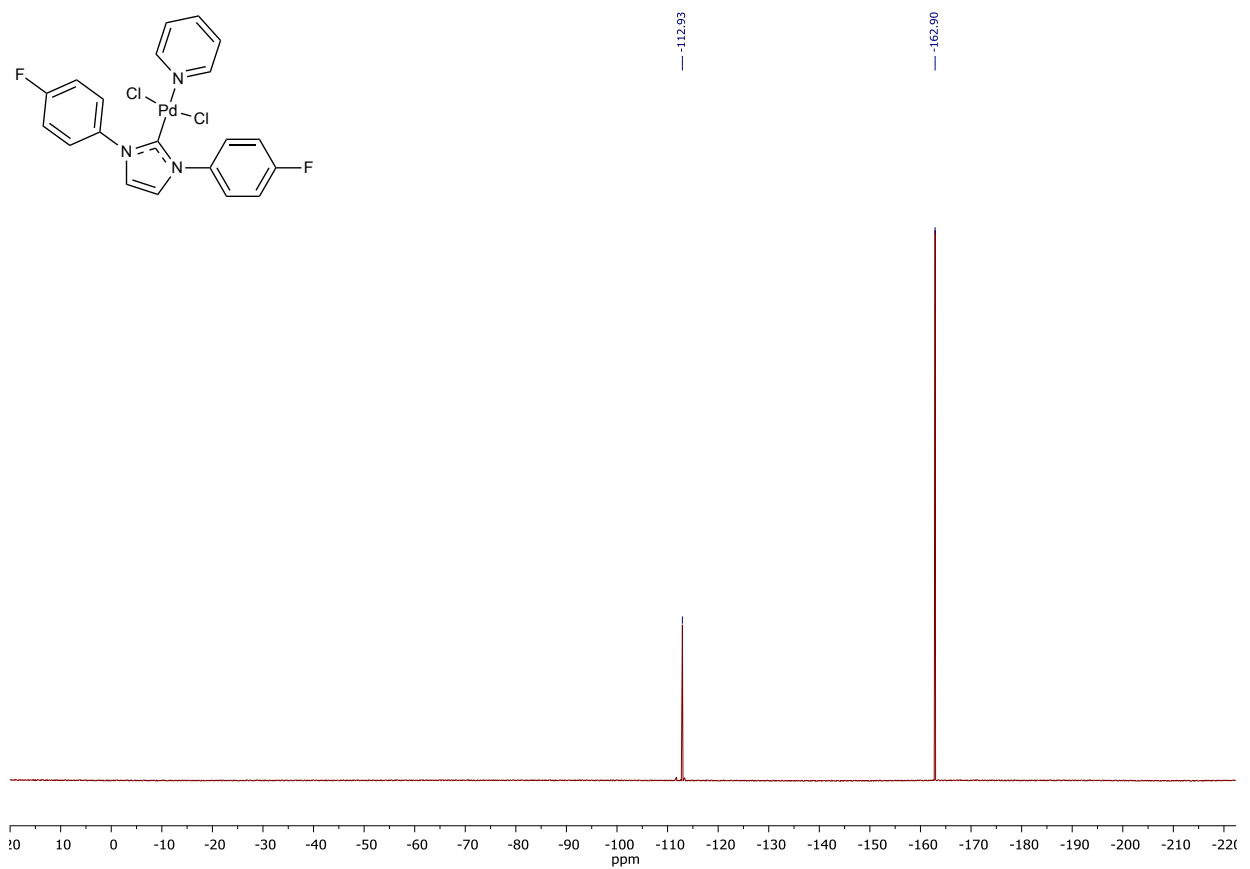
**Figure S29**. $^{19}F\{^1H\}$ NMR spectrum of **3c**. Solvent: CDCl$_3$, 282.4 MHz. Standard: C$_6$F$_6$ with respect to CFCl$_3$.
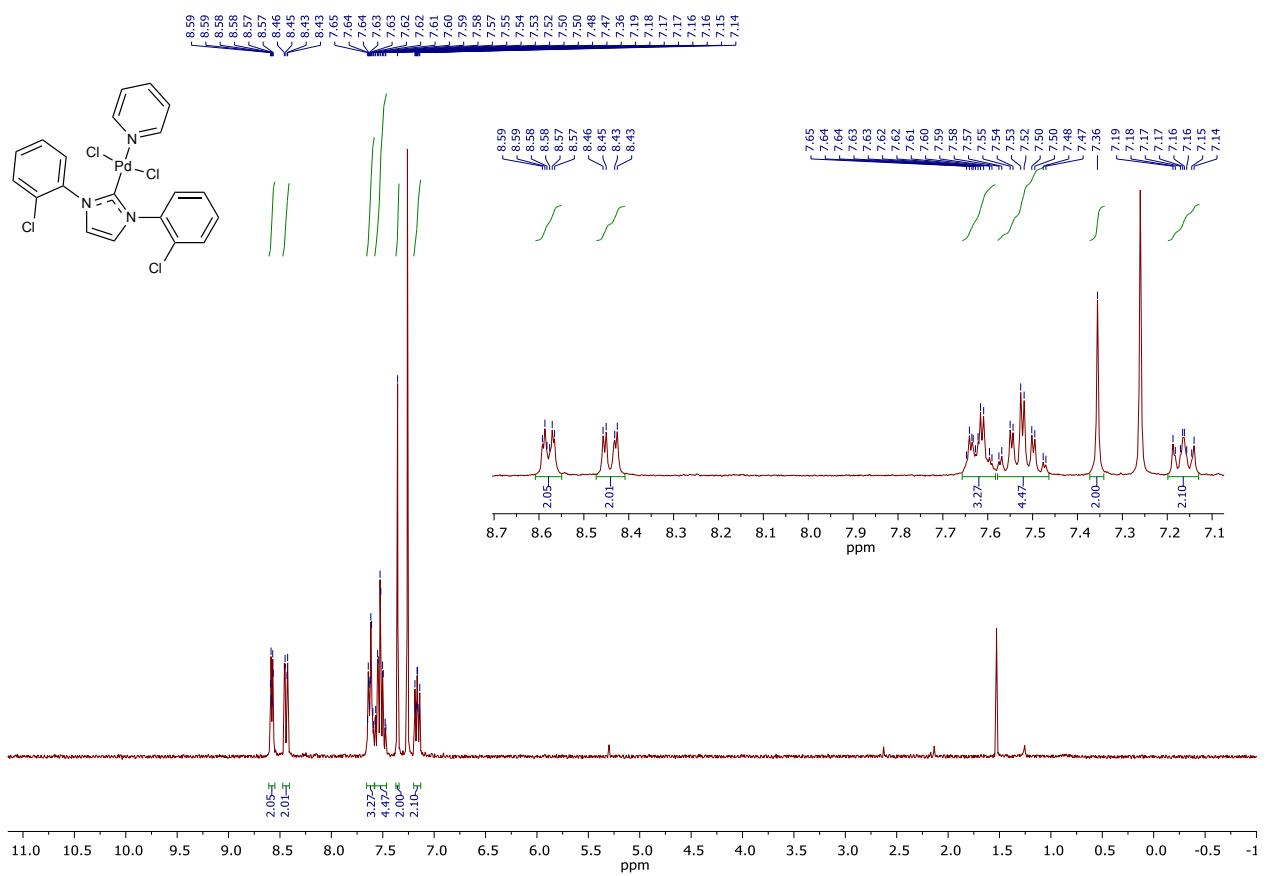
**Figure S30**. $^1$H NMR spectrum of **3d**. Solvent: CDCl$_3$, 300 MHz.
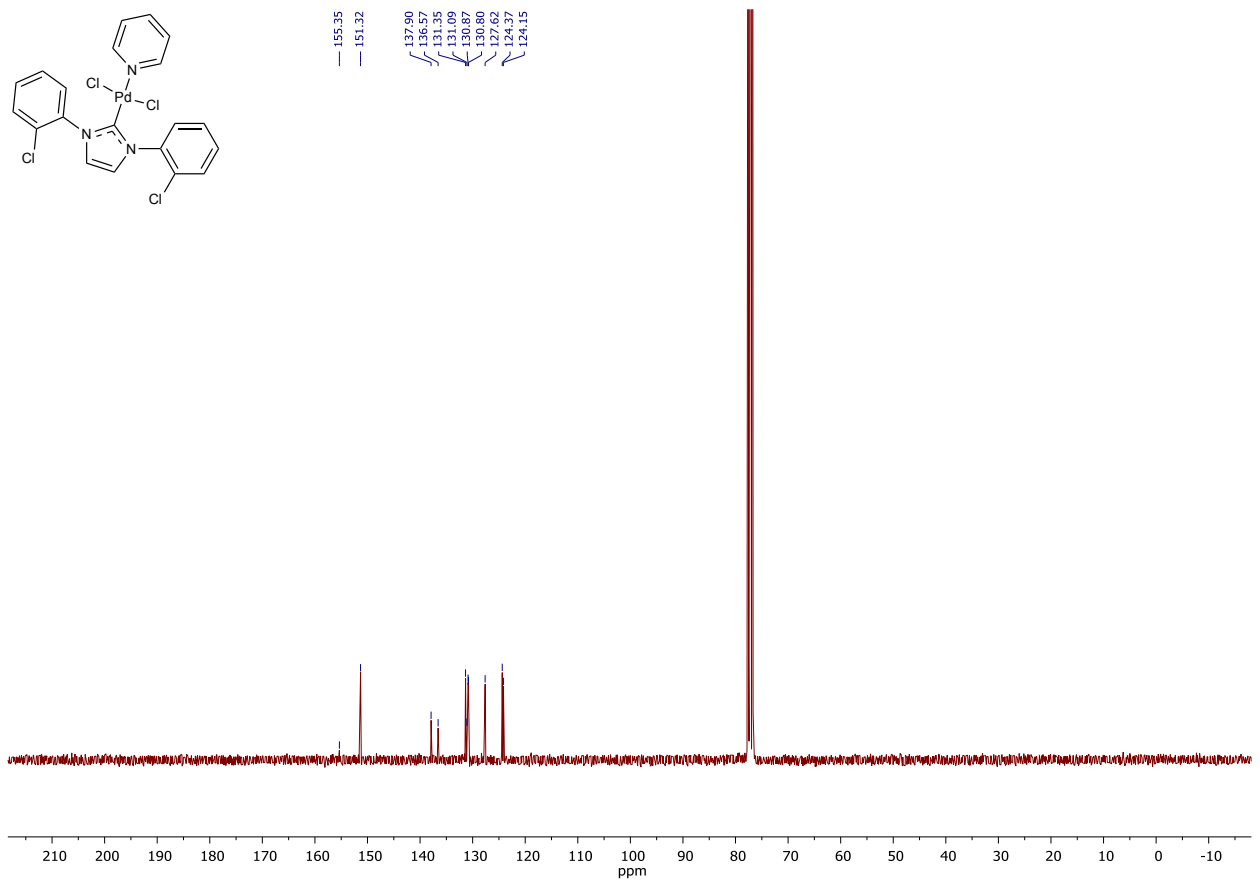


**Figure S31**. $^{13}$C{$^1$H} NMR spectrum of **3d**. Solvent: CDCl$_3$, 75 MHz.

19
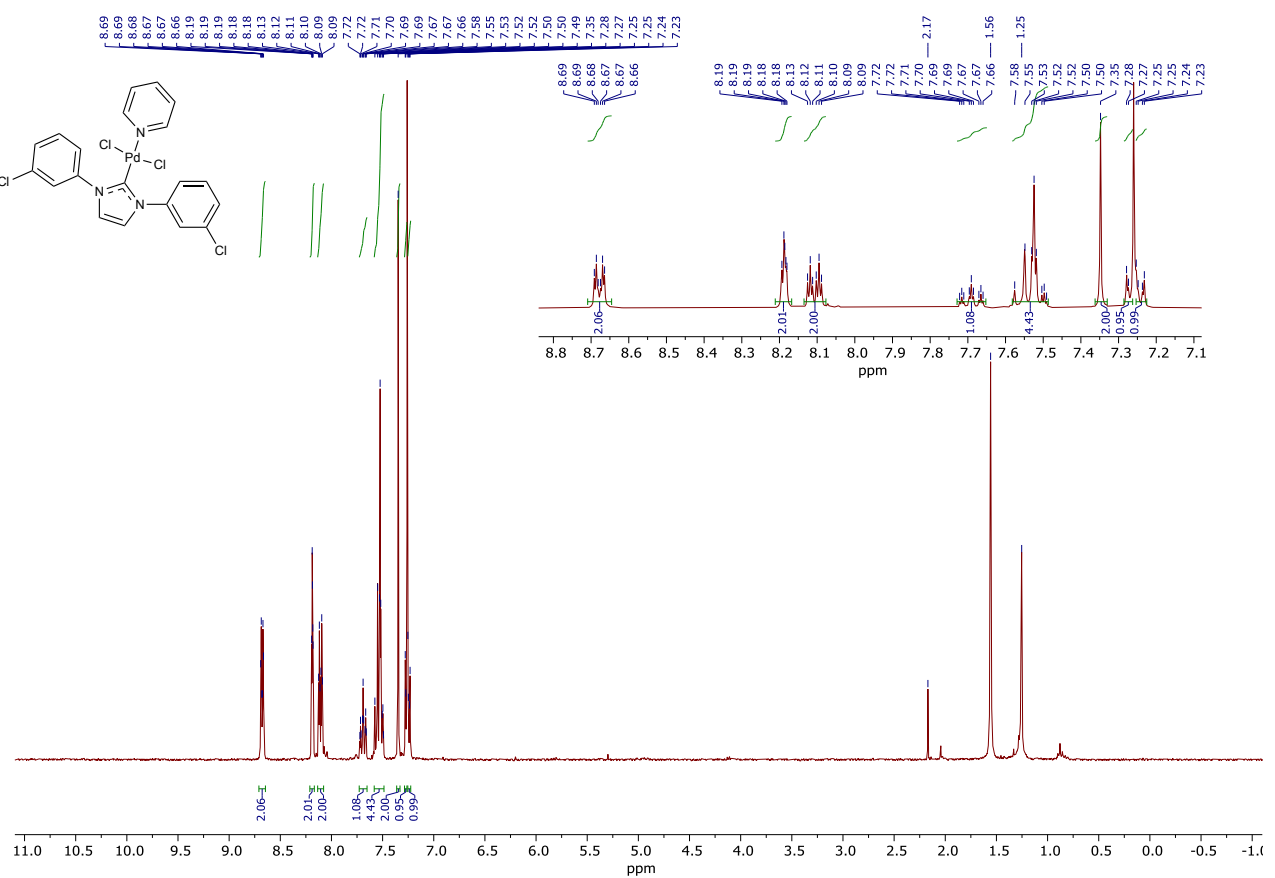
**Figure S32**. $^{1}$H NMR spectrum of **3e**. Solvent: CDCl$_3$, 300 MHz.
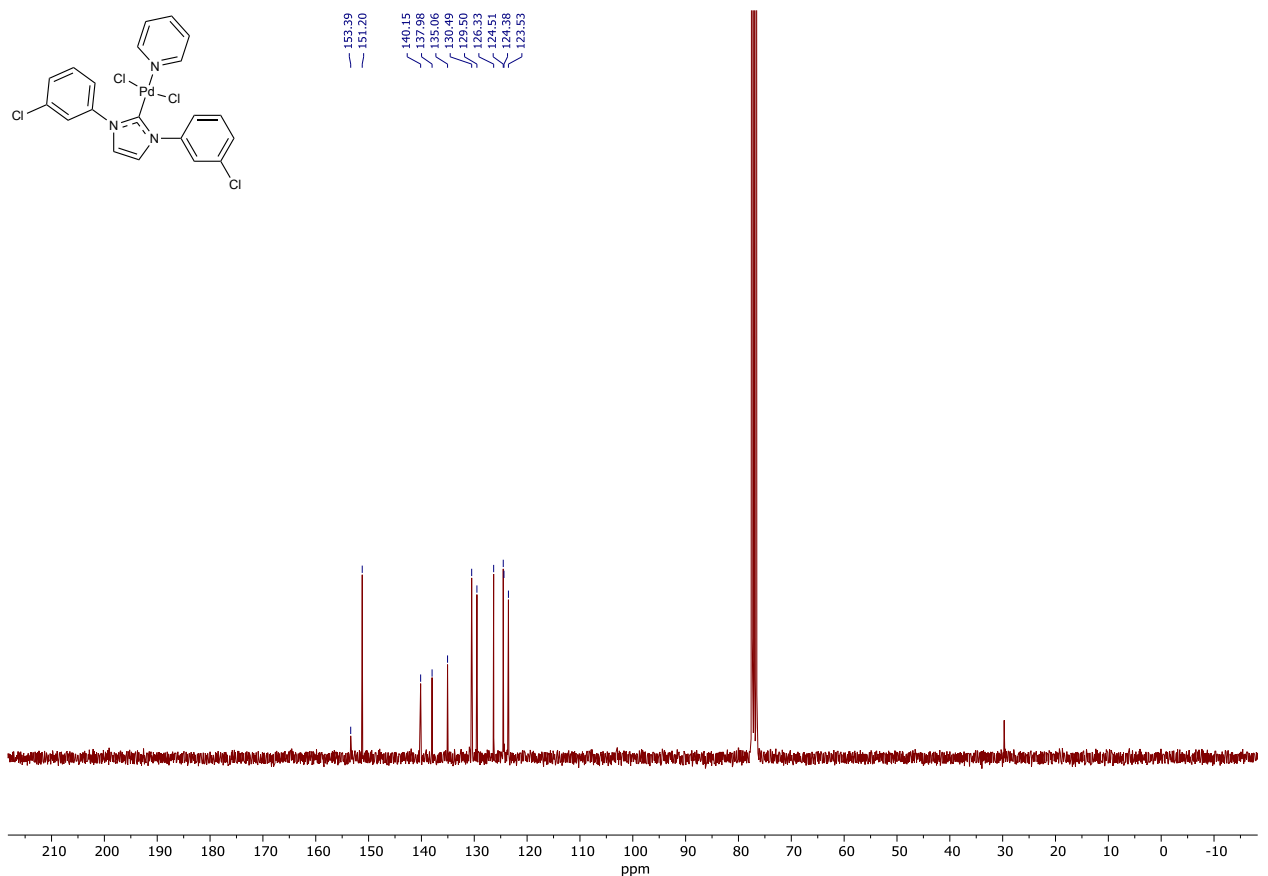


**Figure S33**. $^{13}$C{$^{1}$H} NMR spectrum of **3e**. Solvent: CDCl$_3$, 75 MHz.
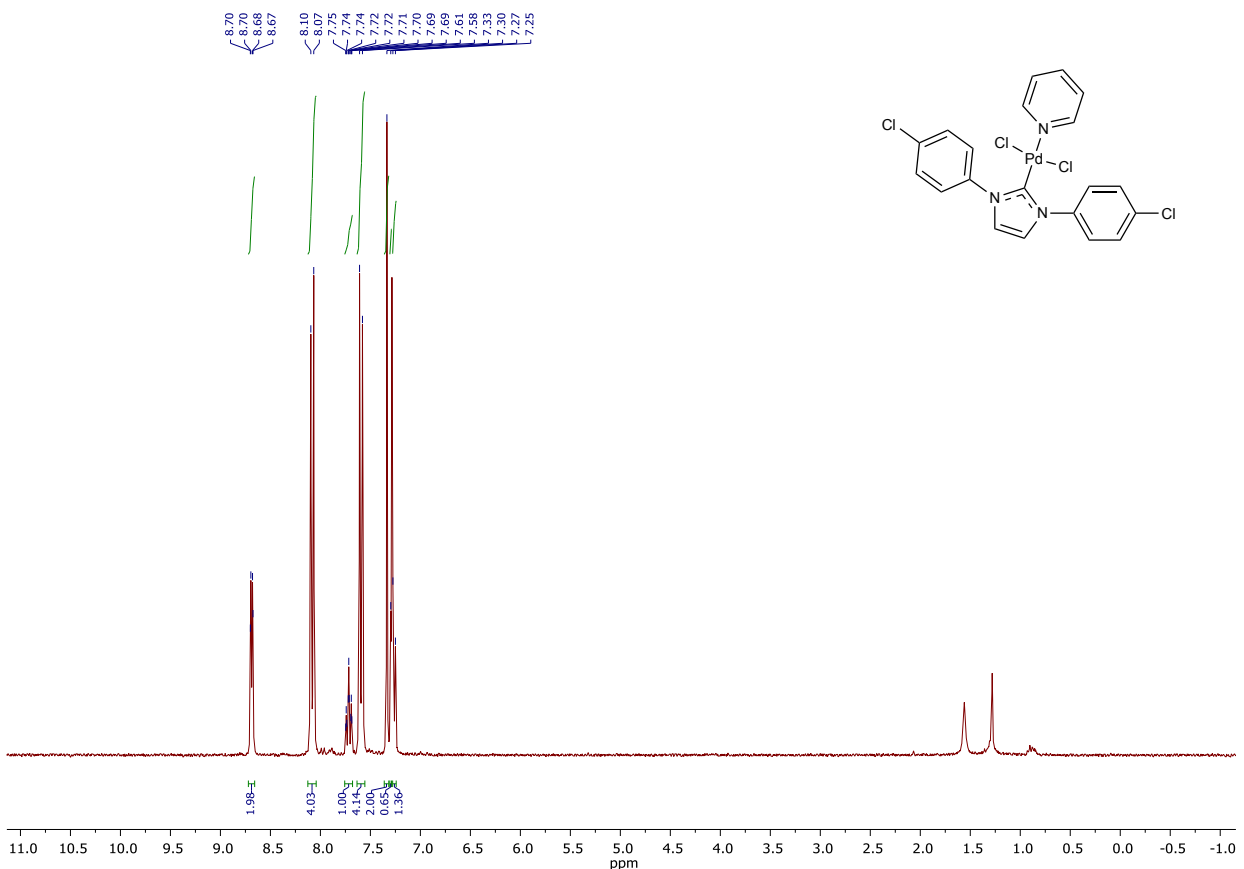
**Figure S34**. $^1$H NMR spectrum of **3f**. Solvent: CDCl$_3$, 300 MHz.
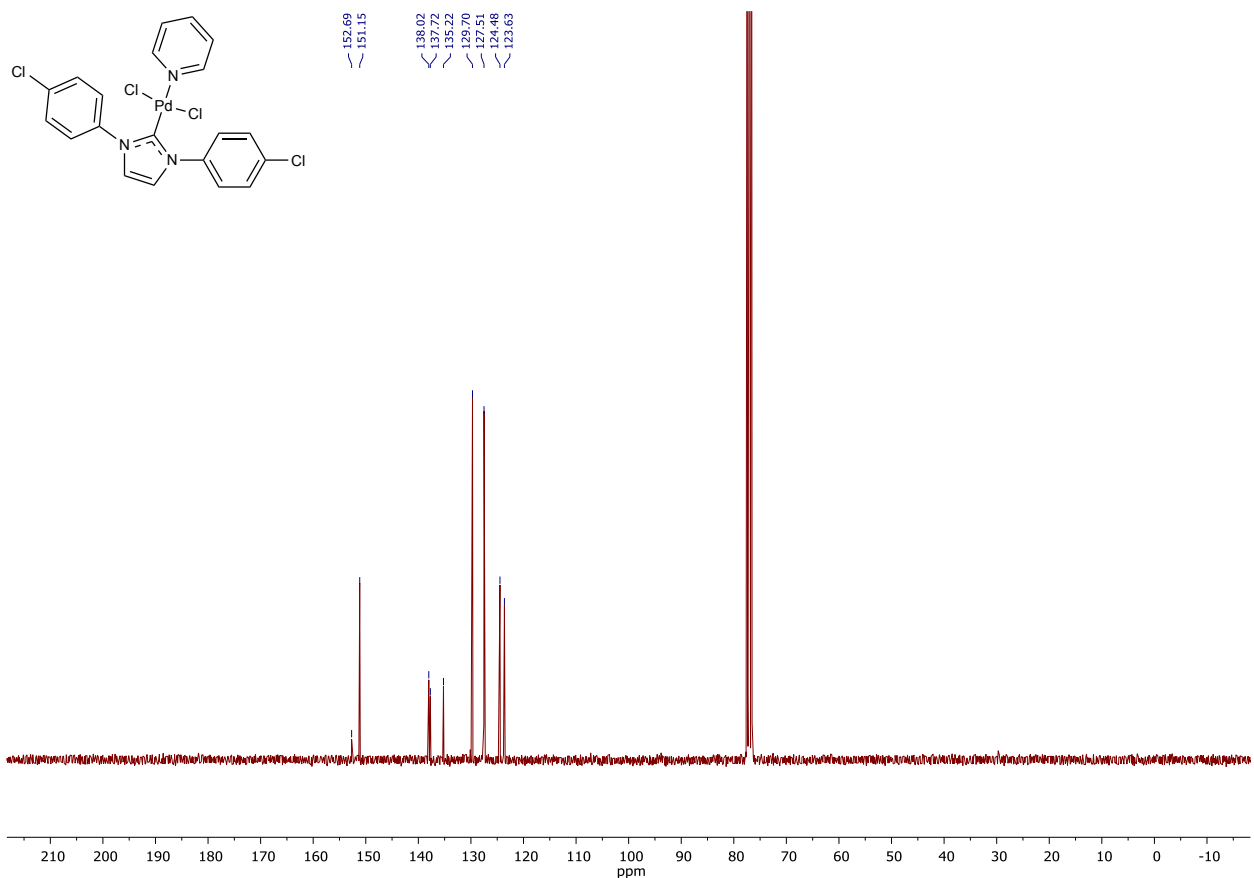


**Figure S35**. $^{13}$C{$^1$H} NMR spectrum of **3f**. Solvent: CDCl$_3$, 75 MHz
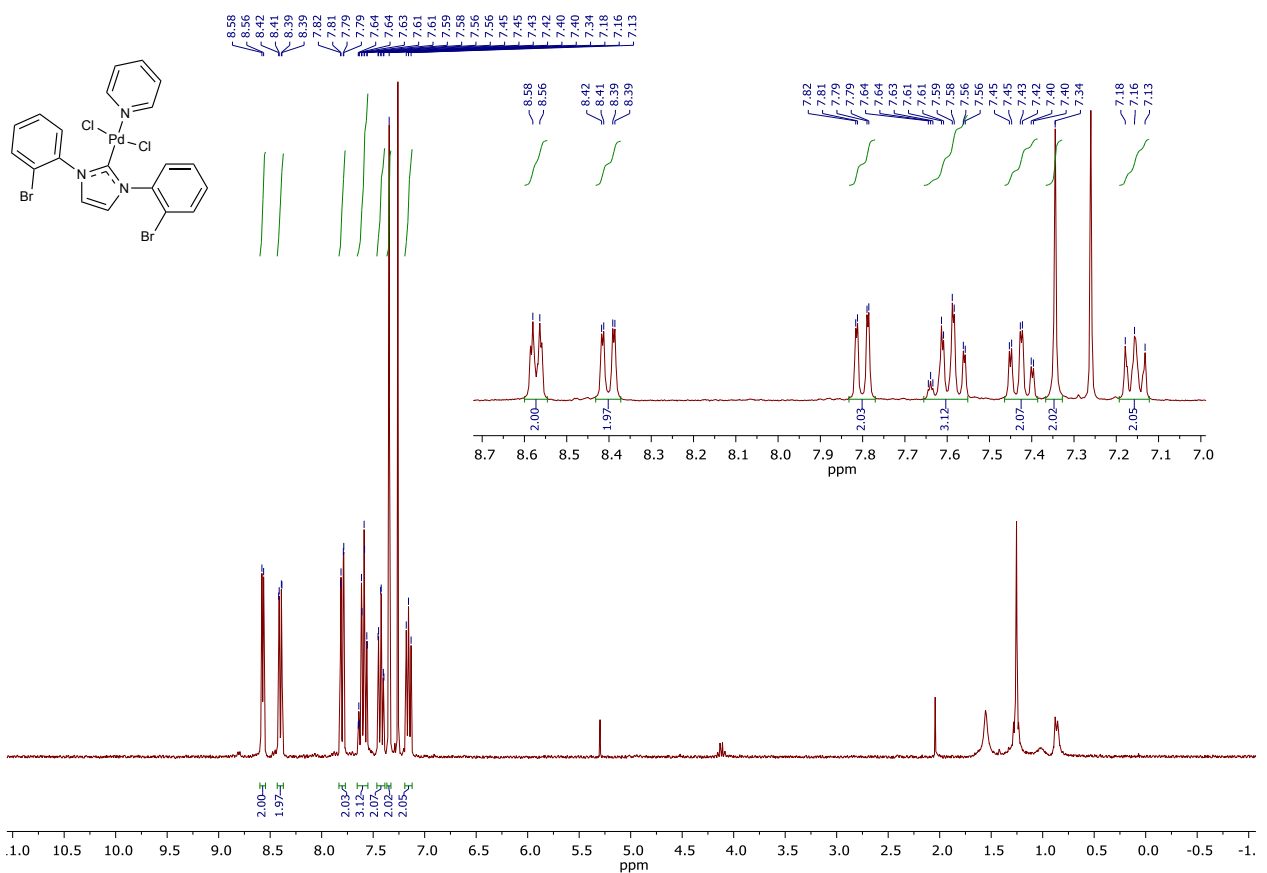
**Figure S36**. $^1$H NMR spectrum of **3g**. Solvent: CDCl$_3$, 300 MHz.
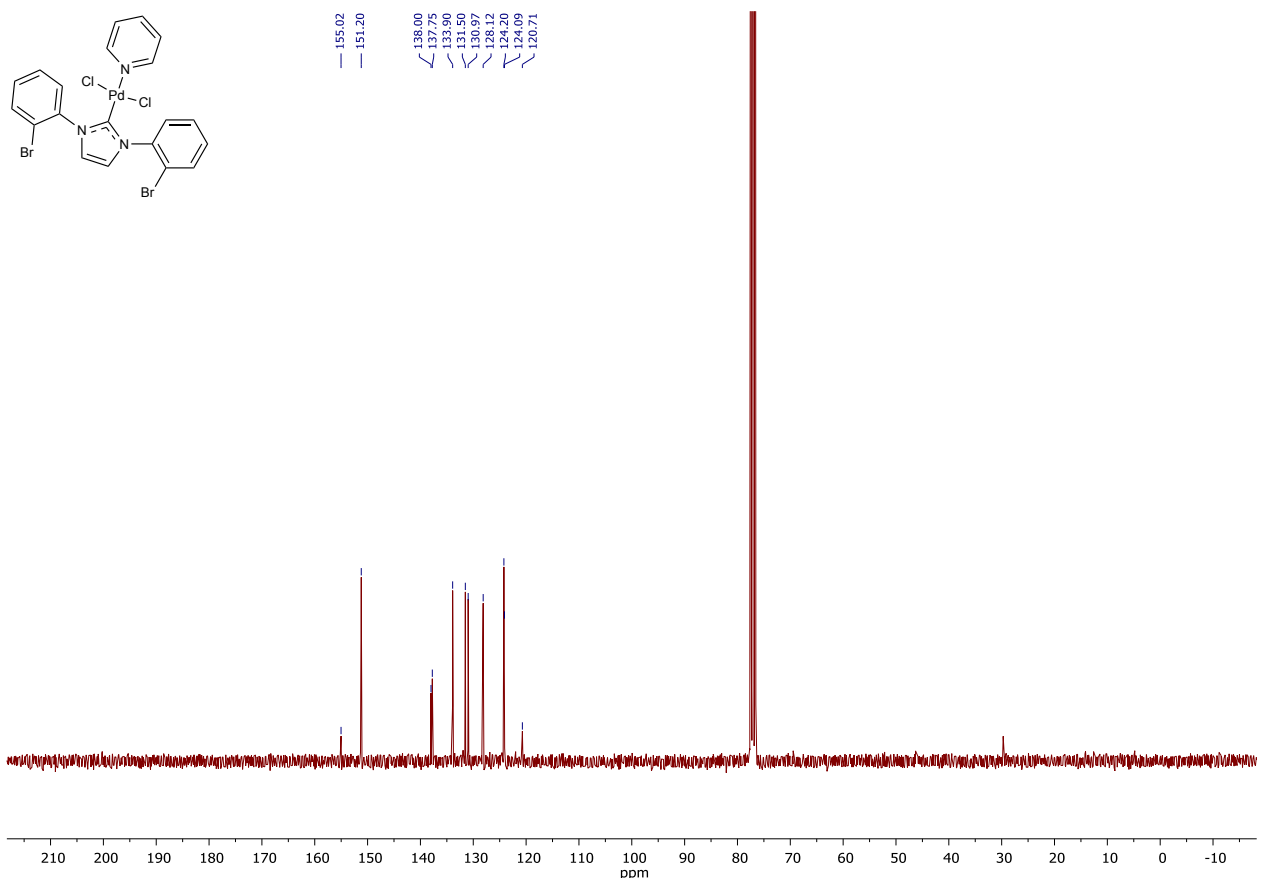


**Figure S37**. $^{13}$C{$^1$H} NMR spectrum of **3g**. Solvent: CDCl$_3$, 75 MHz.
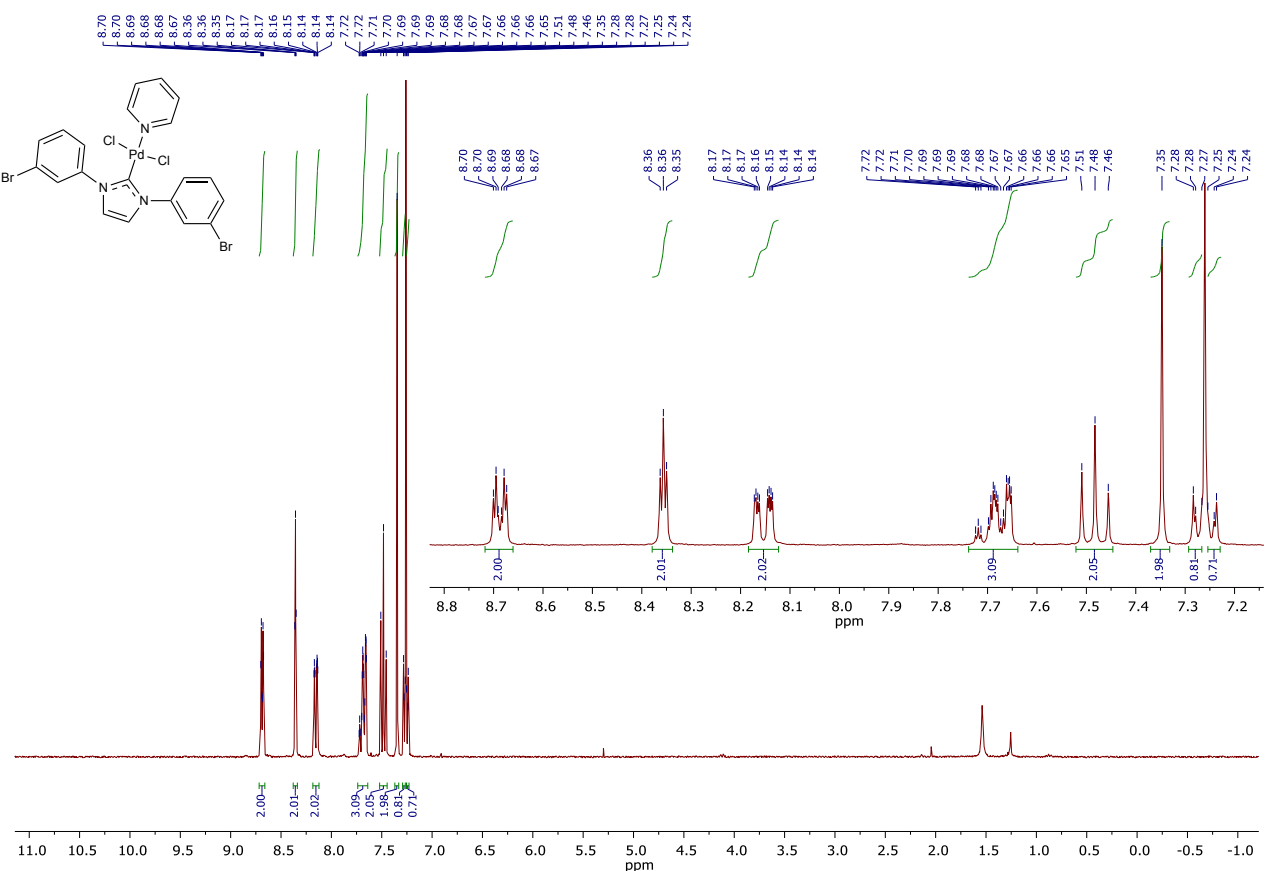
**Figure S38**. ${}^1$H NMR spectrum of **3h**. Solvent: CDCl₃, 300 MHz.
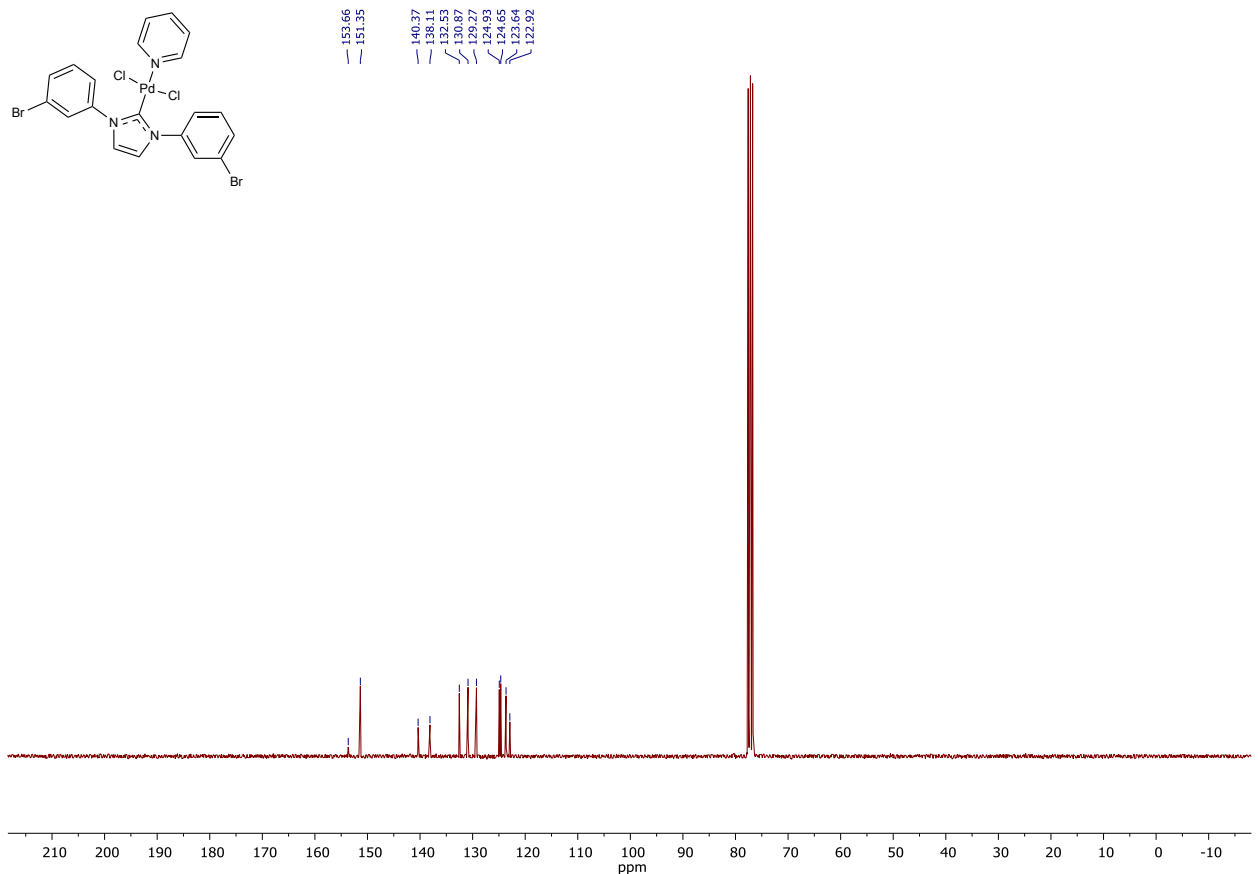


**Figure S39**. ${}^{13}$C{${}^1$H} NMR spectrum of **3h**. Solvent: CDCl₃, 75 MHz.
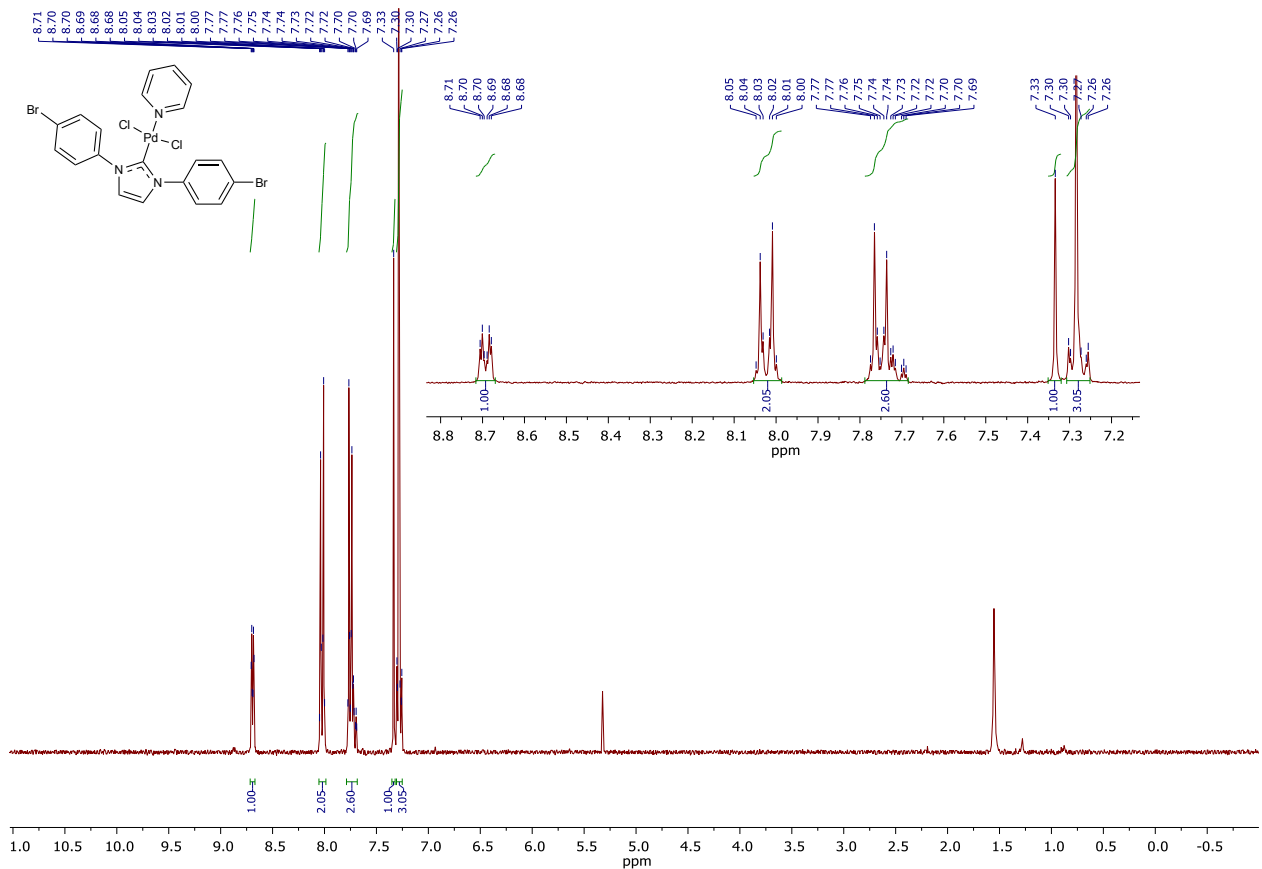
**Figure S40**. $^1$H NMR spectrum of **3i**. Solvent: CDCl$_3$, 300 MHz.
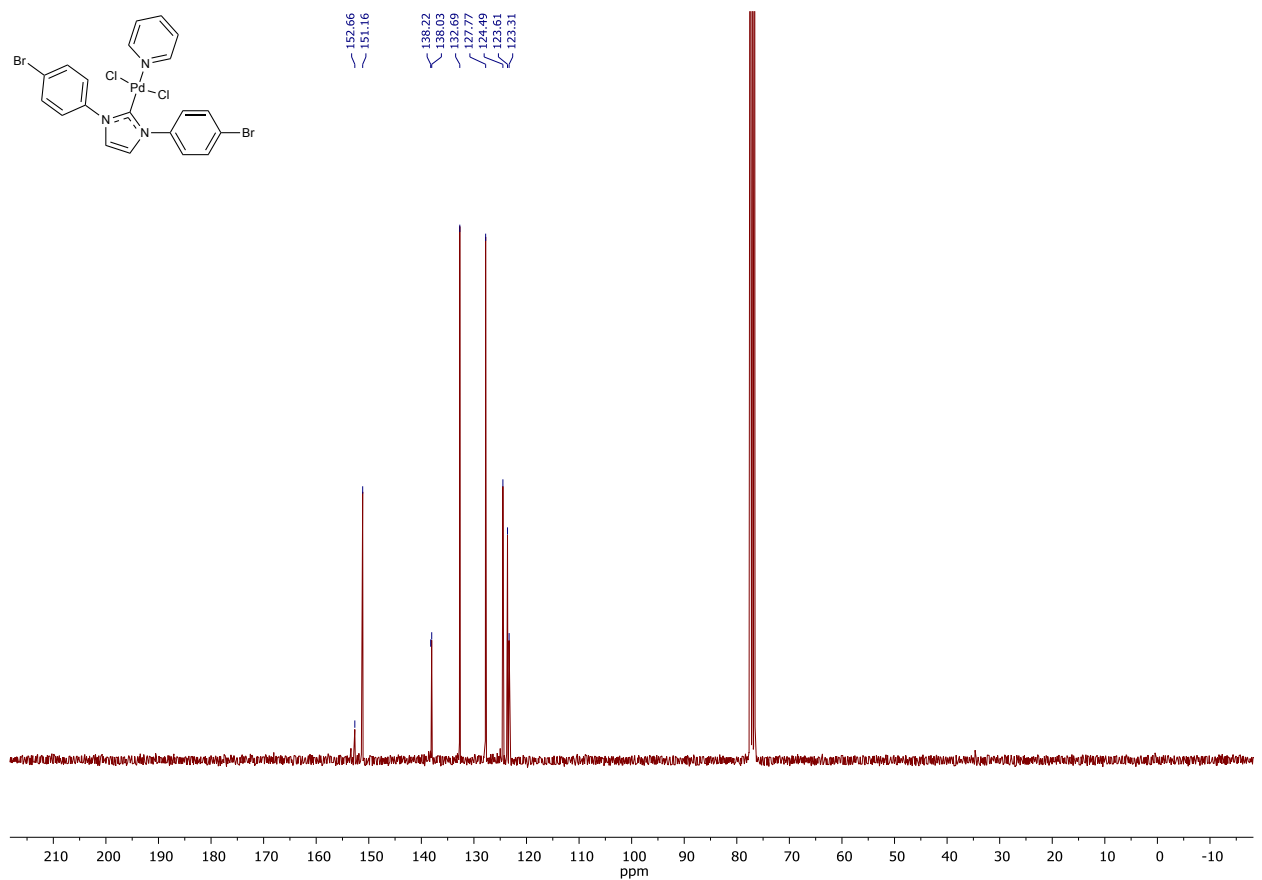


**Figure S41**. $^{13}$C{$^1$H} NMR spectrum of **3i**. Solvent: CDCl$_3$, 75 MHz.
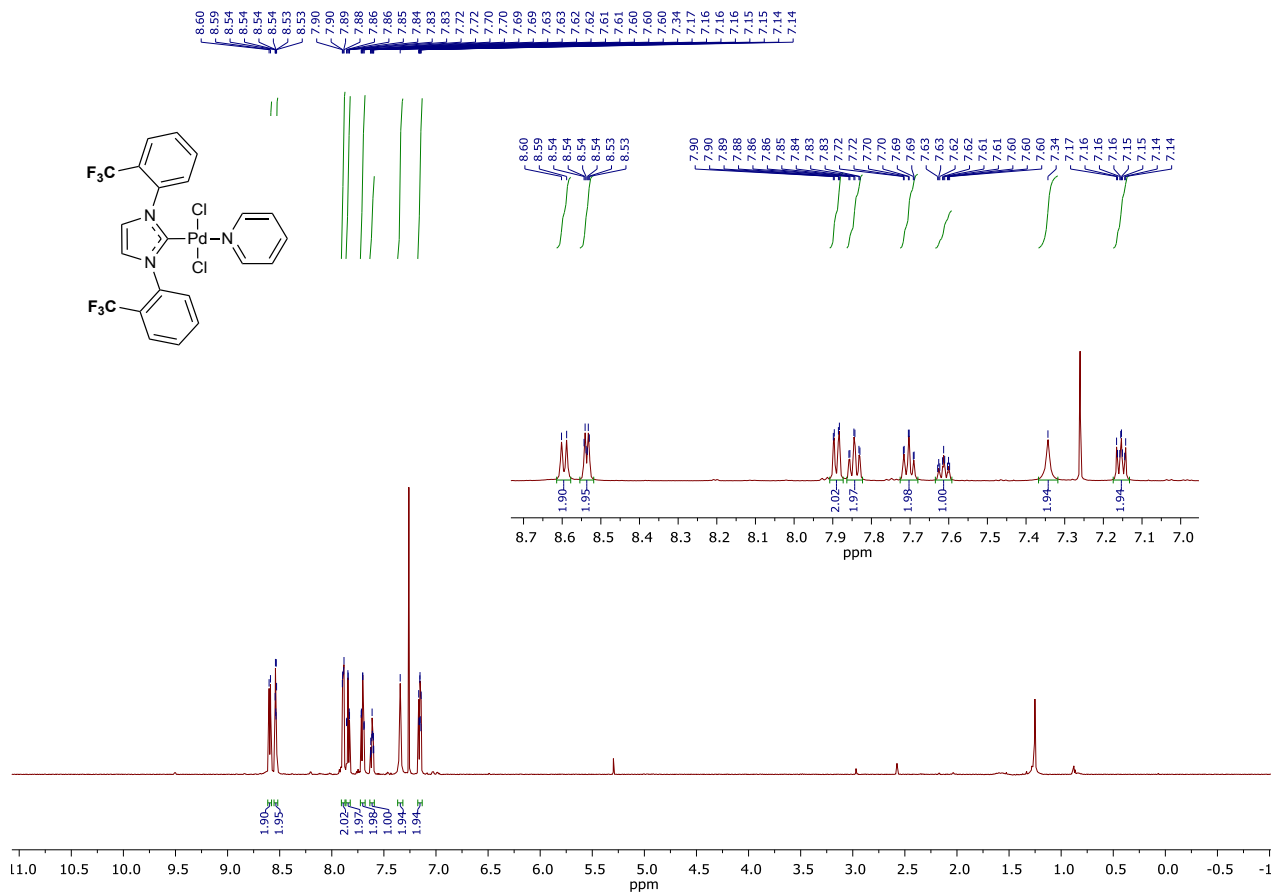
**Figure S42**. $^1H$ NMR spectrum of **3j**. Solvent: CDCl$_3$, 600 MHz.
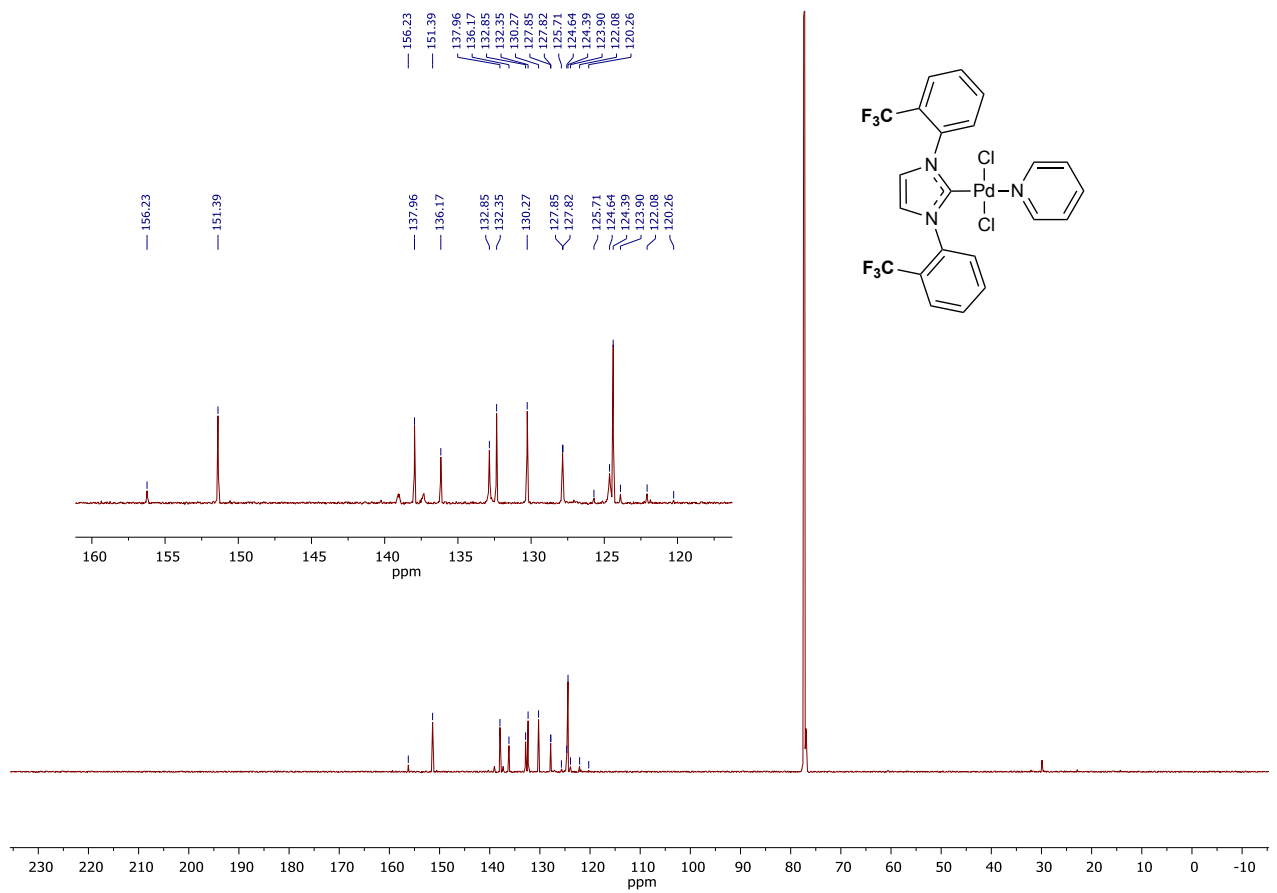


**Figure S43**. $^{13}C\{^1H\}$ NMR spectrum of **3j**. Solvent: CDCl$_3$, 151 MHz.
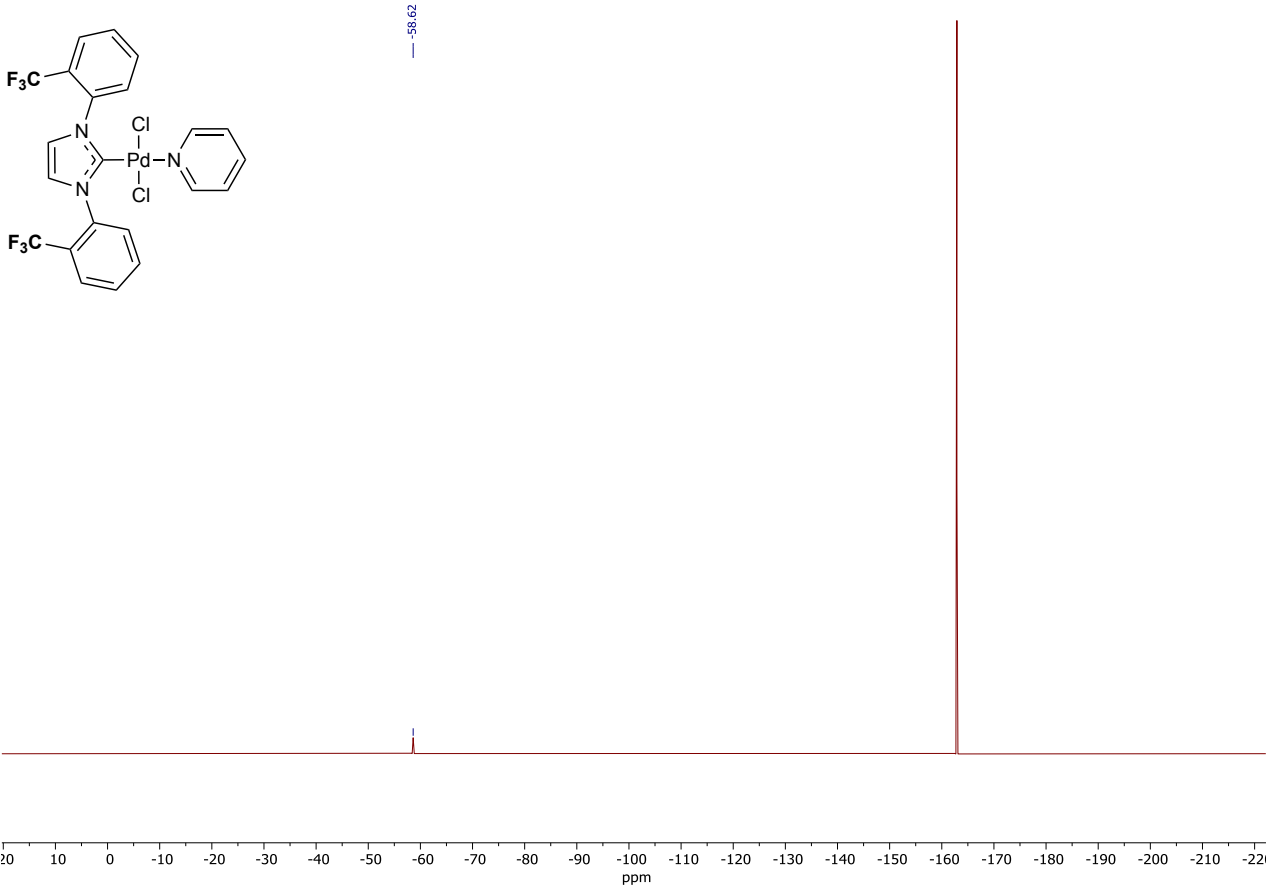
**Figure S44**. $^{19}F\{^1H\}$ NMR spectrum of **3j**. Solvent: CDCl$_3$, 282.4 MHz. Standard: C$_6$F$_6$ with respect to CFCl$_3$.
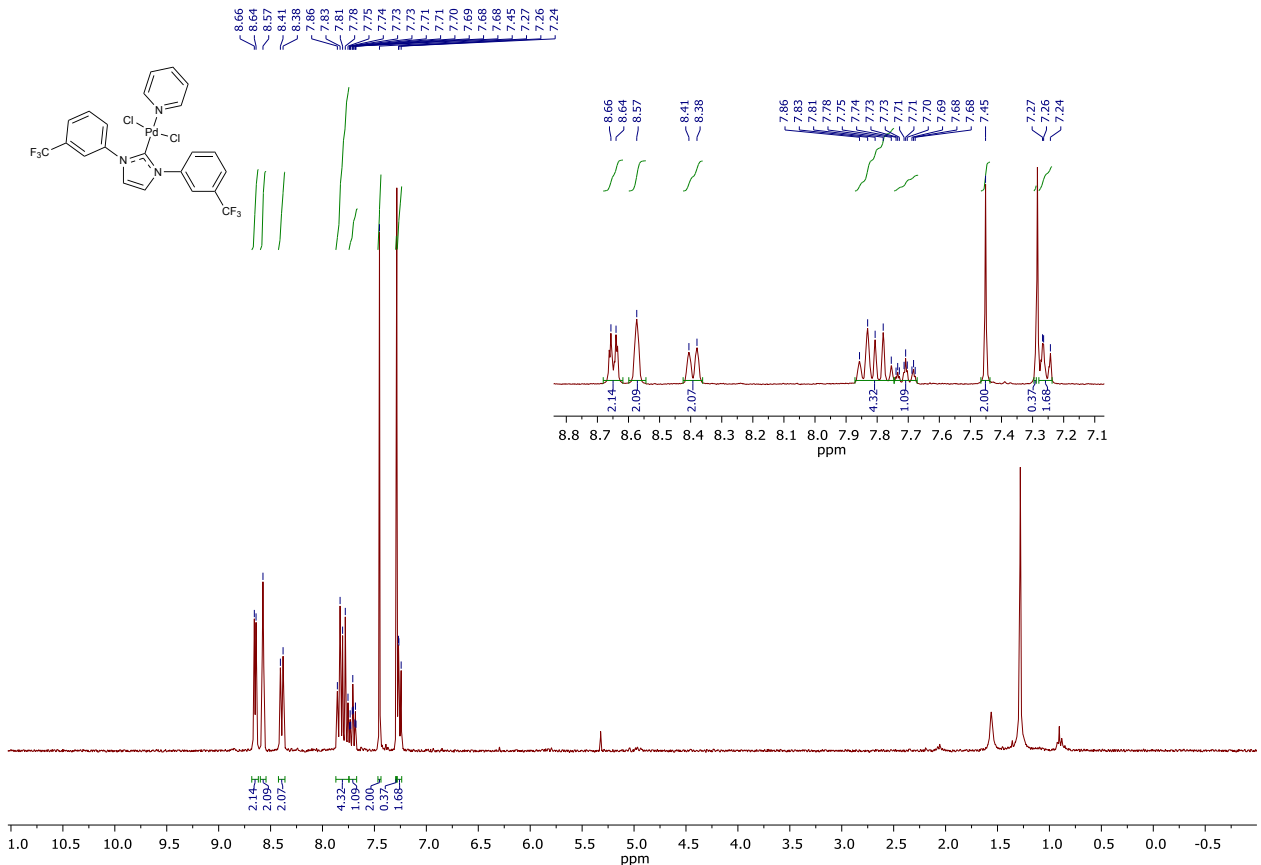


**Figure S45**. $^1H$ NMR spectrum of **3k**. Solvent: CDCl$_3$, 300 MHz.
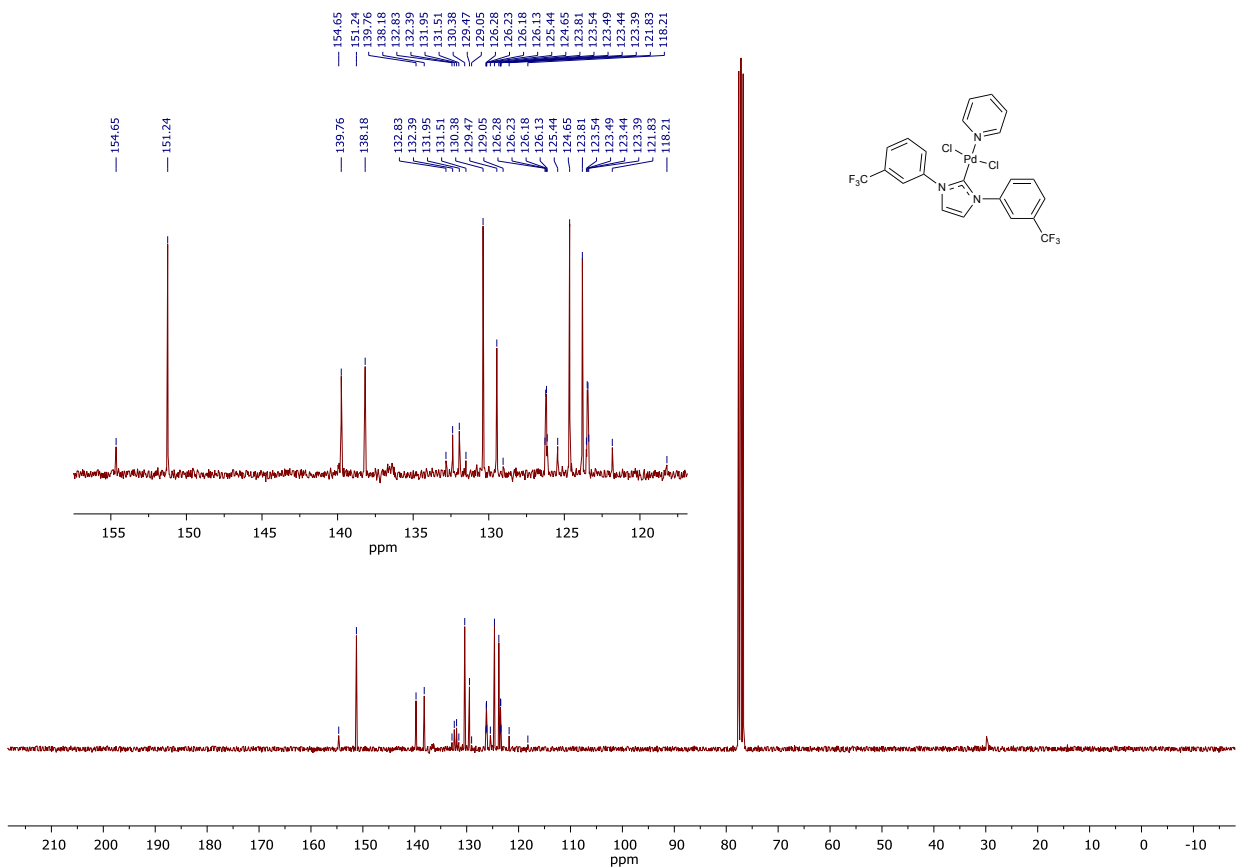
**Figure S46.** $^{13}C\{^1H\}$ NMR spectrum of **3k**. Solvent: $CDCl_3$, 75 MHz.
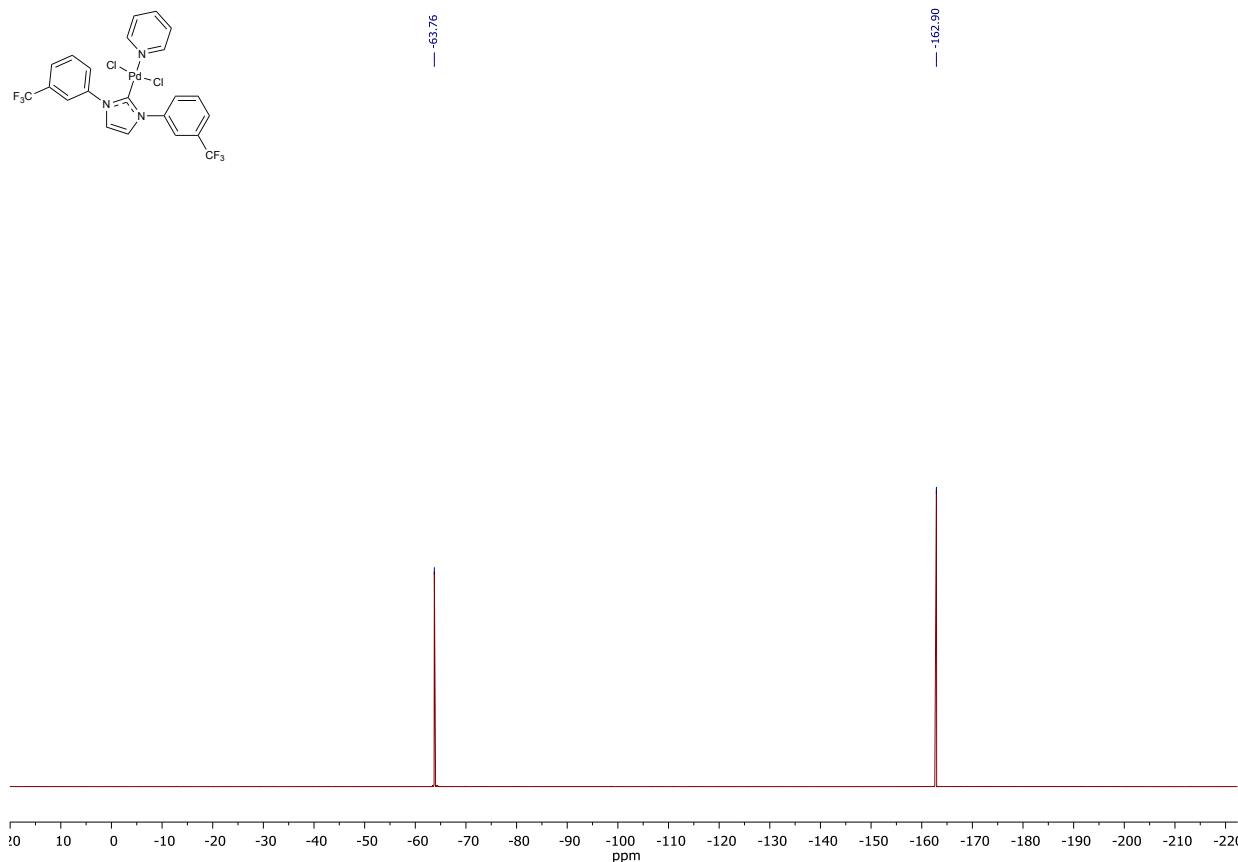


**Figure S47.** $^{19}F\{^1H\}$ NMR spectrum of **3k**. Solvent: $CDCl_3$, 282.4 MHz. Standard: $C_6F_6$ with respect to $CFCl_3$.
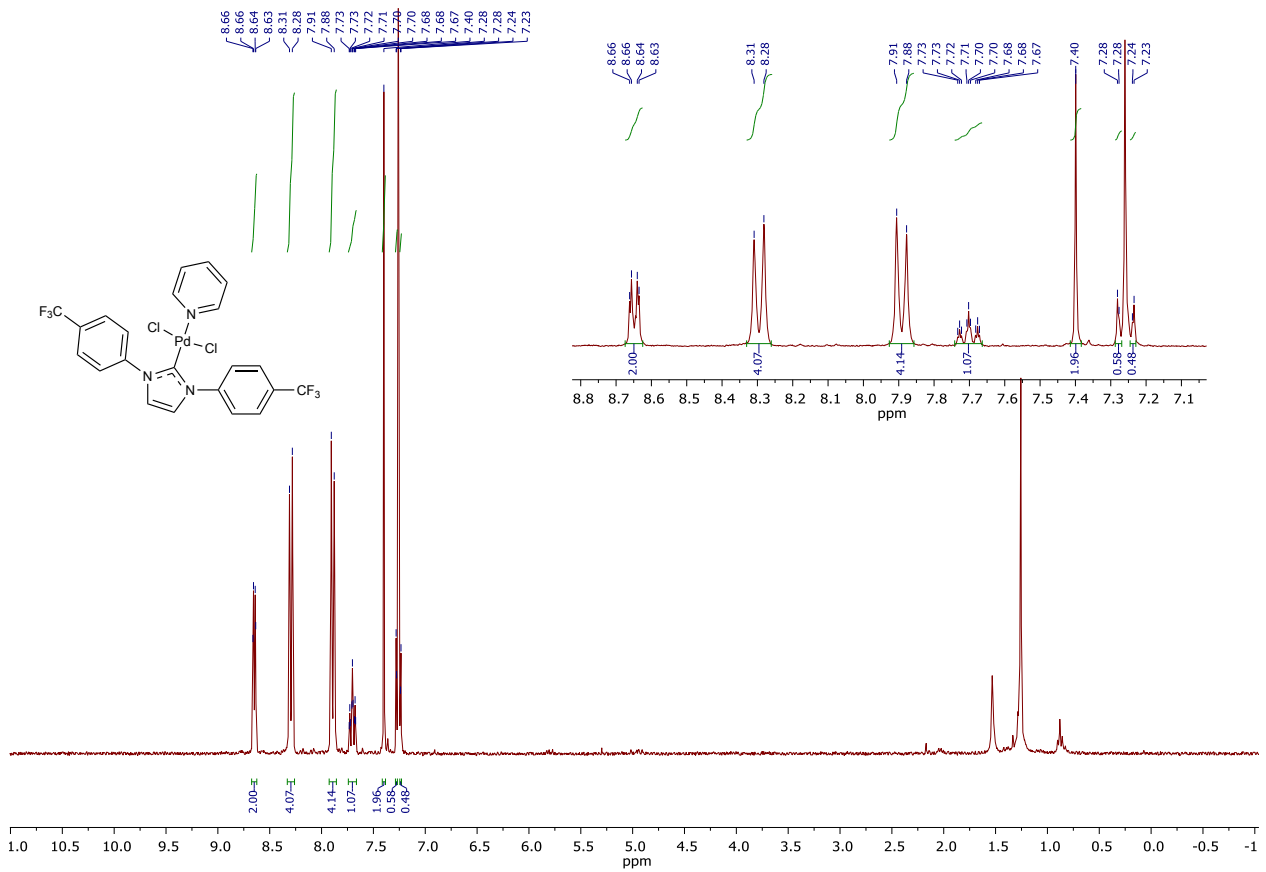
**Figure S48**. $^{1}$H NMR spectrum of **3l**. Solvent: CDCl$_3$, 300 MHz.
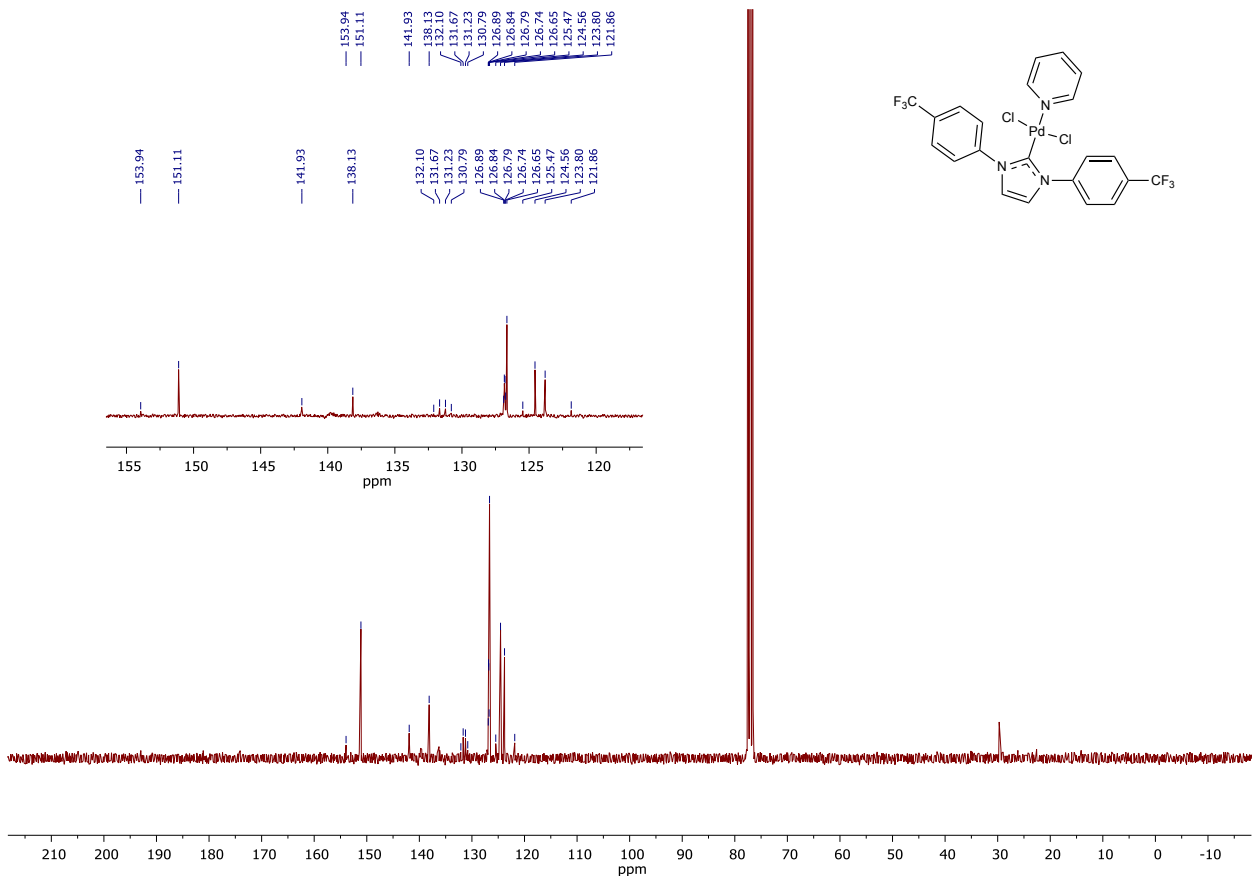


**Figure S49**. $^{13}$C{$^{1}$H} NMR spectrum of **3l**. Solvent: CDCl$_3$, 75 MHz.
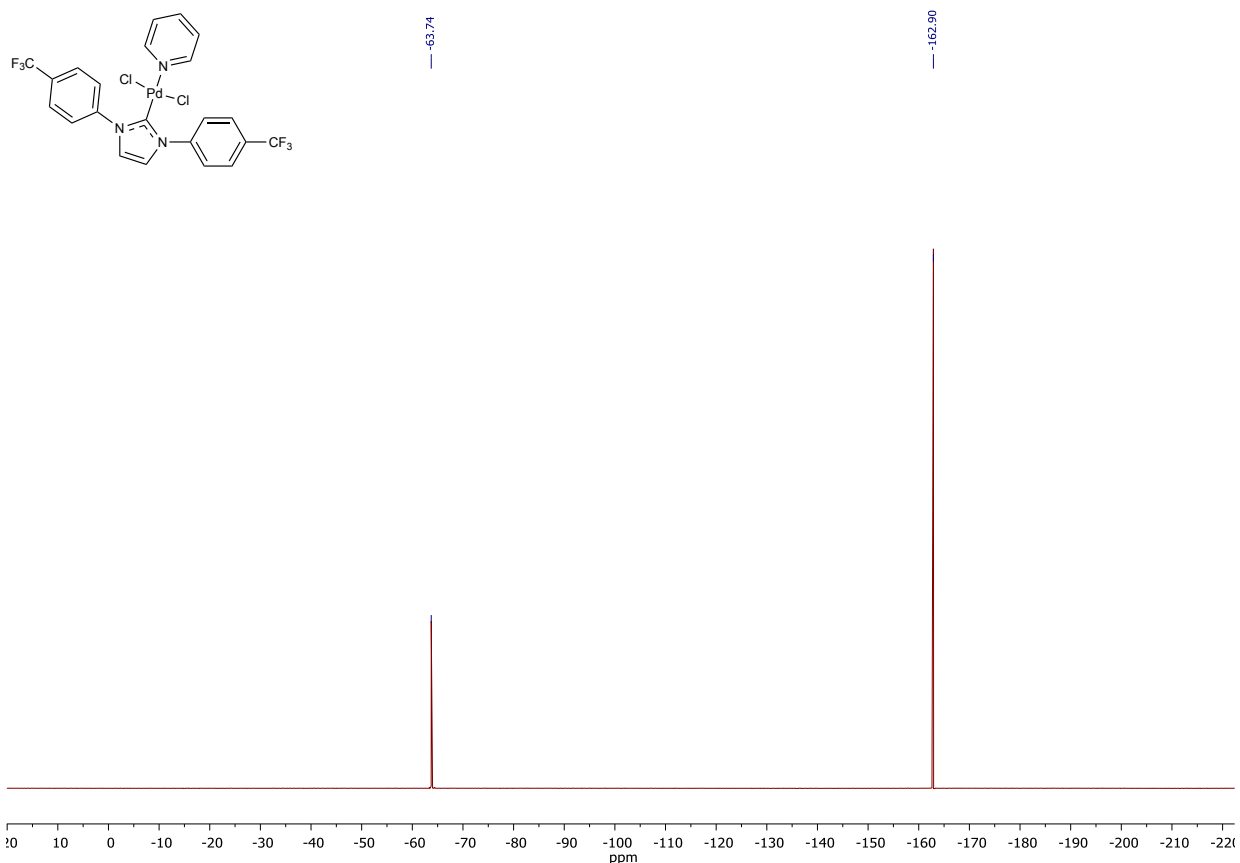
**Figure S50**. $^{19}F\{^{1}H\}$ NMR spectrum of **3l**. Solvent: CDCl$_3$, 282.4 MHz. Standard: C$_6$F$_6$ with respect to CFCl$_3$.

**ESI-HRMS spectra of the obtained compounds.**
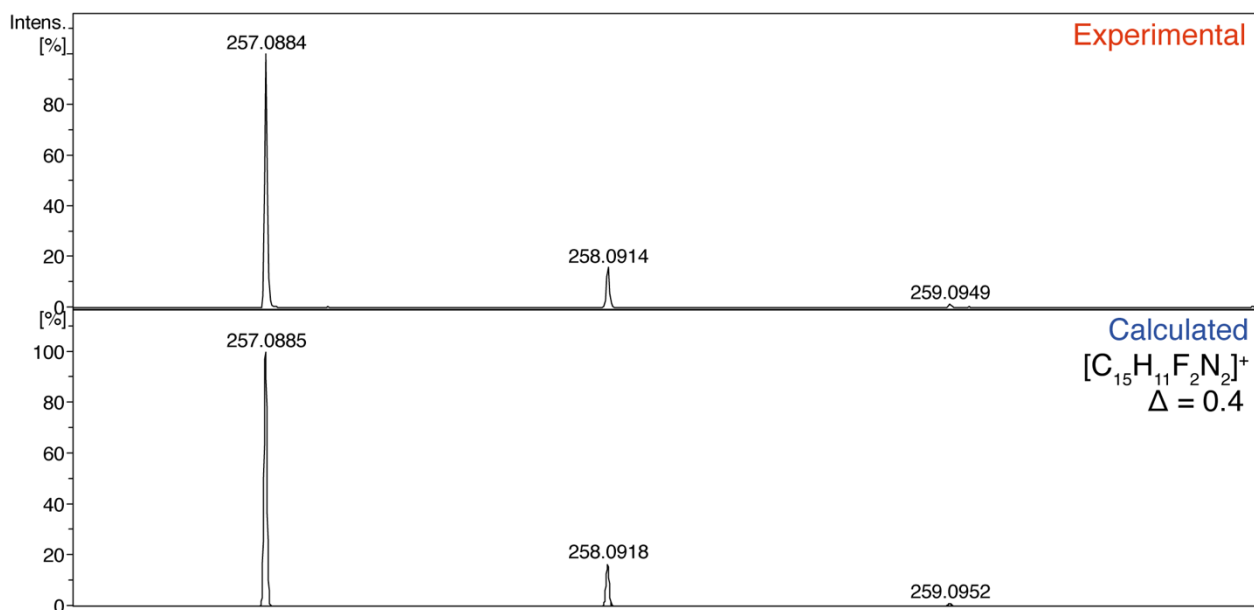


**Figure S51**. Experimental and theoretical ESI-(+)HRMS spectrum of **2c** in CH$_3$CN solution: experimental peak [M+H]$^+$ = 257.0884 Da, calculated for C$_{15}$H$_{11}$F$_2$N$_2$ = 257.0885, $\Delta$ = 0.4 ppm.
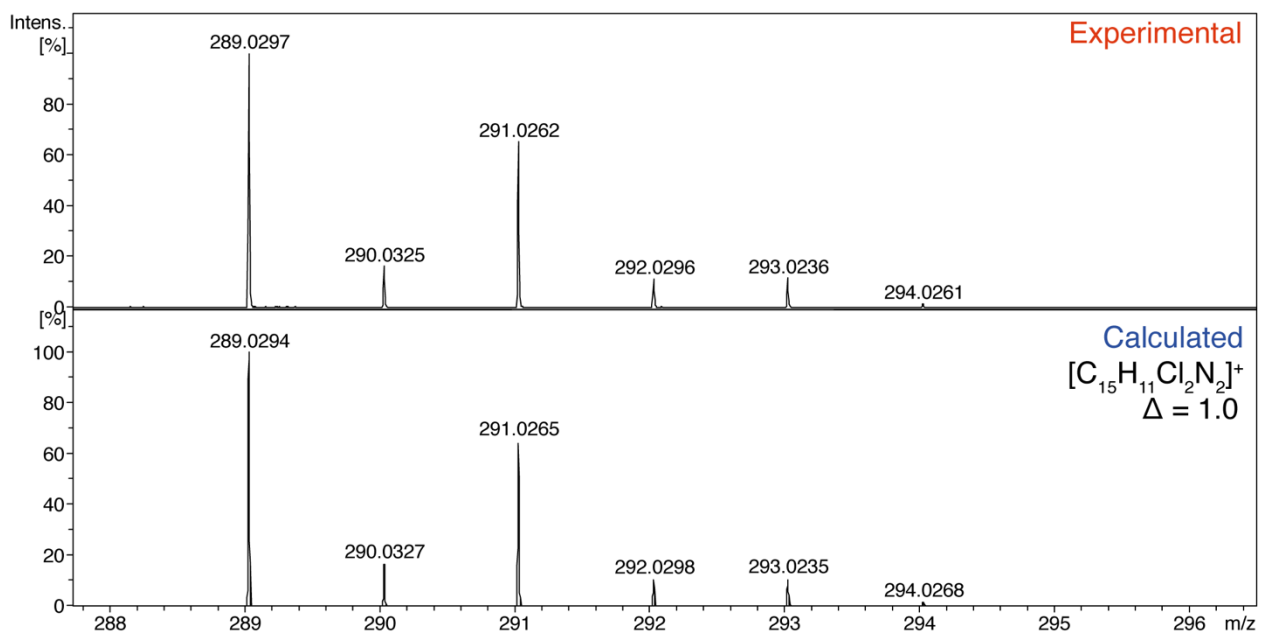
**Figure S52**. Experimental and theoretical ESI-(+)HRMS spectrum of **2d** in CH$_3$CN solution: experimental peak [M+H]$^+$ = 289.0297 Da, calculated for C$_{15}$H$_{11}$Cl$_2$N$_2$ = 289.0294, $\Delta$ = 1.0 ppm.
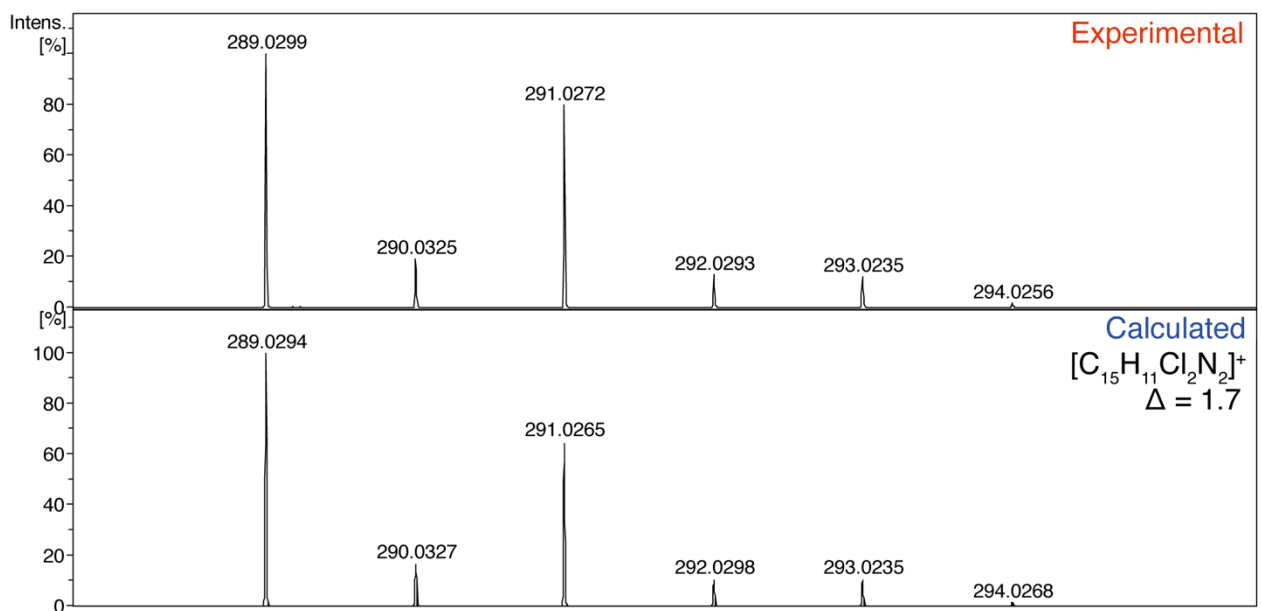


**Figure S53**. Experimental and theoretical ESI-(+)HRMS spectrum of **2e** in CH$_3$CN solution: experimental peak [M+H]$^+$ = 289.0299 Da, calculated for C$_{15}$H$_{11}$Cl$_2$N$_2$ = 289.0294, $\Delta$ = 1.7 ppm.
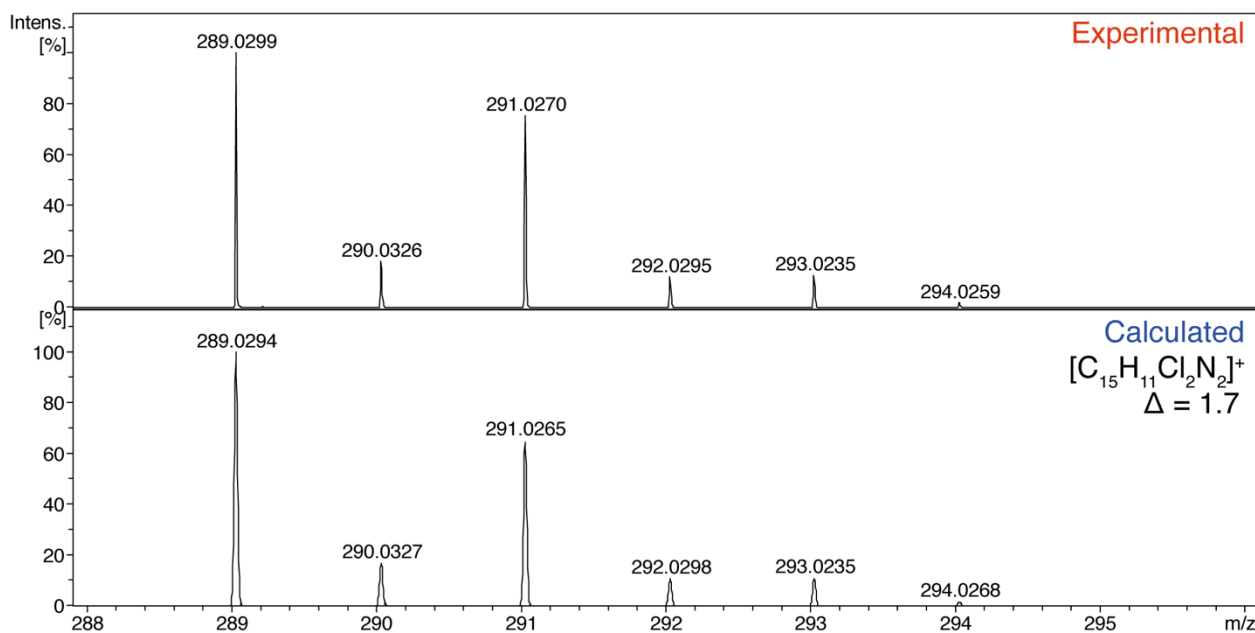
**Figure S54** Experimental and theoretical ESI-(+)HRMS spectrum of **2f** in CH$_3$CN solution: experimental peak [M+H]$^+$ = 289.0299 Da, calculated for C$_{15}$H$_{11}$Cl$_2$N$_2$ = 289.0294, $\Delta$ = 1.7 ppm.
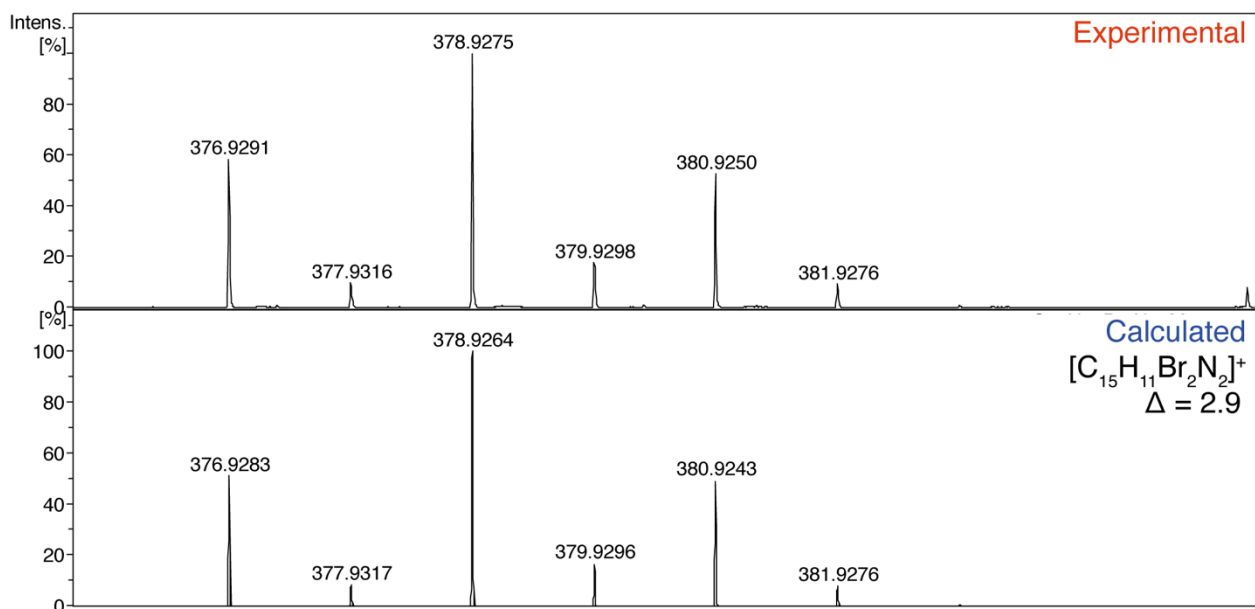


**Figure S55**. Experimental and theoretical ESI-(+)HRMS spectrum of **2g** in CH$_3$CN solution: experimental peak [M+H]$^+$ = 378.9275 Da, calculated for C$_{15}$H$_{11}$Br$_2$N$_2$ = 378.9264, $\Delta$ = 2.9 ppm.
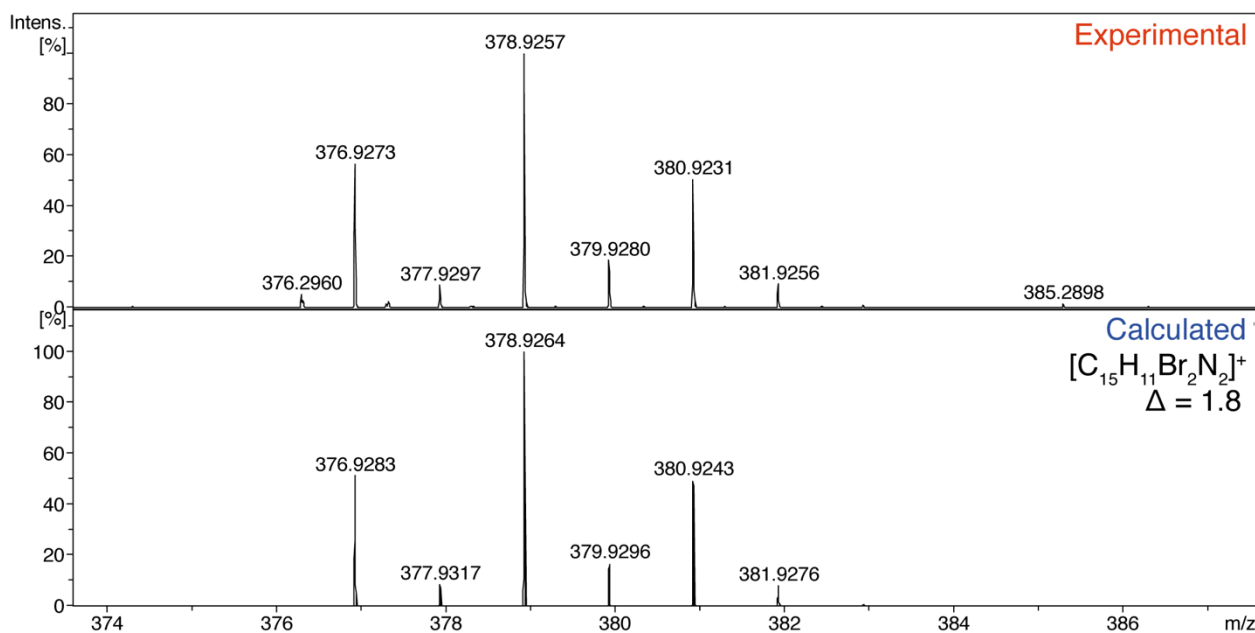
**Figure S56**. Experimental and theoretical ESI-(+)HRMS spectrum of **2h** in CH$_3$CN solution: experimental peak [M+H]$^+$ = 378.9257 Da, calculated for C$_{15}$H$_{11}$Br$_2$N$_2$ = 378.9264, Δ = 1.8 ppm.
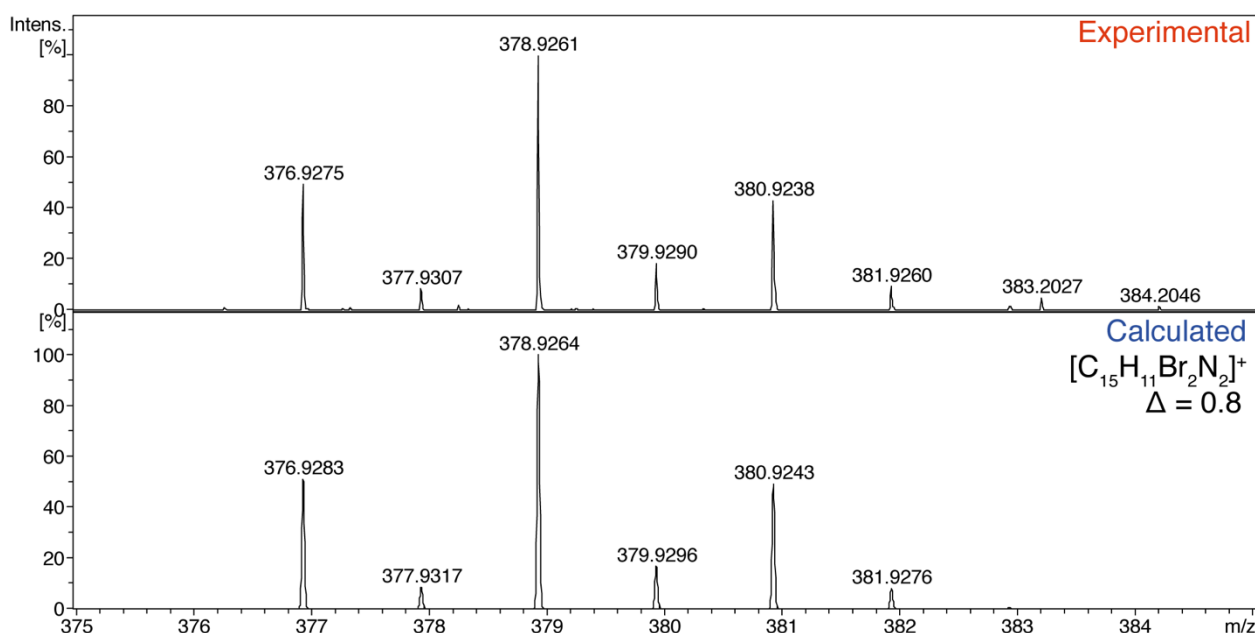


**Figure S57**. Experimental and theoretical ESI-(+)HRMS spectrum of **2i** in CH$_3$CN solution: experimental peak [M+H]$^+$ = 378.9261 Da, calculated for C$_{15}$H$_{11}$Br$_2$N$_2$ = 378.9264, Δ = 0.8 ppm.
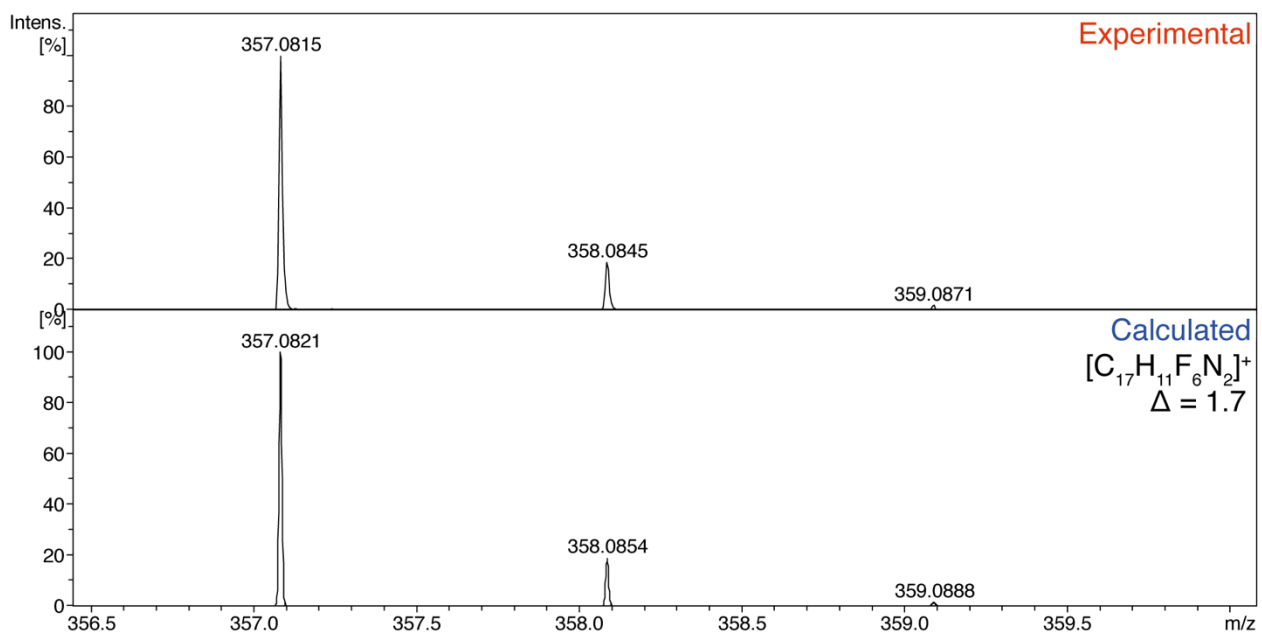
**Figure S58**. Experimental and theoretical ESI-(+)HRMS spectrum of **2j** in CH$_3$CN solution: experimental peak [M+H]$^+$ = 357.0815 Da, calculated for C$_{17}$H$_{11}$F$_6$N$_2$ = 357.0821, $\Delta$ = 1.7 ppm.
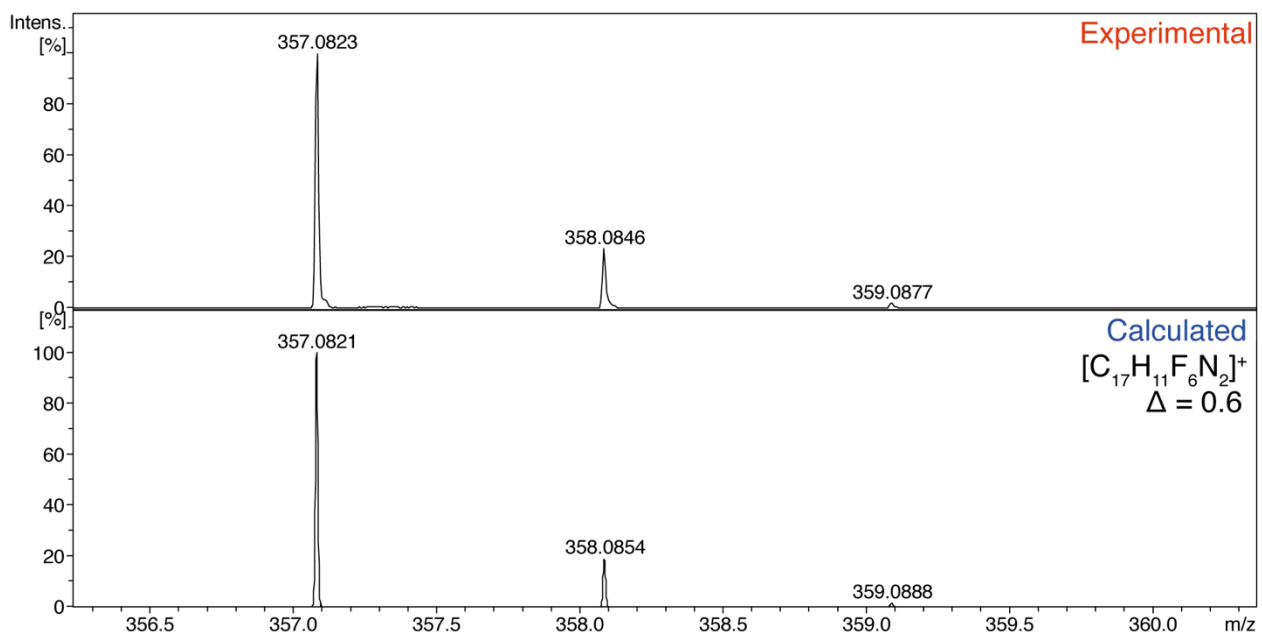


**Figure S59**. Experimental and theoretical ESI-(+)HRMS spectrum of **2k** in CH$_3$CN solution: experimental peak [M+H]$^+$ = 357.0823 Da, calculated for C$_{17}$H$_{11}$F$_6$N$_2$ = 357.0821, $\Delta$ = 0.6 ppm.
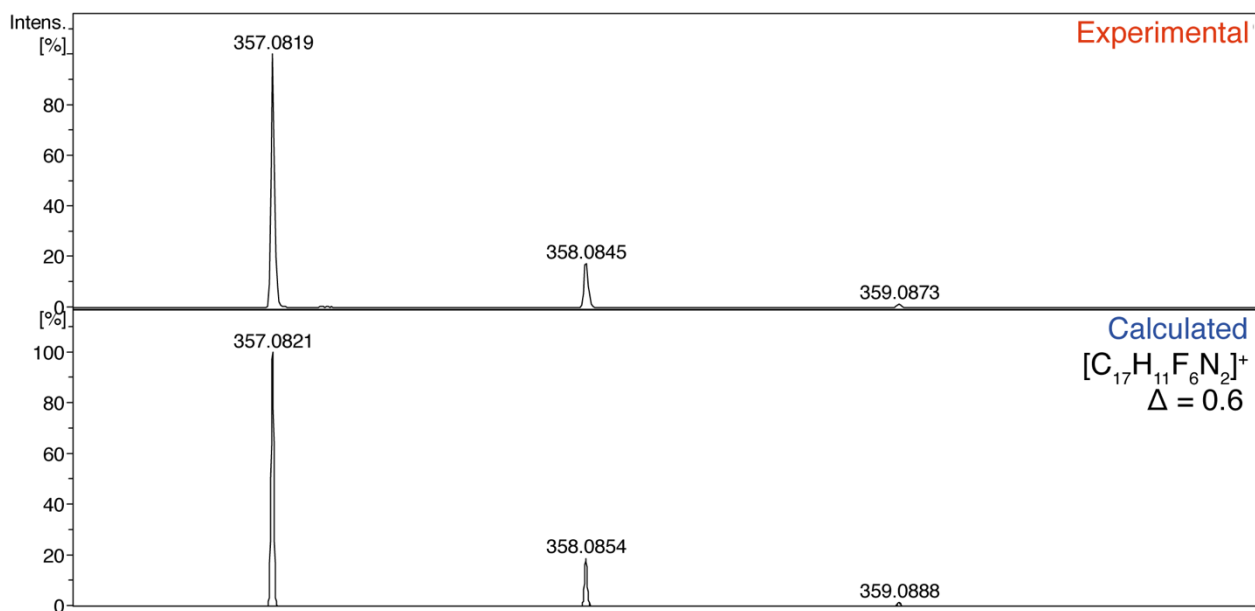
**Figure S60**. Experimental and theoretical ESI-(+)HRMS spectrum of **2l** in $CH_3CN$ solution: experimental peak $[M+H]^+ = 357.0819$ Da, calculated for $C_{17}H_{11}F_6N_2 = 357.0821$, $\Delta = 0.6$ ppm.
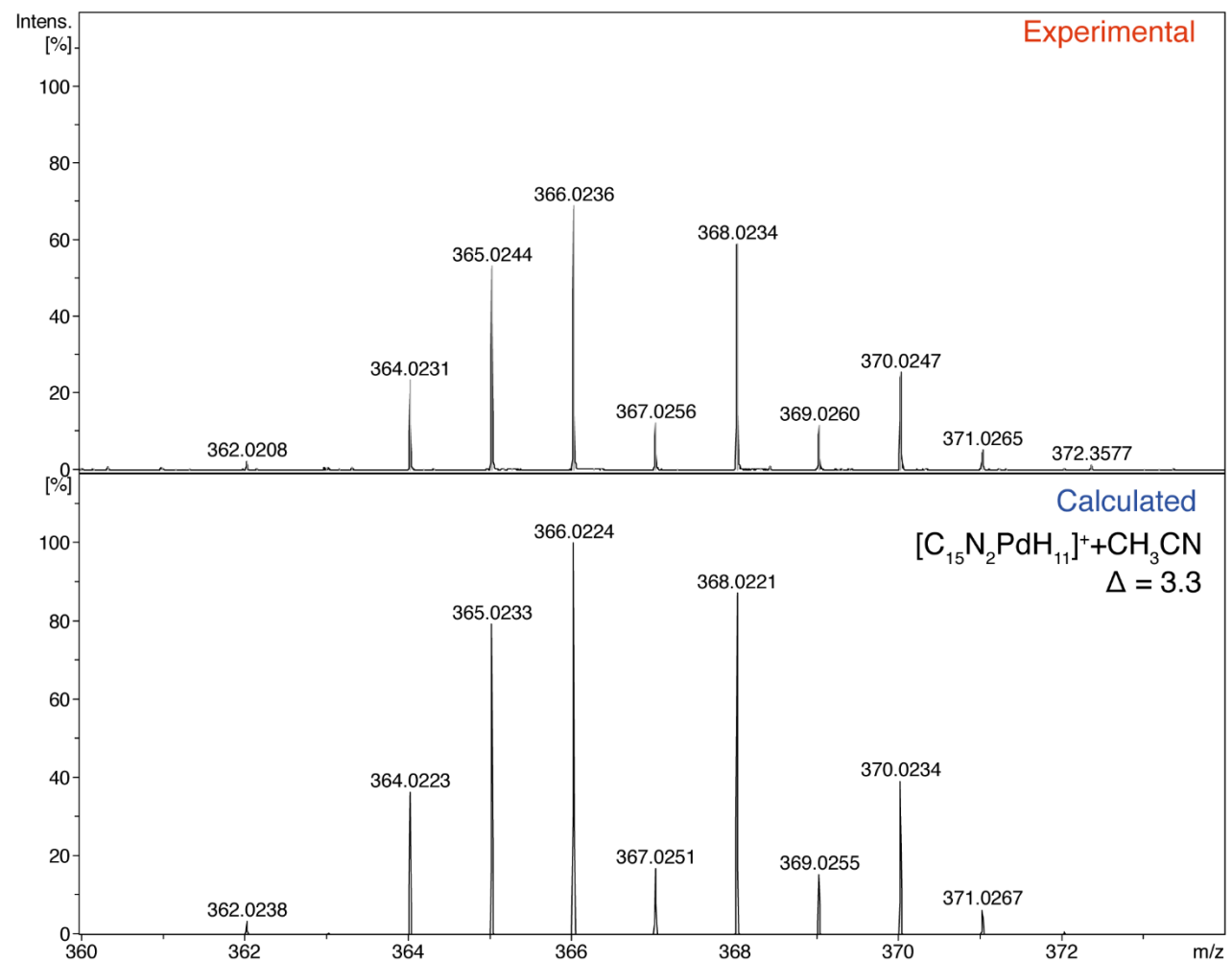


**Figure S61**. Experimental and theoretical ESI-(+)HRMS spectrum of **3** in $CH_3CN$ solution: experimental peak $[M-2Cl-C_6H_5N+CH_3CN]^+ = 366.0236$ Da, calculated for $C_{15}H_{11}N_2PdCH_3CN = 366.0224$, $\Delta = 3.3$ ppm.
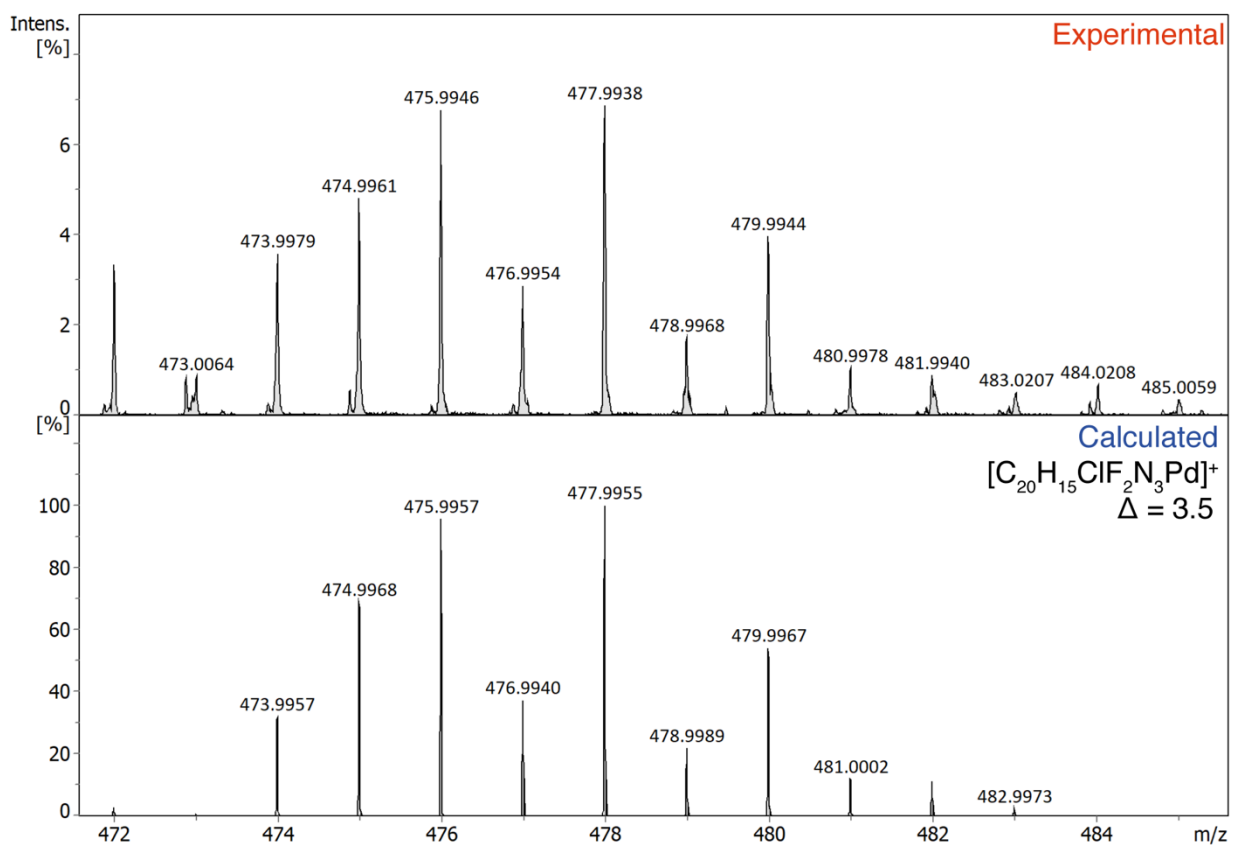
**Figure S62**. Experimental and theoretical ESI-(+)HRMS spectrum of **3c** in $CH_3CN$ solution: experimental peak $[M]^+$ = 477.9938 Da, calculated for $C_{20}H_{15}ClF_2N_3Pd$ = 477.9955, $\Delta$ = 3.5 ppm.
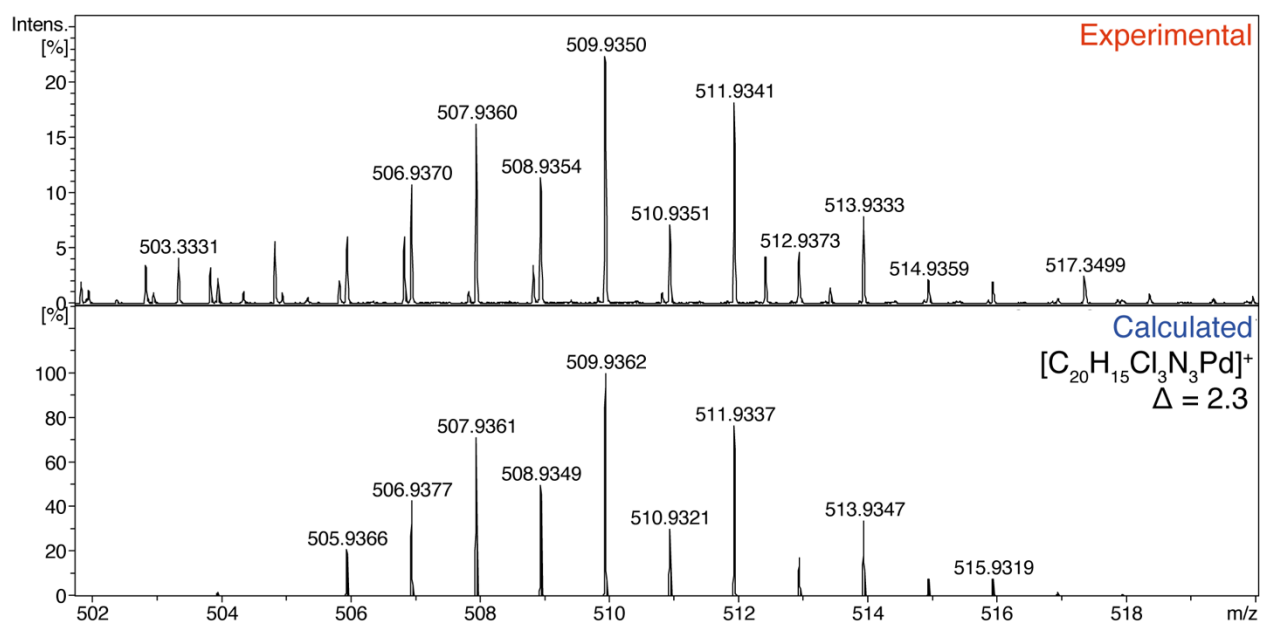


**Figure S63**. Experimental and theoretical ESI-(+)HRMS spectrum of **3d** in $CH_3CN$ solution: experimental peak $[M]^+$ = 509.9350 Da, calculated for $C_{20}H_{15}Cl_3N_3Pd$ = 509.9362, $\Delta$ = 2.3 ppm.
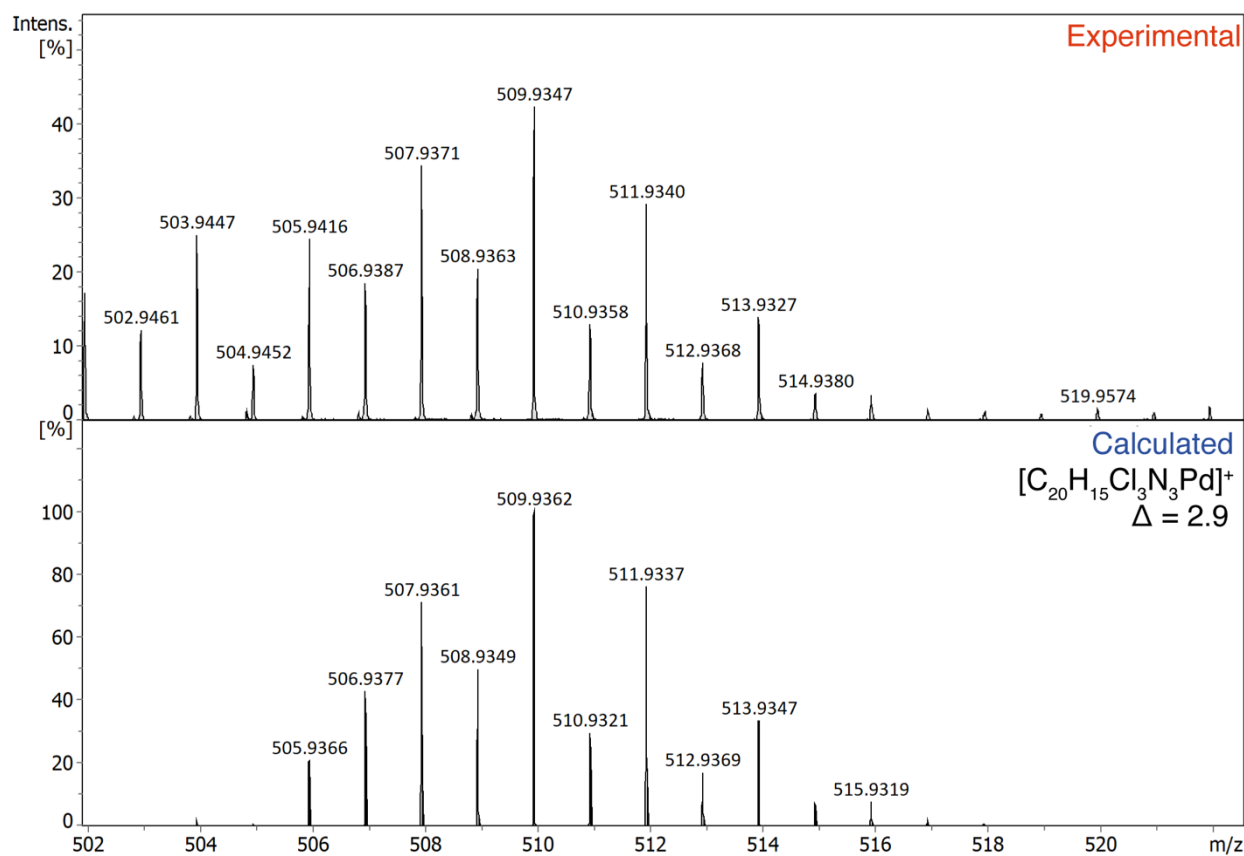
**Figure S64**. Experimental and theoretical ESI-(+)HRMS spectrum of **3e** in $CH_3CN$ solution: experimental peak $[M]^+ = 509.9347$ Da, calculated for $C_{20}H_{15}Cl_3N_3Pd = 509.9362$, $\Delta = 2.9$ ppm.
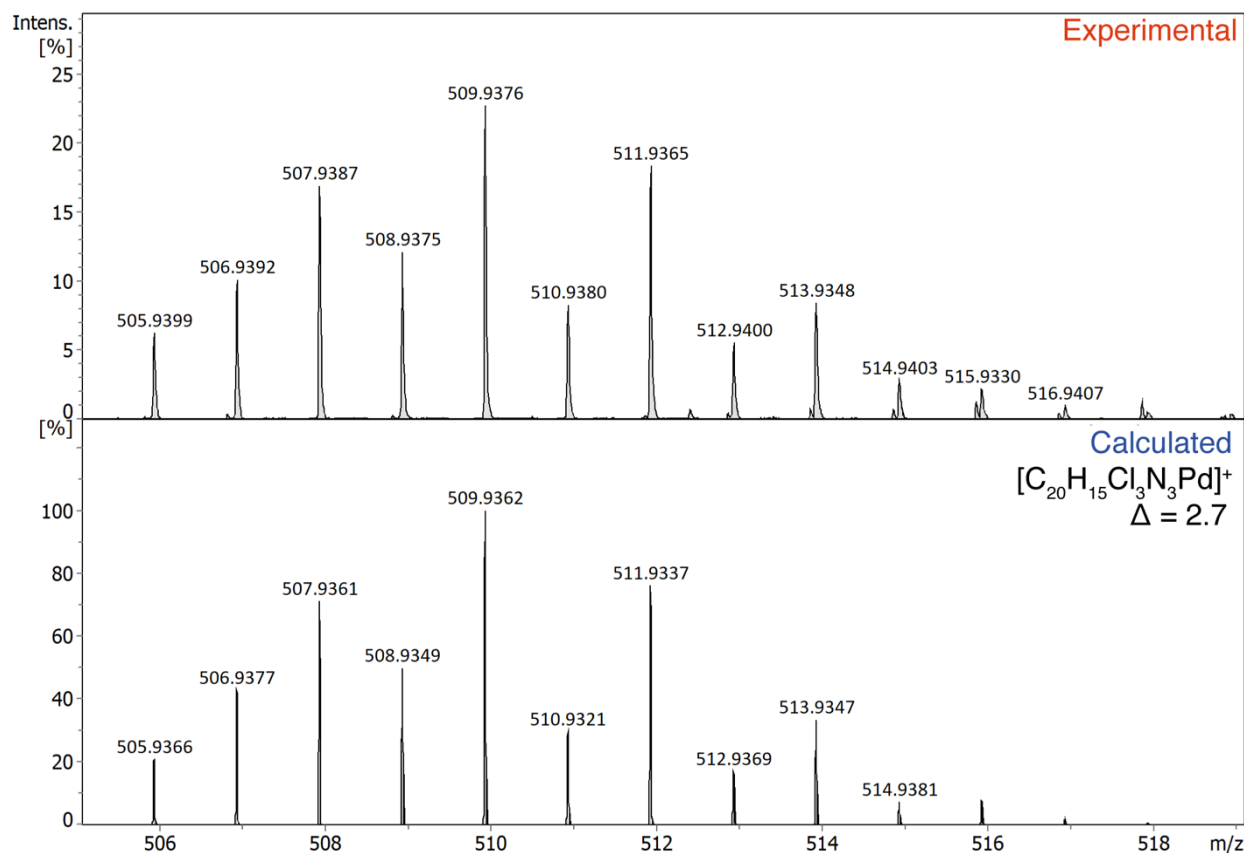


**Figure S65**. Experimental and theoretical ESI-(+)HRMS spectrum of **3f** in $CH_3CN$ solution: experimental peak $[M]^+ = 509.9376$ Da, calculated for $C_{20}H_{15}Cl_3N_3Pd = 509.9362$, $\Delta = 2.7$ ppm.

36
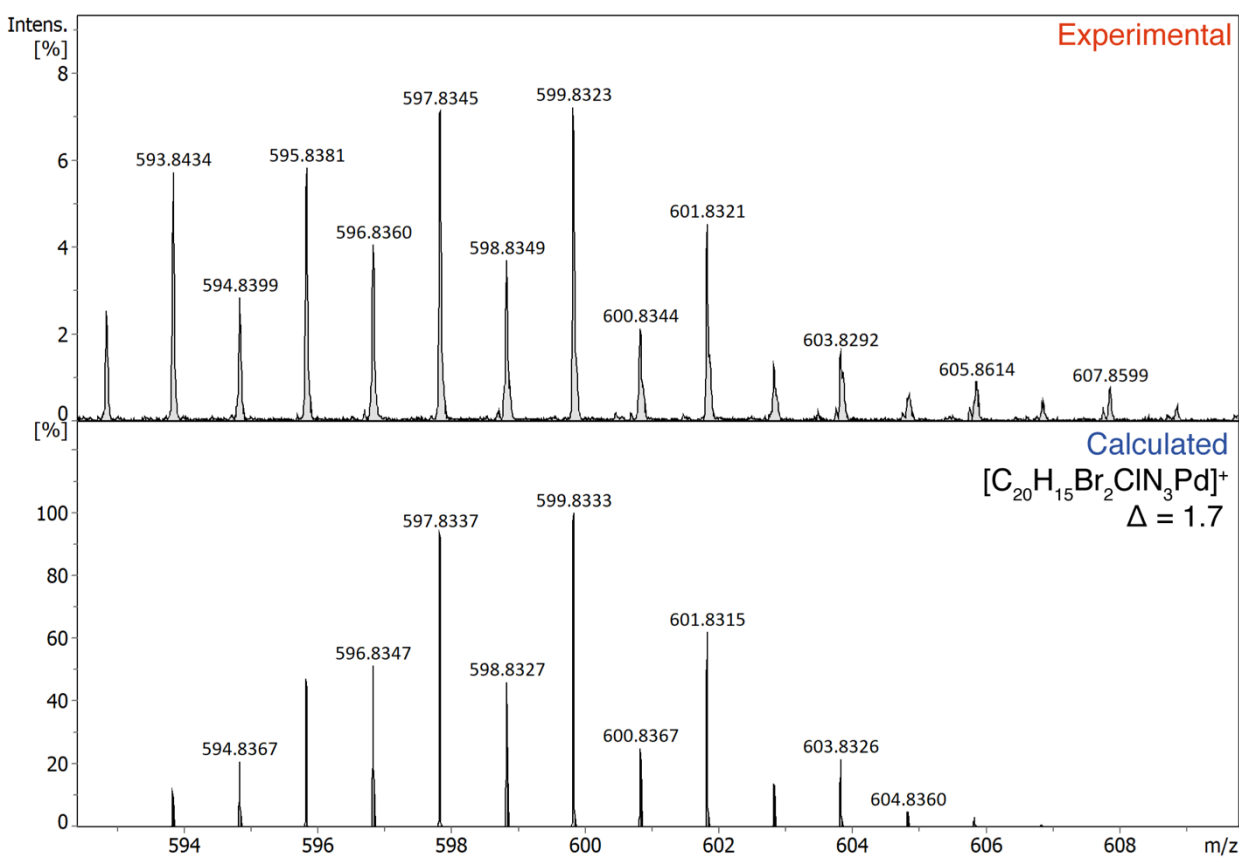
**Figure S66**. Experimental and theoretical ESI-(+)HRMS spectrum of **3g** in CH$_3$CN solution: experimental peak [M]$^+$ = 599.8323 Da, calculated for C$_{20}$H$_{15}$Br$_2$ClN$_3$Pd = 599.8333, Δ = 1.7 ppm.
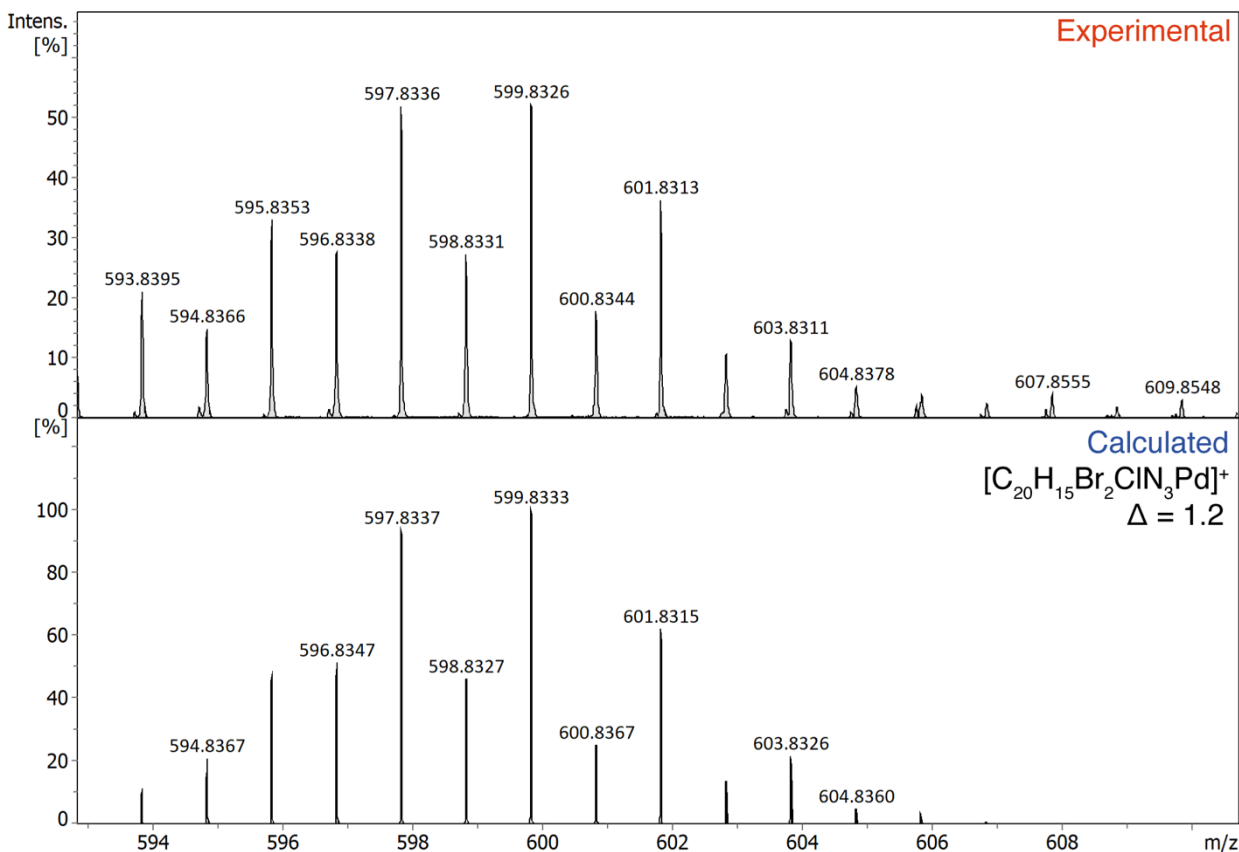


**Figure S67**. Experimental and theoretical ESI-(+)HRMS spectrum of **3h** in CH$_3$CN solution: experimental peak [M]$^+$ = 599.8326 Da, calculated for C$_{20}$H$_{15}$Br$_2$ClN$_3$Pd = 599.8333, Δ = 1.2 ppm.
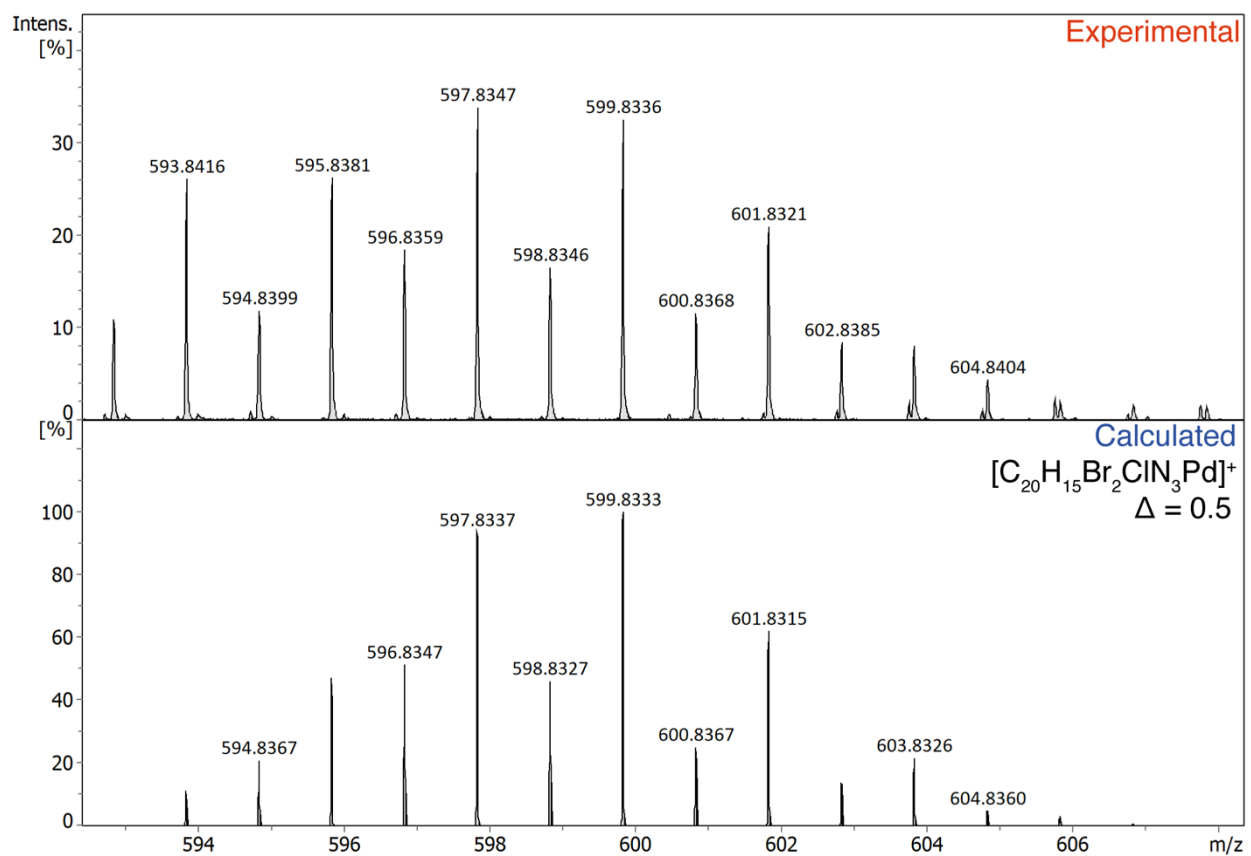
**Figure S68**. Experimental and theoretical ESI-(+)HRMS spectrum of **3i** in $CH_3CN$ solution: experimental peak $[M]^+ = 599.8336$ Da, calculated for $C_{20}H_{15}Br_2ClN_3Pd = 599.8333$, $\Delta = 0.5$ ppm.
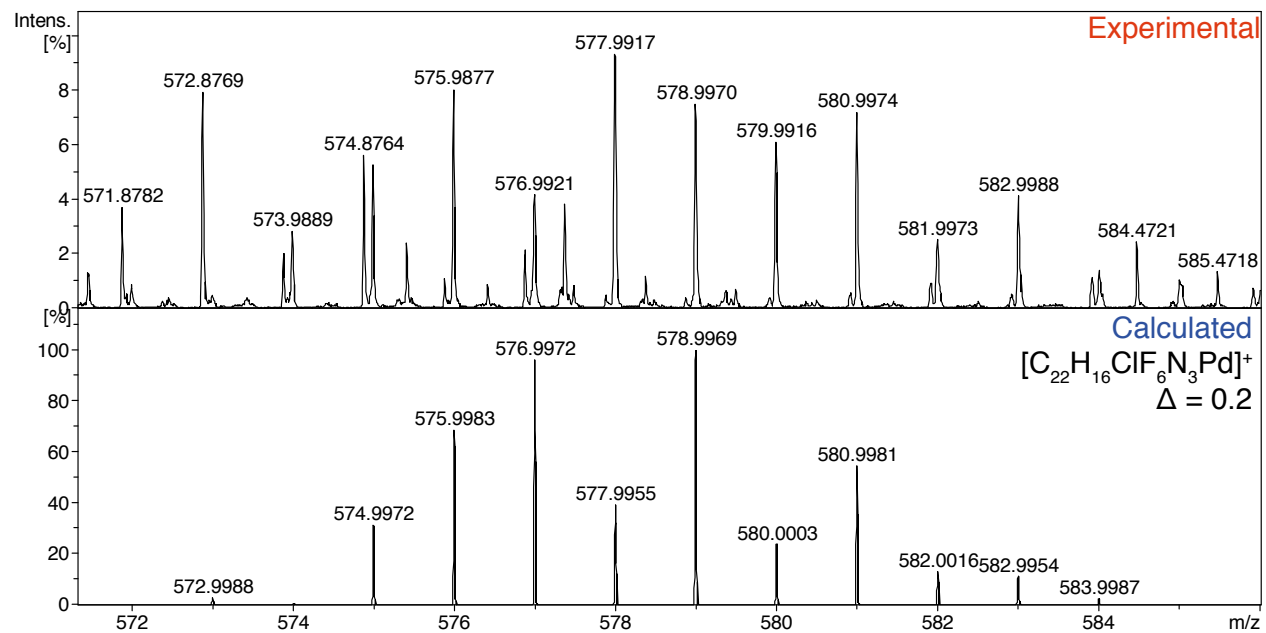


**Figure S69**. Experimental and theoretical ESI-(+)HRMS spectrum of **3j** in $CH_3CN$ solution: experimental peak $[M + H]^+$ $578.9970 =$ Da, calculated for $C_{22}H_{16}ClF_6N_3Pd = 578.9969$, $\Delta = 0.2$ ppm.
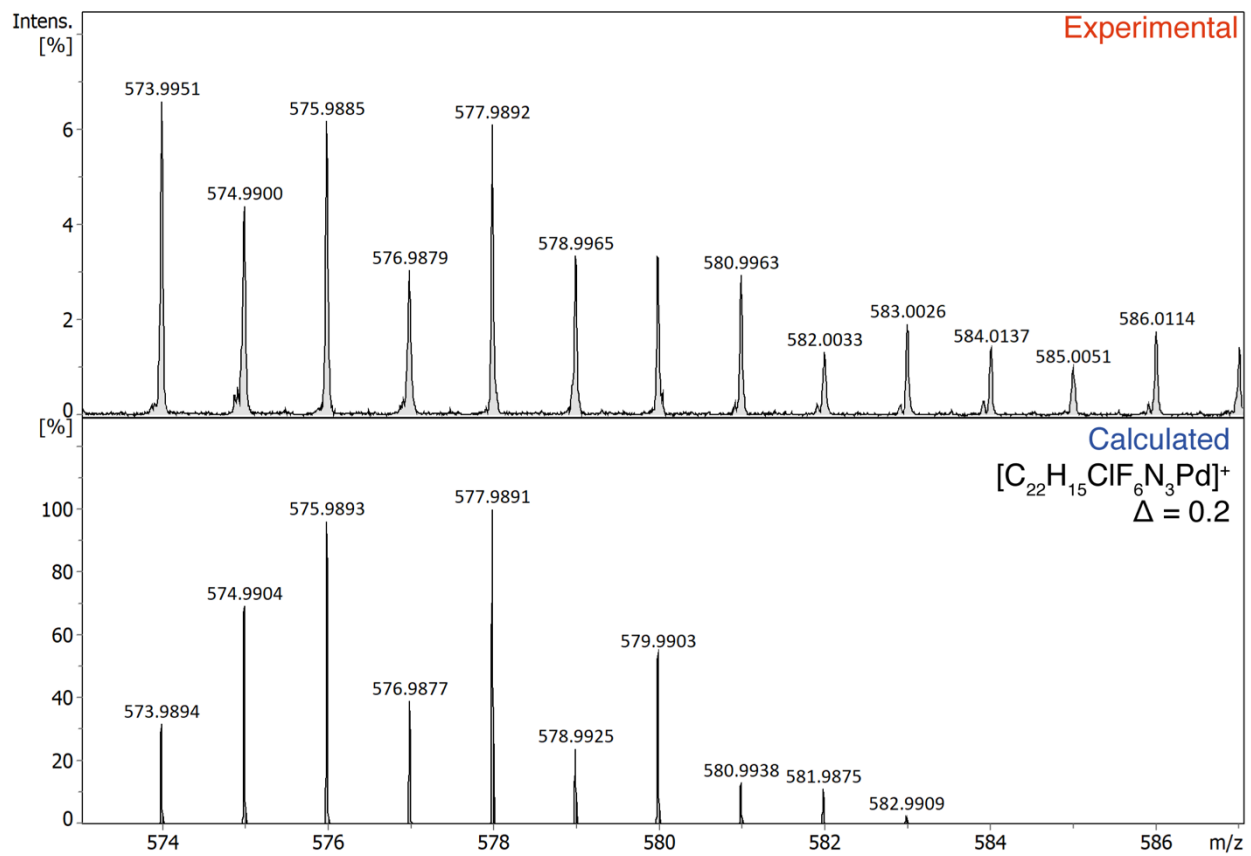
**Figure S70**. Experimental and theoretical ESI-(+)HRMS spectrum of **3k** in CH$_3$CN solution: experimental peak $[M]^+$ = 577.9892 Da, calculated for C$_{22}$H$_{15}$ClF$_6$N$_3$Pd = 577.9891, $\Delta$ = 0.2 ppm.
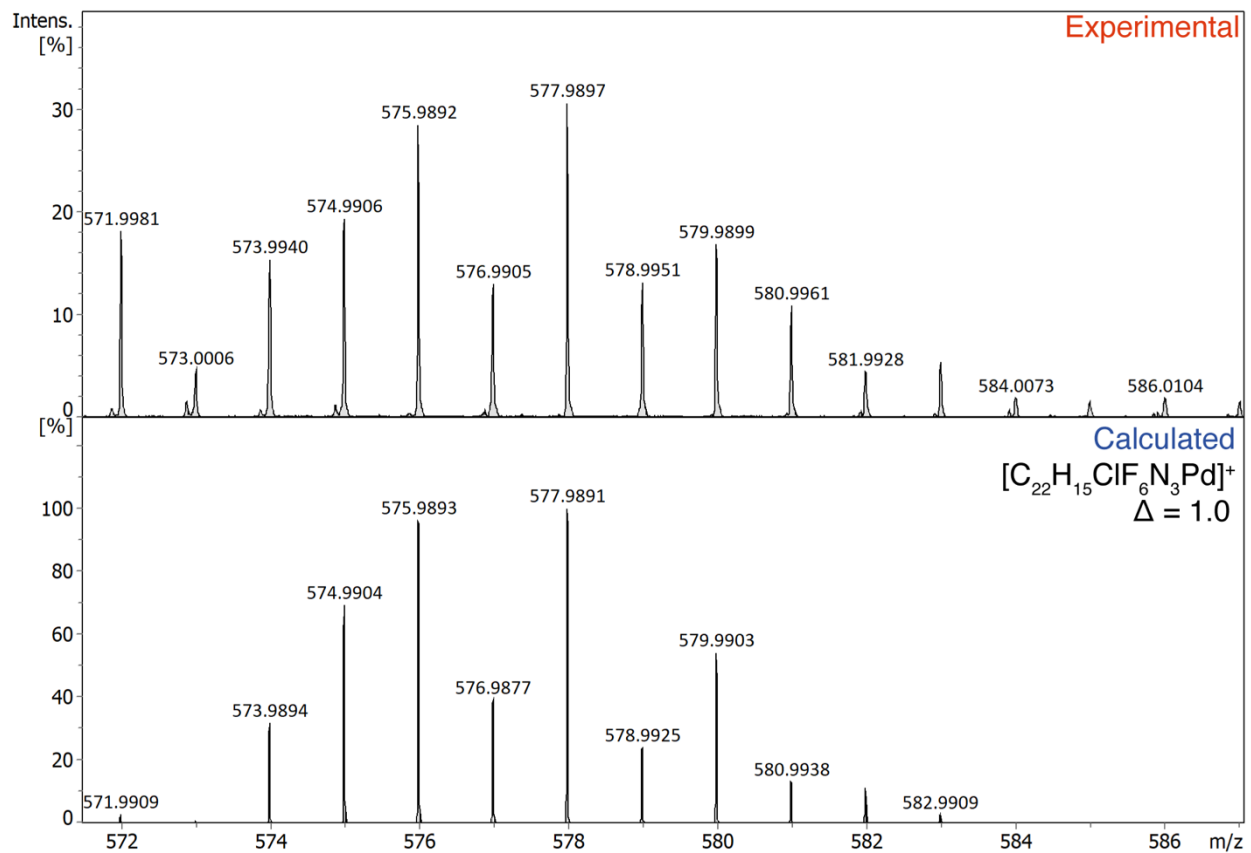


**Figure S71**. Experimental and theoretical ESI-(+)HRMS spectrum of **3l** in CH$_3$CN solution: experimental peak $[M]^+$ = 577.9897 Da, calculated for C$_{22}$H$_{15}$ClF$_6$N$_3$Pd = 577.9891, $\Delta$ = 1.0 ppm.

39

**X-ray crystallographic data and refinement details**

X-ray diffraction data for **3, 3d**, **3e**, **3g, 3iA** and **3k** were collected at 100K on a Bruker Quest D8 diffractometer equipped with a Photon-III area-detector (shutterless φ- and ω-scan technique), using graphite-monochromatized Mo K$_\alpha$-radiation. The intensity data of collected reflections were integrated by the *SAINT* program.[1] Absorption correction based on measurements of equivalent reflections was carried out semi-empirically by multi-scan methods, using *SADABS* and *TWINABS*.[2] X-ray diffraction data for **3i**, **3j**, **3l** were collected at 100K on a Rigaku Synergy S diffractometer equipped with a HyPix6000HE area-detector (kappa geometry, shutterless ω-scan technique), using monochromatized Mo K$_\alpha$-radiation. The intensity data were integrated and corrected for absorption and decay by the CrysAlisPro program.[3] The *SHELXTL* program suite[4] for **3**, **3d**, **3e**, **3g**, **3iA**, **3k** and the *OLEX2* program[5] for **3i**, **3j** and **3l** were used for further calculations. The structures were solved by dual methods using *SHELXT*[6] and refined by the full-matrix least-squares method on on $F^2$ using *SHELXL-2018*.[7] Positions of all non-hydrogen atoms were found from the electron density-difference map; the atoms were refined with individual anisotropic displacement parameters. Hydrogen atoms in **3** and two hydrogen atoms belonging to the minor component of the disordered pyridine ligand in **3j** were placed in ideal calculated positions (d(C-H)=0.950Å) and refined as riding atoms with relative isotropic displacement parameters: $U_{iso}(H)=1.2U_{eq}(C)$. Positions of all other hydrogen atoms were found from the electron density-difference map; the H-atoms were refined with individual isotropic displacement parameters. Disorders in **3** and in **3j** were modeled by applying the same isotropic displacement parameters for disordered similar atoms (EADP); similar bond distances were restrained to be equal within 0.003Å. Disorder of the CF$_3$ group in **3k** and **3l** was modeled by applying the EADP *SHELXL* instruction; the C-F bond distances were restrained to be equal within 0.003Å and F..F distances were set to be equal within 0.03Å (SADI). The Cl/Br disorder in **3iA** was modeled by applying the same isotropic displacement parameters only.

Crystals **3e** and **3l** were refined as 2-component non-merohedral twins. The *SHELXTL* program suite[4] and the *Mercury* program[8] were used for molecular graphics herein and in the manuscript, correspondingly.

Crystal data, data collection and structure refinement details for **3**, **3d**, **3e**, **3g**, **3i**, **3iA**, **3j, 3k** and **3l** are summarized in Table S1. The structures have been deposited at the Cambridge Crystallographic Data Center with the reference CCDC numbers 2238012, 2217756, 2211738, 2211739, 2211740, 2217757, 2238013, 2211741, 2211742, correspondingly; they also contain the supplementary crystallographic data. These data can be obtained free of charge from the CCDC *via* http://www.ccdc.cam.ac.uk/data_request/cif

**Table S1.** Crystal data and structure refinement for **3**, **3d**, **3e**, **3g**, **3i**, **3iA**, **3j**, **3k** and **3l**.

| Identification code | **3** | **3d** | **3e** |
|---|---|---|---|
| Empirical formula | $C_{20}H_{17}Cl_2N_3Pd$ | $C_{20}H_{15}Cl_4N_3Pd$ | $C_{20}H_{15}Cl_4N_3Pd$ |
| Formula weight | 476.66 | 545.55 | 545.55 |
| Temperature, K | 100(2) | 100(2) | 100(2) |
| Wavelength, Å | 0.71073 | 0.71073 | 0.71073 |
| Crystal system | Triclinic | Monoclinic | Monoclinic |
| Space group | P $\bar{1}$ | P2$_1$/c | C2/c |
| Unit cell dimensions | | | |
| a, Å | 11.1768(2) | 13.5230(3) | 9.0789(6) |
| b, Å | 13.3155(2) | 11.9245(3) | 14.4880(10) |
| c, Å | 14.9335(3) | 14.5709(4) | 16.3561(12) |
| α, ° | 116.1390(10) | 90 | 90 |
| β, ° | 93.4870(10) | 115.6740(10) | 103.025(2) |
| γ, ° | 103.2910(10) | 90 | 90 |
| Volume, Å$^3$ | 1908.02(6) Å$^3$ | 2117.66(9) | 2096.0(3) |
| Z' / Z | 2 / 4 | 1 / 4 | 0.5 / 4 |
| Density calcd., g·cm$^{-3}$ | 1.659 | 1.711 | 1.729 |
| μ, mm$^{-1}$ | 1.261 | 1.392 | 1.406 |
| F(000) | 952 | 1080 | 1080 |
| Crystal size, mm | 0.37×0.30×0.20 | 0.18×0.10×0.09 | 0.36×0.35×0.21 |
| θ range, ° | 2.203-36.340 | 2.307-33.216 | 2.698-35.664 |
| Index ranges | -18<=h<=18, | -20<=h<=20, | -14<=h<=14, |
| | -22<=k<=22, | -18<=k<=18, | 0<=k<=23, |
| | -24<=l<=24 | -22<=l<=22 | 0<=l<=26 |
| Reflections | | | |
| collected | 151435 | 86820 | 4887[*] |
| independent [R$_{int}$] | 18465 [0.0326] | 8115 [0.1122] | 4887 [0[*]] |
| observed | 16154 | 5400 | 4654 |
| Completeness to θ$_{full}$ / θ$_{max}$ | 0.999 / 0.999 | 1.000 / 1.000 | 0.997 / 0.998 |
| T$_{max}$ / T$_{min}$ | 0.4977 / 0.4243 | 0.5659 / 0.5116 | 0.438 / 0.338 |
| Data/restraints/parameters | 18465 / 211 / 664 | 8115 / 6 / 314 | 4887 / 0 / 161 |
| Goodness-of-fit on F$^2$ | 1.040 | 1.017 | 1.113 |
| R1 / wR2 indices (I>2σ(I)) | 0.0236 / 0.0498 | 0.0461 / 0.0884 | 0.0222 / 0.0533 |
| R1 / wR2 indices (all data) | 0.0307 / 0.0530 | 0.0883 / 0.1027 | 0.0247 / 0.0546 |
| Extinction coefficient | 0.00146(13) | 0.0022(3) | 0.00106(15) |
| Δρ(ē)$_{max}$ / Δρ(ē)$_{min}$, ē·Å$^{-3}$ | 0.641 /-1.040 | 1.150 / -1.569 | 0.708 / -0.867 |
| CCDC number | 2238012 | 2217756 | 2211738 |

**Table S1 (*cont.*).** Crystal data and structure refinement for **3**, **3d**, **3e**, **3g**, **3i**, **3iA**, **3j, 3k** and **3l**.

| Identification code | 3g | 3i | 3iA |
|---|---|---|---|
| Empirical formula | $C_{20}H_{15}Br_2Cl_2N_3Pd$ | $C_{20}H_{15}Br_2Cl_2N_3Pd$ | $C_{20}H_{15}Br_{2.41}Cl_{1.59}N_3Pd$ |
| Formula weight | 634.47 | 634.47 | 652.65 |
| Temperature, K | 100(2) | 100.0(1) | 100(2) |
| Wavelength, Å | 0.71073 | 0.71073 | 0.71073 |
| Crystal system | Monoclinic | Monoclinic | Monoclinic |
| Space group | $P2_1/c$ | I2/a (C2/c) | C2/c (I2/a) |
| Unit cell dimensions | | | |
| a, Å | 13.4034(3) | 6.96427(16) | 22.0556(4) |
| b, Å | 12.0835(3) | 14.9658(3) | 15.0381(3) |
| c, Å | 14.6627(3) | 21.8956(5) | 6.98560(10) |
| β, ° | 115.2760(10) | 98.197(2) | 100.1093(6) |
| Volume, Å$^3$ | 2147.41(9) | 2258.77(9) | 2280.97(7) |
| Z' / Z | 1 / 4 | 0.5 / 4 | 0.5 / 4 |
| Density calcd., g·cm$^{-3}$ | 1.962 | 1.866 | 1.900 |
| μ, mm$^{-1}$ | 4.846 | 4.607 | 5.230 |
| F(000) | 1224 | 1224 | 1253.5 |
| Crystal size, mm | 0.98×0.39×0.21 | 0.17×0.10×0.05 | 0.20×0.17×0.12 |
| θ range, ° | 2.280-36.995 | 2.722-33.997 | 3.124 to 34.351°. |
| Index ranges | -22<=h<=22, | -10<=h<=10, | -34<=h<=34, |
| | -20<=k<=20, | -22<=k<=23, | -23<=k<=23, |
| | -24<=l<=24 | -34<=l<=34 | -11<=l<=11 |
| Reflections | | | |
| collected | 96150 | 26930 | 42511 |
| independent [R$_{int}$] | 10918 [0.0283] | 4576 [0.0329] | 4772 [0.0361] |
| observed | 10170 | 3895 | 4059 |
| Completeness to θ$_{full}$ / θ$_{max}$ | 0.999 / 1.000 | 0.999 / 0.995 | 0.998 / 0.999 |
| T$_{max}$ / T$_{min}$ | 0.276 / 0.123 | 1.000 / 0.636 | 0.6471 / 0.4765 |
| Data/restraints/parameters | 10918 / 0 / 311 | 4576 / 0 / 159 | 4772 / 0 / 163 |
| Goodness-of-fit on F$^2$ | 1.064 | 1.044 | 1.043 |
| R1 / wR2 indices (I>2σ(I)) | 0.0249 / 0.0592 | 0.0238 / 0.0572 | 0.0230 / 0.0495 |
| R1 / wR2 indices (all data) | 0.0277 / 0.0603 | 0.0323 / 0.0598 | 0.0316 / 0.0529 |
| Extinction coefficient | 0.00214(13) | - | - |
| Δρ(ē)$_{max}$ / Δρ(ē)$_{min}$, ē·Å$^{-3}$ | 1.892 / -1.371 | 1.170 / -0.555 | 0.719 / -0.794 |
| CCDC number | 2211739 | 2211740 | 2217757 |

**Table S1 (*cont.*).** Crystal data and structure refinement for **3**, **3d**, **3e**, **3g**, **3i**, **3iA**, **3j, 3k** and **3l**..

| Identification code | 3j | 3k | 3l |
|---|---|---|---|
| Empirical formula | $C_{22}H_{15}Cl_2F_6N_3Pd$ | $C_{22}H_{15}Cl_2F_6N_3Pd$ | $C_{22}H_{15}Cl_2F_6N_3Pd$ |
| Formula weight | 612.67 | 612.67 | 612.67 |
| Temperature, K | 100.0(2) | 100(2) | 100.0(1) |
| Wavelength, Å | 0.71073 | 0.71073 | 0.71073 |
| Crystal system | Orthorhombic | Orthorhombic | Monoclinic |
| Space group | Pbcn | Fdd2 | I2/a (C2/c) |
| Unit cell dimensions | | | |
| a, Å | 18.1381(3) | 36.2866(7) | 6.9530(3) |
| b, Å | 16.7952(3) | 8.7886(2) | 14.9603(5) |
| c, Å | 7.55530(10) | 14.5007(3) | 22.6625(8) |
| β, ° | 90 | 90 | 95.962(3) |
| Volume, Å$^3$ | 2301.59(6) | 4624.40(17) | 2344.58(15) |
| Z' / Z | 0.5 / 4 | 0.5 / 8 | 0.5 / 4 |
| Density calcd., g·cm$^{-3}$ | 1.768 | 1.760 | 1.736 |
| μ, mm$^{-1}$ | 1.103 | 1.098 | 1.083 |
| F(000) | 1208 | 2416 | 1208 |
| Crystal size, mm | 0.14×0.05×0.03 | 0.47×0.23×0.12 | 0.19×0.04×0.03 |
| θ range, ° | 2.246-35.829 | 2.245-32.595 | 2.723-35.755 |
| Index ranges | -28<=h<=27, | -54<=h<=54, | -11<=h<=11, |
|  | -25<=k<=26, | -13<=k<=13, | -24<=k<=24, |
|  | -12<=l<=11 | -21<=l<=21 | -36<=l<=36 |
| Reflections | | | |
| collected | 29059 | 49547 | 9367[*] |
| independent [$R_{int}$] | 4845 [0.0296] | 4224 [0.0270] | 9367 [0[*]] |
| observed | 4017 | 4142 | 6894 |
| Completeness to $θ_{full}$ / $θ_{max}$ | 0.999 / 0.897 | 1.000 / 1.000 | 0.999 / 0.931 |
| $T_{max}$ / $T_{min}$ | 0.974 / 0.911 | 0.747 / 0.666 | 1.403 / 0.644 |
| Data / restraints / parameters | 4845 / 3 / 193 | 4224 / 74 / 208 | 9367 / 85 / 208 |
| Goodness-of-fit on F$^2$ | 1.040 | 1.070 | 1.034 |
| R1 / wR2 indices (I>2σ(I)) | 0.0259 / 0.0627 | 0.0143 / 0.0350 | 0.0381 / 0.1180 |
| R1 / wR2 indices (all data) | 0.0356 / 0.0662 | 0.0150 / 0.0355 | 0.0536 / 0.1292 |
| Absolute struct. parameter | - | -0.020(6) | - |
| Extinction coefficient | - | 0.00020(3) | - |
| Δρ($\bar{e}$)$_{max}$ / Δρ($\bar{e}$)$_{min}$, $\bar{e}$·Å$^{-3}$ | 0.630 / -0.727 | 0.319 / -0.573 | 1.296 / -0.791 |
| CCDC number | 2238013 | 2211741 | 2211742 |

* Due to the refinement of **3e** and **3k** as regular non-merohedral twins, equivalent reflections were merged by a conventional way, setting the collected reflection number to be equal to the number of independent reflections and, therefore, making $R_{int}$=0.

R1 = $\Sigma||F_o|-|F_c||/\Sigma|F_o|$, wR2 = $[\Sigma[w(F_o^2-F_c^2)^2]/ \Sigma[w(F_o^2)^2]]^{1/2}$

# Crystal structure of 3

The asymmetric unit of **3** contains two symmetrically non-equivalent molecules. The first one exhibits a disordered pyridine molecule. The second one is entirely disordered over two positions.
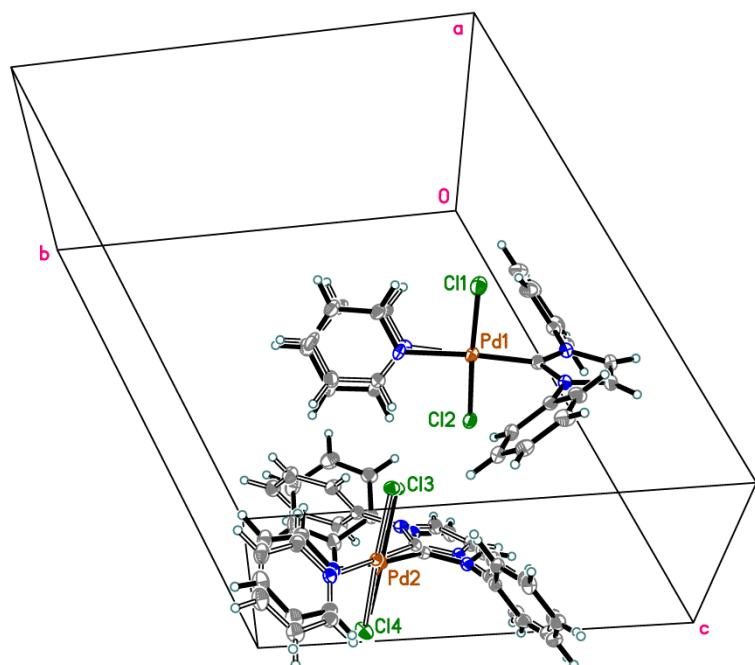


**Fig. S72.** Two crystallographically non-equivalent molecules of **3** in the unit cell (p=50%).
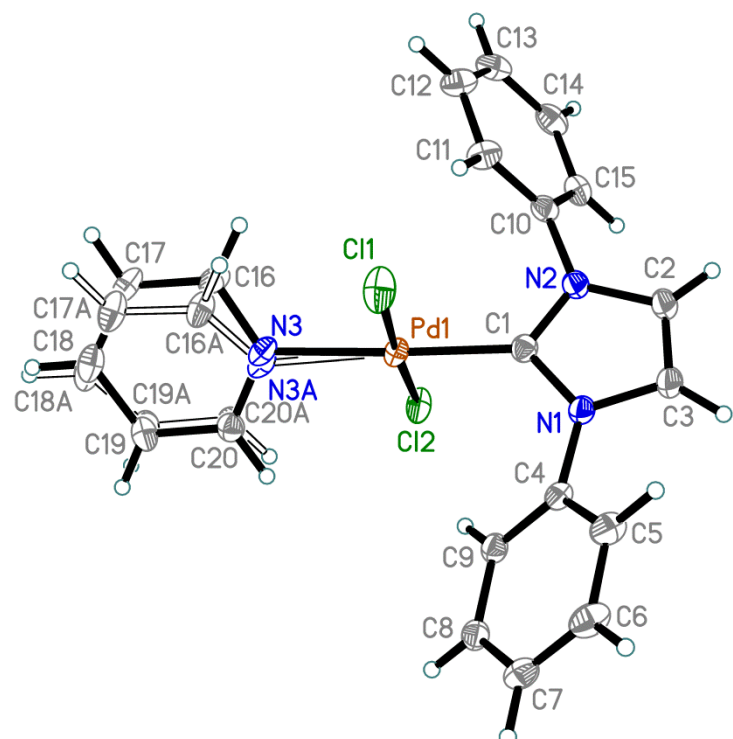


**Fig. S73.** The molecular structure of the first molecule of **3** (p=50%) exhibiting pyridine disorder. The disorder ratio for atoms N3, C16..C20 / N3A, C16A..C20A is 0.504(5) : 0.496(5).
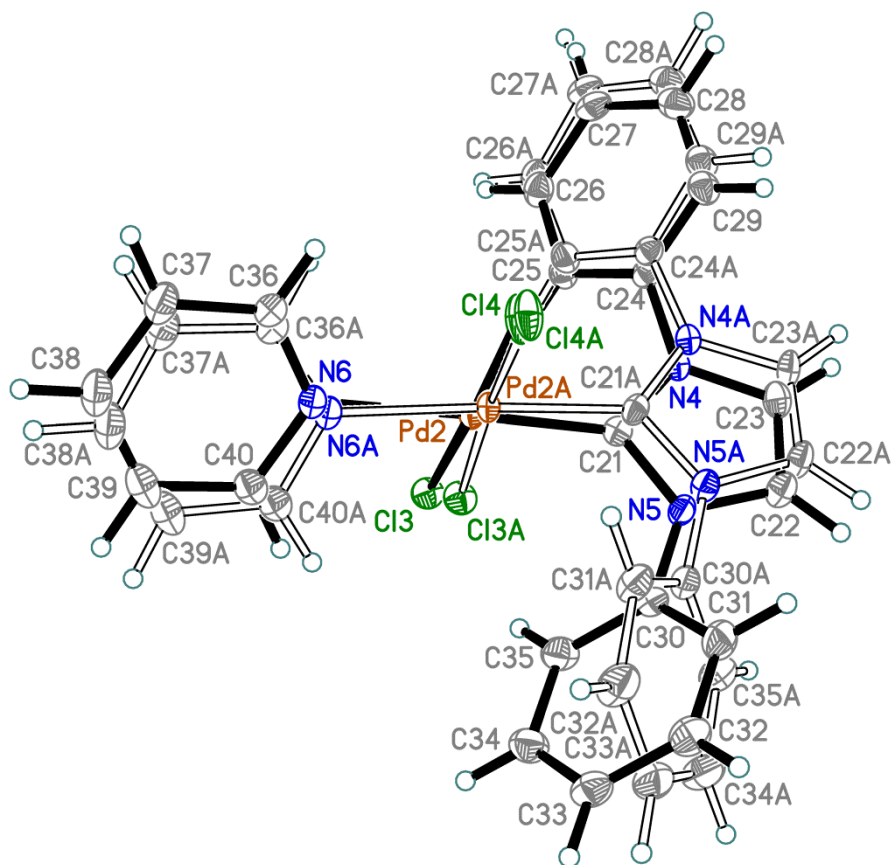
**Fig. S74.** Overlay of two components of disorder for the second crystallographically non-equivalent molecule of **3** (p=50%). The disorder ratio is 0.5065(15): 0.4935(15).
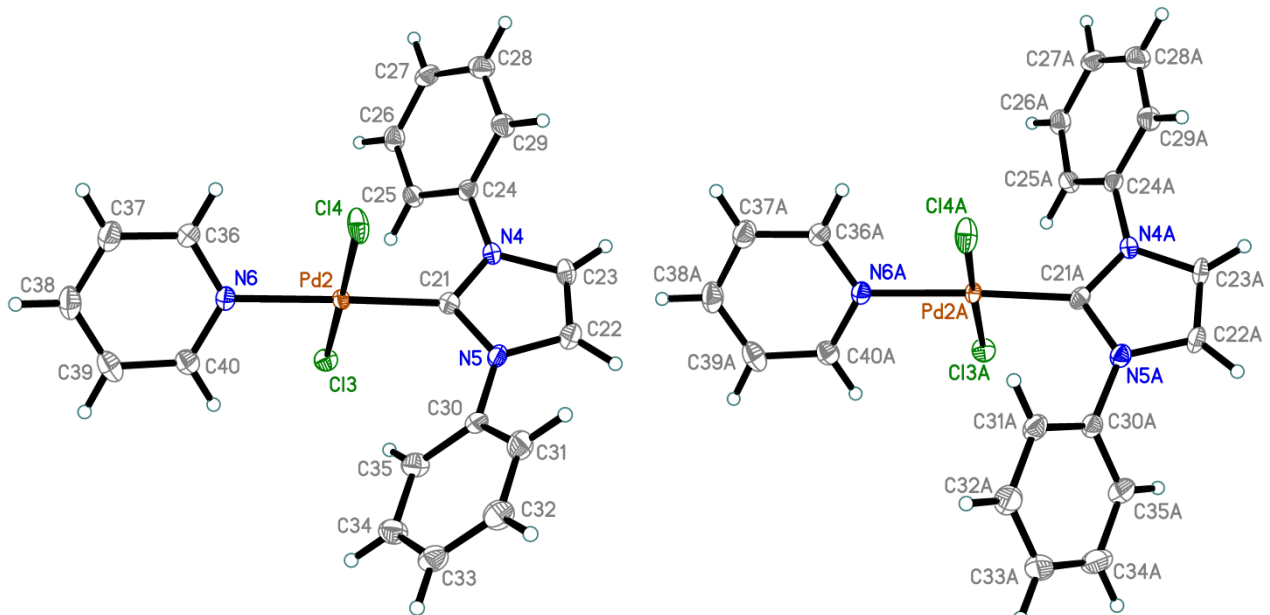


**Fig. S75.** Two components of disorder of the second molecule of **3** (p=50%).

**Table S2.** Selected bond distances (Å) for **3**.

| | | | | | |
|---|---|---|---|---|---|
| Pd1-C1 | 1.9599(11) | C4-C9 | 1.3907(15) | N3-C16 | 1.330(2) |
| Pd1-N3 | 2.0789(17) | C4-C5 | 1.3918(15) | N3-C20 | 1.331(2) |
| Pd1-N3A | 2.1063(17) | C5-C6 | 1.3903(18) | C16-C17 | 1.388(2) |
| Pd1-Cl1 | 2.3228(3) | C6-C7 | 1.3885(18) | C17-C18 | 1.386(2) |
| Pd1-Cl2 | 2.3090(3) | C7-C8 | 1.3904(16) | C18-C19 | 1.387(2) |
| N1-C1 | 1.3578(14) | C8-C9 | 1.3941(16) | C19-C20 | 1.387(2) |
| N1-C3 | 1.3947(14) | C10-C15 | 1.3882(16) | N3A-C20A | 1.351(2) |
| N1-C4 | 1.4353(14) | C10-C11 | 1.3891(16) | N3A-C16A | 1.351(2) |
| N2-C1 | 1.3542(14) | C11-C12 | 1.3901(17) | C16A-C17A | 1.390(2) |
| N2-C2 | 1.3934(15) | C12-C13 | 1.3877(18) | C17A-C18A | 1.379(2) |
| N2-C10 | 1.4377(14) | C13-C14 | 1.3860(19) | C18A-C19A | 1.382(2) |
| C2-C3 | 1.3451(17) | C14-C15 | 1.3908(18) | C19A-C20A | 1.392(2) |
| Pd2-C21 | 1.970(2) | C22-C23 | 1.336(3) | C32-C33 | 1.3874(19) |
| Pd2-N6 | 2.094(6) | C24-C29 | 1.388(2) | C33-C34 | 1.3879(18) |
| Pd2-Cl3 | 2.3038(11) | C24-C25 | 1.3917(19) | C34-C35 | 1.3911(18) |
| Pd2-Cl4 | 2.2999(16) | C25-C26 | 1.3895(19) | N6-C36 | 1.345(2) |
| N4-C21 | 1.349(3) | C26-C27 | 1.389(2) | N6-C40 | 1.347(2) |
| N4-C23 | 1.396(2) | C27-C28 | 1.389(2) | C36-C37 | 1.391(2) |
| N4-C24 | 1.435(2) | C28-C29 | 1.388(2) | C37-C38 | 1.380(2) |
| C21-N5 | 1.363(2) | C30-C35 | 1.3893(19) | C38-C39 | 1.377(2) |
| N5-C22 | 1.391(3) | C30-C31 | 1.3910(18) | C39-C40 | 1.389(2) |
| N5-C30 | 1.434(3) | C31-C32 | 1.3888(19) | | |
| Pd2A-C21A | 1.967(2) | C22A-C23A | 1.334(4) | C32A-C33A | 1.3877(19) |
| Pd2A-N6A | 2.095(6) | C24A-C29A | 1.387(2) | C33A-C34A | 1.390(2) |
| Pd2A-Cl3A | 2.2892(11) | C24A-C25A | 1.3911(19) | C34A-C35A | 1.3913(19) |
| Pd2A-Cl4A | 2.3000(16) | C25A-C26A | 1.389(2) | N6A-C36A | 1.345(2) |
| N4A-C21A | 1.349(3) | C26A-C27A | 1.389(2) | N6A-C40A | 1.348(2) |
| N4A-C23A | 1.397(2) | C27A-C28A | 1.389(2) | C36A-C37A | 1.390(2) |
| N4A-C24A | 1.435(2) | C28A-C29A | 1.388(2) | C37A-C38A | 1.380(2) |
| C21A-N5A | 1.362(2) | C30A-C31A | 1.3883(19) | C38A-C39A | 1.376(2) |
| N5A-C22A | 1.392(3) | C30A-C35A | 1.3918(19) | C39A-C40A | 1.389(2) |
| N5A-C30A | 1.431(3) | C31A-C32A | 1.3900(19) | | |

## Crystal structure of 3d
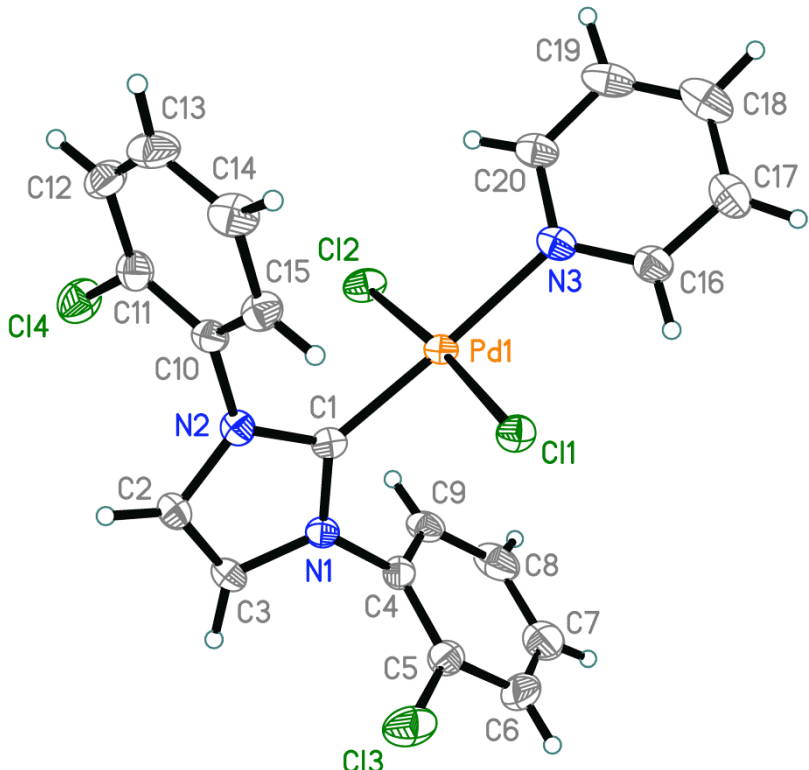


**Fig. S76.** The molecular structure of **3d** (p=50%).

**Table S3.** Selected bond distances (Å) for **3d**.

| | | | | | |
|---|---|---|---|---|---|
| Pd1-C1 | 1.956(3) | N3-C20 | 1.360(4) | C10-C15 | 1.392(4) |
| Pd1-N3 | 2.112(3) | Cl3-C5 | 1.738(4) | C11-C12 | 1.384(4) |
| Pd1-Cl1 | 2.3128(7) | Cl4-C11 | 1.738(3) | C12-C13 | 1.387(5) |
| Pd1-Cl2 | 2.2935(8) | C2-C3 | 1.339(4) | C13-C14 | 1.374(5) |
| N1-C1 | 1.351(4) | C4-C5 | 1.384(4) | C14-C15 | 1.389(4) |
| N1-C3 | 1.397(4) | C4-C9 | 1.390(4) | C16-C17 | 1.387(5) |
| N1-C4 | 1.429(4) | C5-C6 | 1.395(5) | C17-C18 | 1.384(6) |
| N2-C1 | 1.351(4) | C6-C7 | 1.377(6) | C18-C19 | 1.370(6) |
| N2-C2 | 1.399(4) | C7-C8 | 1.370(6) | C19-C20 | 1.380(5) |
| N2-C10 | 1.436(4) | C8-C9 | 1.380(5) | | |
| N3-C16 | 1.342(4) | C10-C11 | 1.390(4) | | |

## Crystal structure of 3e

Complex **3e** is located on a 2-fold rotation axis passing through atoms C11, N2, Pd1 and C1.
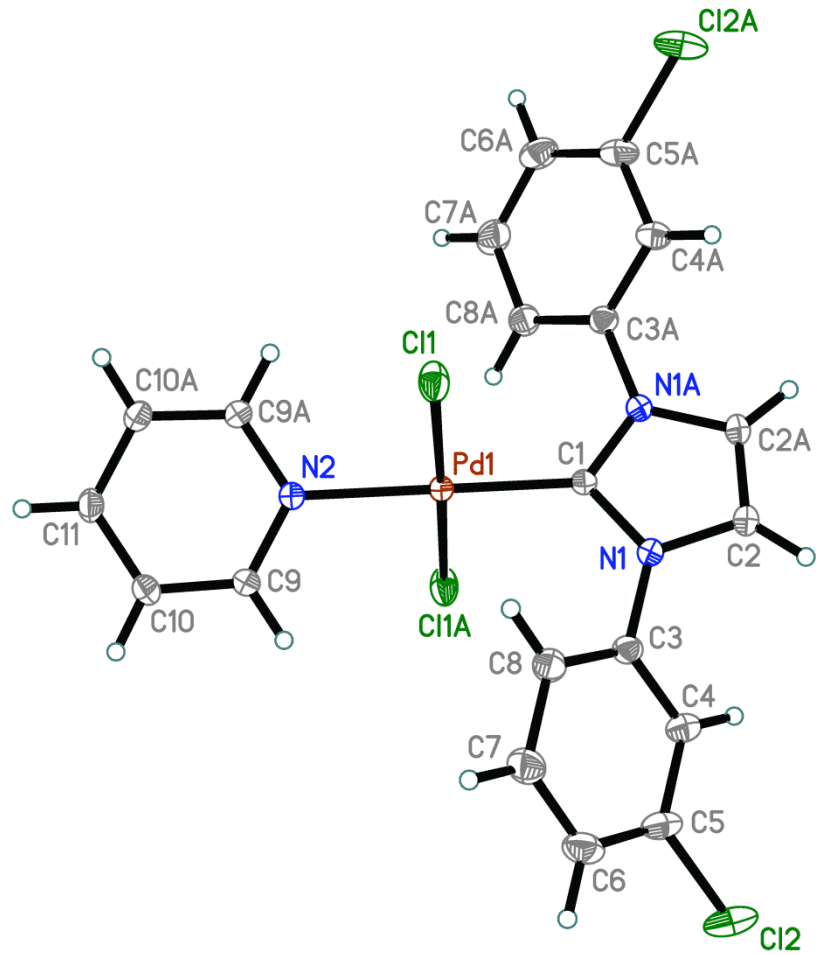


**Fig. S77.** The molecular structure of **3e** (p=50%). Symmetry transformation to generate equivalent atoms: (A) -x+1, +y, -z+1/2.

**Table S4.** Selected bond distances (Å) for **3e**.

| Pd1-Cl1 | 2.3002(3) | N2-C9 | 1.3471(12) | C5-C6 | 1.387(2) |
|---------|-----------|-------|------------|-------|----------|
| Pd1-C1 | 1.9645(14) | C2-C2A | 1.346(2) | C6-C7 | 1.393(2) |
| Pd1-N2 | 2.0601(13) | C3-C4 | 1.3896(16) | C7-C8 | 1.3896(18) |
| N1-C1 | 1.3616(12) | C3-C8 | 1.3929(17) | C9-C10 | 1.3808(16) |
| N1-C2 | 1.3928(14) | C4-C5 | 1.3904(16) | C10-C11 | 1.3902(14) |
| N1-C3 | 1.4302(14) | Cl2-C5 | 1.7355(13) | | |

Symmetry transformation to generate equivalent atoms: (A) -x+1, +y, -z+1/2.

# Crystal structure of 3g
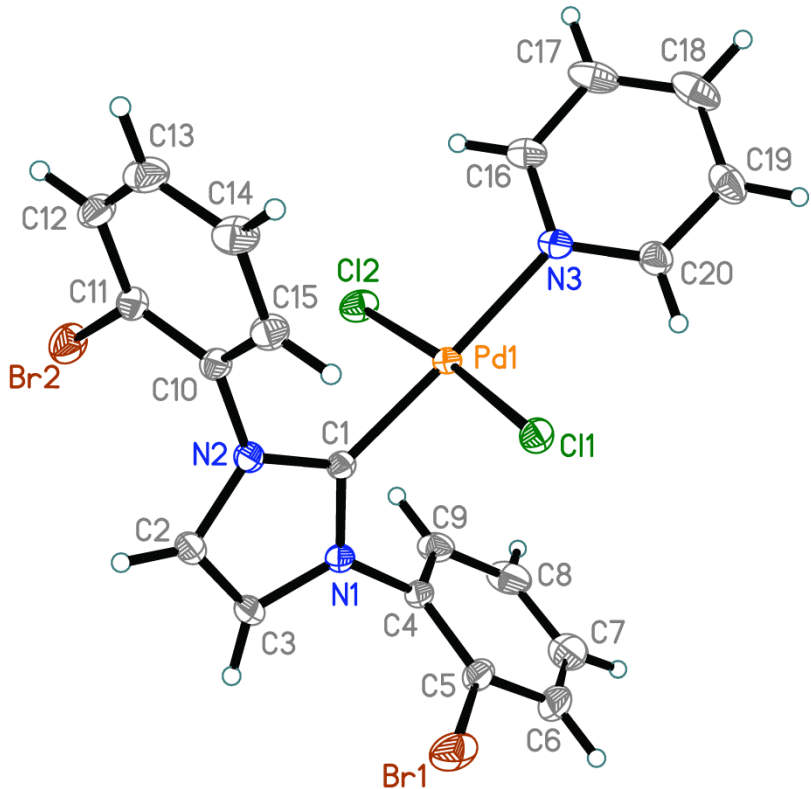


**Fig. S78.** The molecular structure of **3g** (p=50%).

**Table S5.** Selected bond distances (Å) for **3g**.

| Pd1-Cl1 | 2.3145(3) | N2-C10 | 1.4307(17) | C10-C15 | 1.393(2) |
|---------|-----------|--------|------------|---------|----------|
| Pd1-Cl2 | 2.2917(3) | N3-C20 | 1.340(2) | C10-C11 | 1.3941(19) |
| Pd1-C1 | 1.9514(12) | N3-C16 | 1.3516(18) | C11-C12 | 1.388(2) |
| Pd1-N3 | 2.1145(12) | C2-C3 | 1.3458(19) | C12-C13 | 1.390(2) |
| Br1-C5 | 1.8914(17) | C4-C9 | 1.391(2) | C13-C14 | 1.388(2) |
| Br2-C11 | 1.8939(14) | C4-C5 | 1.3922(19) | C14-C15 | 1.388(2) |
| N1-C1 | 1.3529(16) | C5-C6 | 1.389(2) | C16-C17 | 1.387(2) |
| N1-C3 | 1.3966(17) | C6-C7 | 1.383(3) | C17-C18 | 1.385(3) |
| N1-C4 | 1.4294(17) | C7-C8 | 1.389(3) | C18-C19 | 1.375(3) |
| N2-C1 | 1.3513(16) | C8-C9 | 1.388(2) | C19-C20 | 1.392(2) |
| N2-C2 | 1.3972(17) | | | | |

## Crystal structure of 3i

Complex **3i** is located on a 2-fold rotation axis passing through atoms C11, N2, Pd1 and C1.
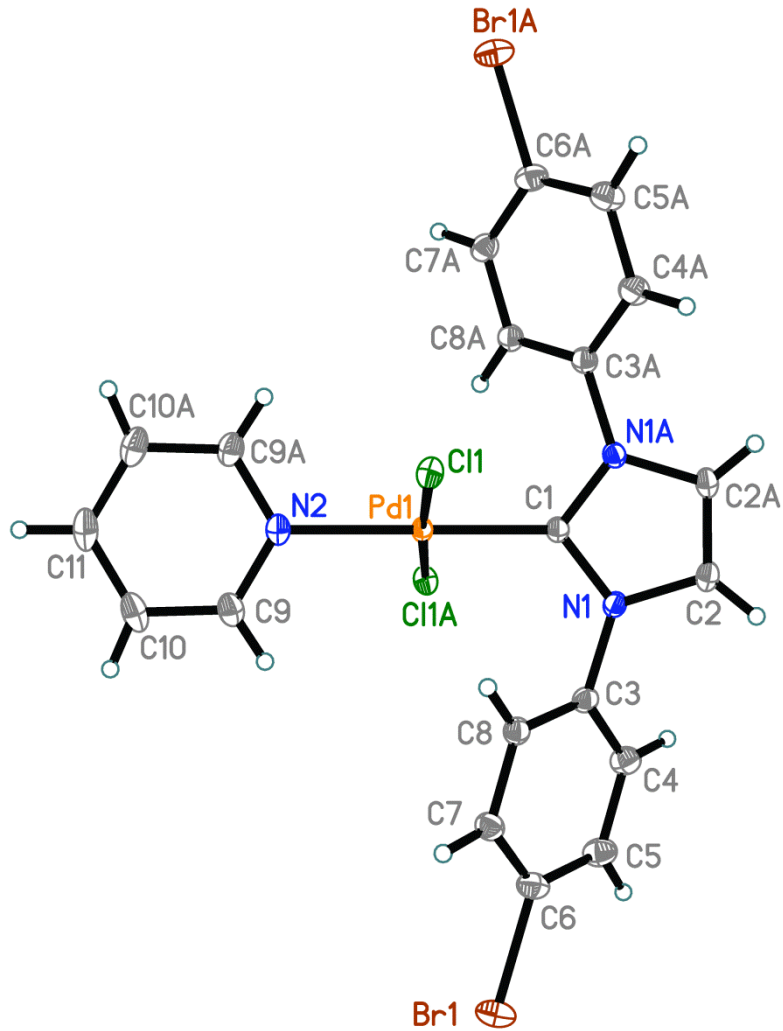


**Fig. S79.** The molecular structure of **3i** (p=50%). Symmetry transformation to generate equivalent atoms: (A) -x+1/2, +y, -z+1.

**Table S6.** Selected bond distances (Å) for **3i**.

| | | | | | |
|---|---|---|---|---|---|
| Pd1-Cl1 | 2.3163(3) | N1-C3 | 1.4303(17) | C6-C7 | 1.389(2) |
| Pd1-C1 | 1.9500(18) | C2-C2A | 1.348(3) | C7-C8 | 1.391(2) |
| Pd1-N2 | 2.0765(16) | C3-C4 | 1.392(2) | N2-C9 | 1.3401(17) |
| Br1-C6 | 1.8992(14) | C3-C8 | 1.3948(19) | C9-C10 | 1.389(2) |
| C1-N1 | 1.3538(15) | C4-C5 | 1.391(2) | C10-C11 | 1.383(2) |
| N1-C2 | 1.3951(17) | C5-C6 | 1.389(2) | | |

Symmetry transformation to generate equivalent atoms: (A) -x+1/2, +y, -z+1.

## Crystal structure of 3iA

Complex **3iA** is located on a 2-fold rotation axis passing through atoms C11, N2, Pd1 and C1.
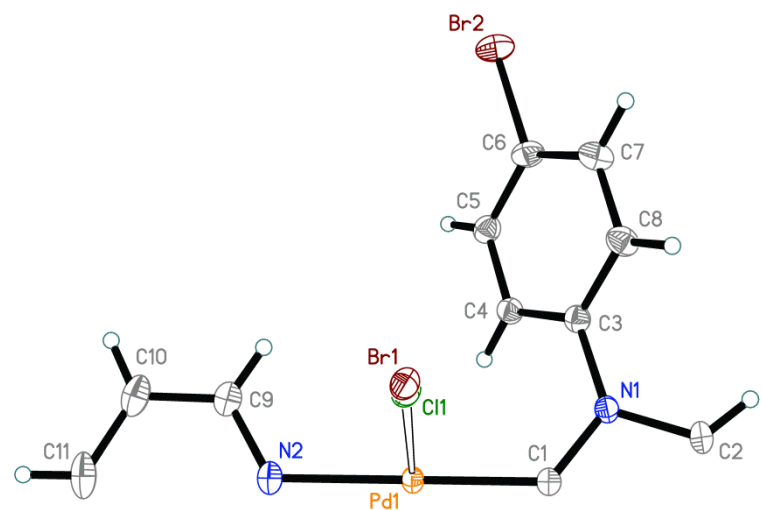


**Fig. S80.** The asymmetric unit **3iA** (p=50%). The Cl1/Br1 ratio is 0.7951(15):0.2049(15), correspondingly.
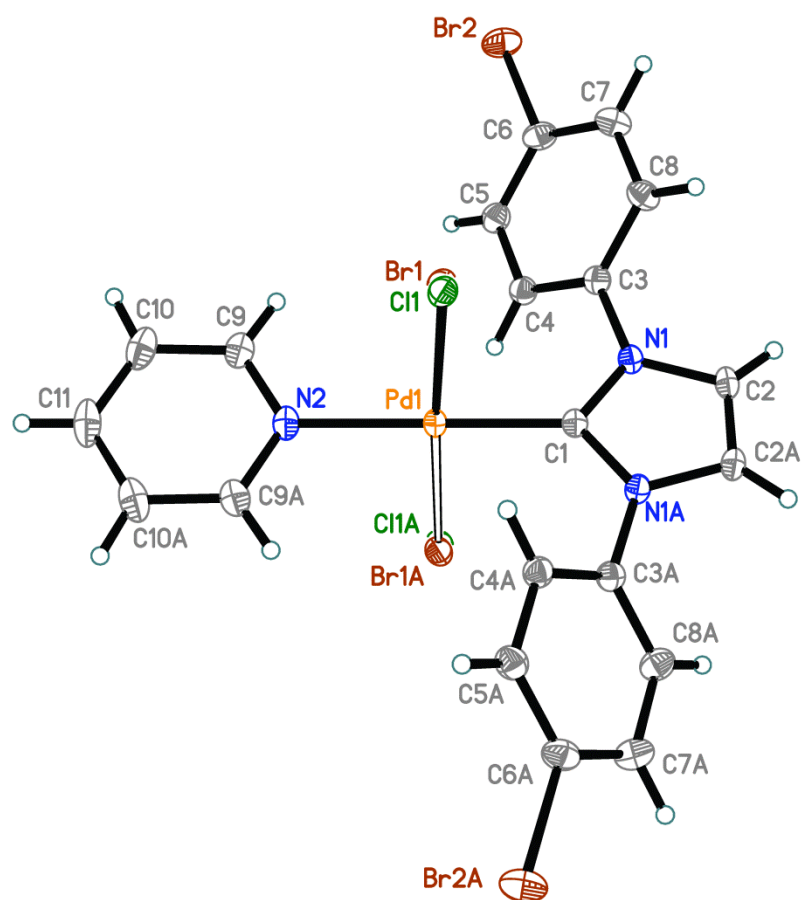


**Fig. S81.** The molecular structure of **3i** (p=50%). Symmetry transformation to generate equivalent atoms: (A) -x+1, +y, -z+1/2.

**Table S7.** Selected bond distances (Å) for **3i**.

| | | | | | |
|---|---|---|---|---|---|
| Pd1-Cl1 | 2.325(7) | N1-C2 | 1.3955(18) | C4-C5 | 1.391(2) |
| Pd1-Br1 | 2.394(11) | N1-C3 | 1.4340(18) | C5-C6 | 1.391(2) |
| Pd1-C1 | 1.9472(19) | N2-C9 | 1.3373(18) | C6-C7 | 1.387(2) |
| Pd1-N2 | 2.0780(17) | C2-C2#1 | 1.347(3) | C7-C8 | 1.391(2) |
| Br2-C6 | 1.8942(15) | C3-C8 | 1.388(2) | C9-C10 | 1.386(2) |
| N1-C1 | 1.3542(16) | C3-C4 | 1.392(2) | C10-C11 | 1.381(2) |

Symmetry transformation to generate equivalent atoms: (A) -x+1, +y, -z+1/2.

The structures **3i** and **3iA** are isostructural. Due to crystal structure determination of **3i** and **3iA** on different diffractometers and different software, their cell settings slightly differ.

The presence of the Cl/Br disorder at the Pd atom directly comes from X-ray data, including analysis of the electron density-difference (deformation) map. The found X-ray structure of **3iA** corresponds to a mixture of three co-crystalized complexes: (3Br-NHC)(py)PdCl$_2$, (3Br-NHC)(py)PdClBr, (3Br-NHC)(py)PdBr$_2$, the ratio of which remains unknown. Based on the Cl/Br ratio found by the X-ray diffraction analysis, the content of the (3Br-NHC)(py)PdCl$_2$ complex is between 59% and 79%.

## Crystal structure of 3j

Complex **3j** is located on a 2-fold rotation axis passing through atoms C12, N2, Pd1 and C1.
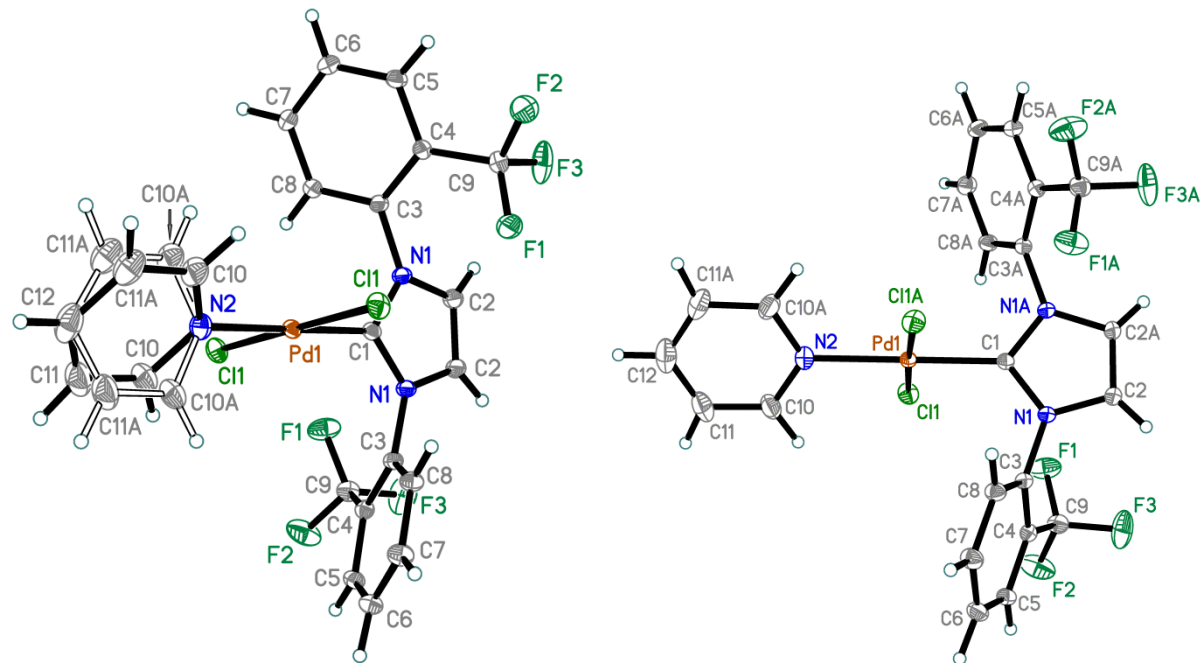


**Fig. S82.** The molecular structure of **3j** (p=50%). The disorder ratio for pyridine molecule (left) is 0.910(3) : 0.090(3) for atoms C10, C11 / C10A, C11A. The disorder is omitted (right); the symmetry transformation to generate equivalent atoms: (A) -x+1, +y, -z+1/2.

**Table S8.** Selected bond distances (Å) for **3j**.

| | | | | | |
|---|---|---|---|---|---|
| Pd1-Cl1 | 2.2988(3) | C3-C8 | 1.3899(17) | C9-F3 | 1.3422(17) |
| Pd1-C1 | 1.9601(17) | C4-C5 | 1.3944(18) | N2-C10 | 1.3455(19) |
| Pd1-N2 | 2.0943(16) | C4-C9 | 1.5017(18) | N2-C10A | 1.345(4) |
| N1-C1 | 1.3555(14) | C5-C6 | 1.3891(18) | C10-C11 | 1.392(2) |
| N1-C2 | 1.3929(16) | C6-C7 | 1.3876(19) | C11-C12 | 1.375(2) |
| N1-C3 | 1.4377(16) | C7-C8 | 1.3892(18) | C10A-C11A | 1.392(4) |
| C2-C2B | 1.352(3) | C9-F1 | 1.3334(16) | C11A-C12 | 1.375(4) |
| C3-C4 | 1.3978(17) | C9-F2 | 1.3354(16) | | |

The symmetry transformation to generate equivalent atoms: (B) -x+1, +y, -z+1/2.

# Crystal structure of 3k

Complex **3k** is located on a 2-fold rotation axis passing through atoms C11, N2, Pd1 and C1.
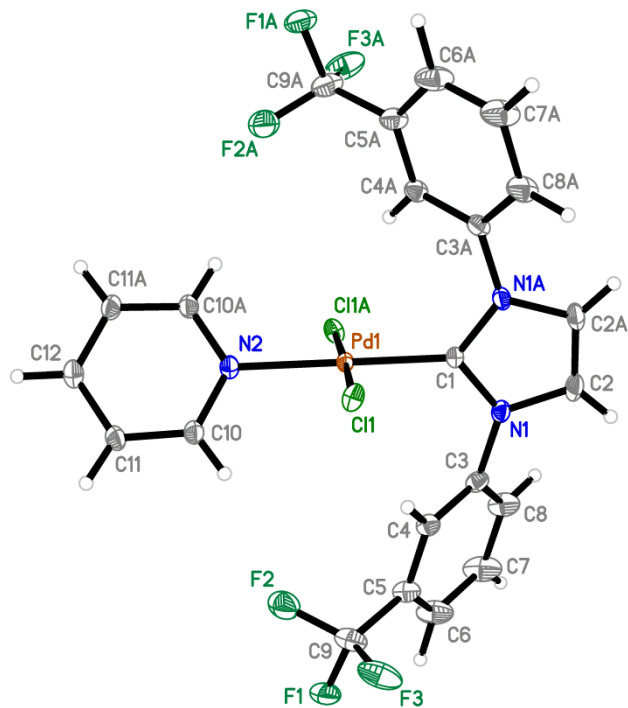


**Fig. S83.** The molecular structure of **3k** (p=50%). The CF₃-disorder is omitted. Symmetry transformation to generate equivalent atoms: (A) -x+1/2, -y+3/2, +z.
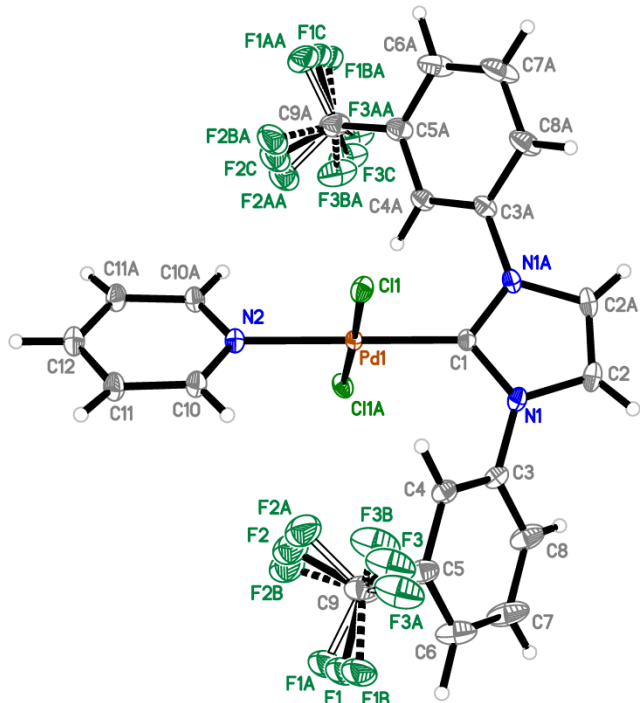


**Fig. S84.** The molecular structure of **3k** (p=50%). The CF₃-disorder ratio for atoms F1, F2, F3 / F1A, F2A, F3A / F1B, F2B, F3B (and for atoms F1C, F2C, F3C / F1AA, F2AA, F3AA / F1BA, F2BA, F3BA) is 0.617(4) : 0.131(4) : 0.252(4). Symmetry transformation to generate equivalent atoms: -x+1/2, -y+3/2, +z.

**Table S9.** Selected bond distances (Å) for **3k**.

| Pd1-Cl1 | 2.3022(3) | C4-C5 | 1.391(2) | C9-F2A | 1.346(4) |
|---------|-----------|-------|----------|--------|----------|
| Pd1-C1 | 1.971(3) | C5-C6 | 1.390(3) | C9-F3A | 1.346(4) |
| Pd1-N2 | 2.064(3) | C5-C9 | 1.497(3) | C9-F1B | 1.345(3) |
| C1-N1 | 1.359(2) | C6-C7 | 1.384(3) | C9-F2B | 1.347(3) |
| N1-C2 | 1.394(2) | C7-C8 | 1.391(3) | C9-F3B | 1.346(3) |
| N1-C3 | 1.434(2) | C9-F1 | 1.343(2) | N2-C10 | 1.341(2) |
| C2-C2#1 | 1.343(4) | C9-F2 | 1.353(3) | C10-C11 | 1.382(2) |
| C3-C4 | 1.385(2) | C9-F3 | 1.346(2) | C11-C12 | 1.388(2) |
| C3-C8 | 1.391(2) | C9-F1A | 1.347(4) | | |

Symmetry transformation to generate equivalent atoms: (A) -x+1/2, -y+3/2, +z.


## Crystal structure of 3l

Complex **3l** is located on a 2-fold rotation axis passing through atoms C11, N2, Pd1 and C1.
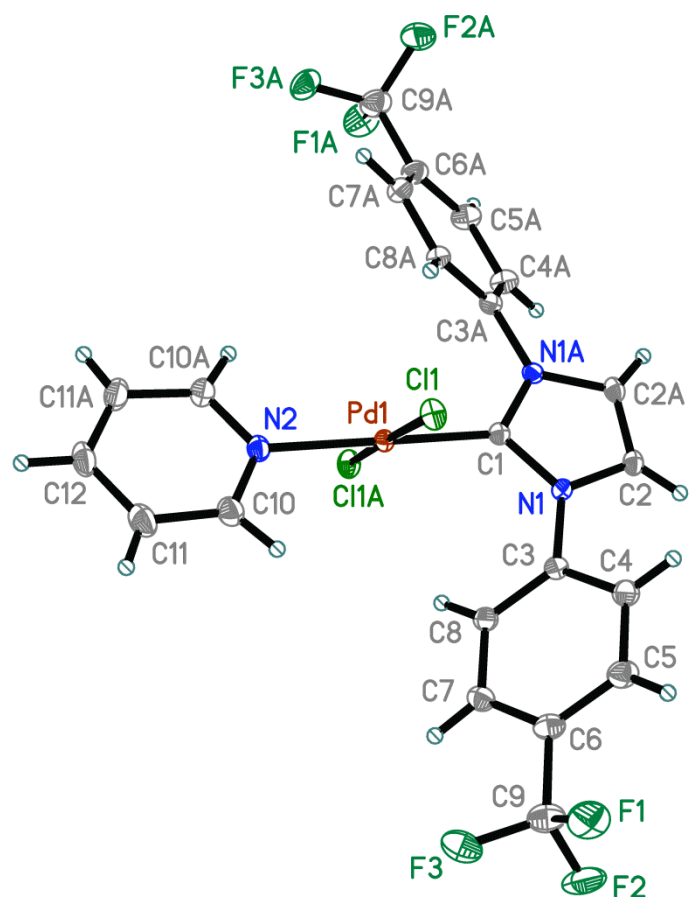


**Fig. S85.** The molecular structure of **3l** (p=50%). The CF$_3$-disorder is omitted. Symmetry transformation to generate equivalent atoms: (A) -x+3/2, +y, -z+1.
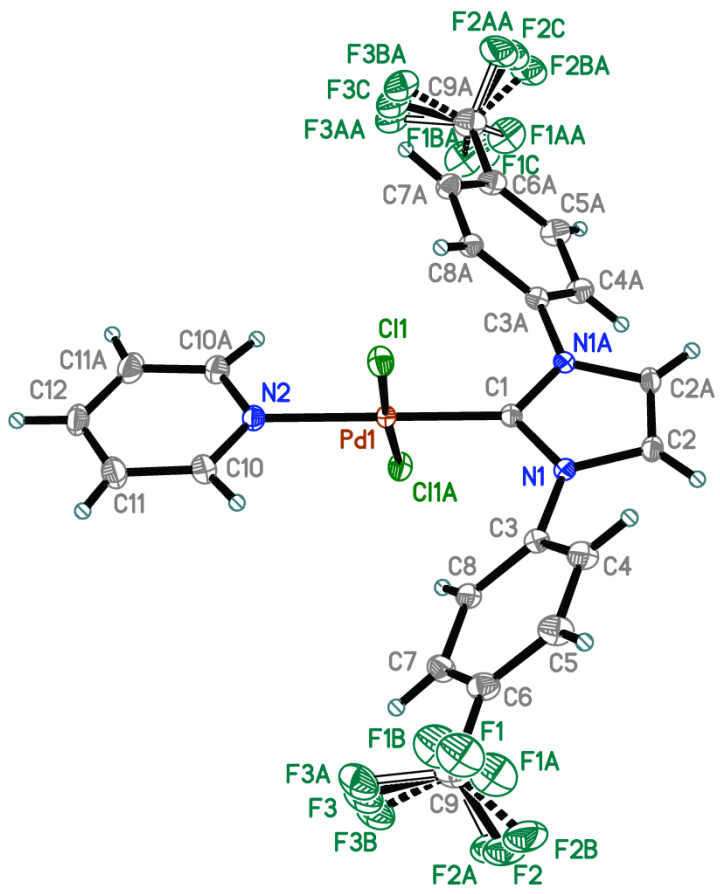
**Fig. S86.** The molecular structure of **3l** (p=50%). The CF$_3$-disorder ratio for atoms F1, F2, F3 / F1A, F2A, F3A / F1B, F2B, F3B (and for atoms F1C, F2C, F3C / F1AA, F2AA, F3AA / F1BA, F2BA, F3BA) is 0.720(4) : 0.140(4) : 0.140(4). Symmetry transformation to generate equivalent atoms: -x+3/2, +y, -z+1.

**Table S10.** Selected bond distances (Å) for **3l**.

| | | | | | |
|---|---|---|---|---|---|
| Pd1-Cl1 | 2.3140(6) | C4-C5 | 1.393(3) | C9-F2A | 1.347(3) |
| Pd1-C1 | 1.948(2) | C5-C6 | 1.384(3) | C9-F3A | 1.345(3) |
| Pd1-N2 | 2.076(2) | C6-C7 | 1.397(3) | C9-F1B | 1.347(3) |
| C1-N1 | 1.357(2) | C6-C9 | 1.501(3) | C9-F2B | 1.347(3) |
| N1-C2 | 1.394(2) | C7-C8 | 1.393(3) | C9-F3B | 1.345(3) |
| N1-C3 | 1.431(2) | C9-F1 | 1.350(2) | N2-C10 | 1.339(2) |
| C2-C2#1 | 1.351(4) | C9-F2 | 1.345(2) | C10-C11 | 1.389(3) |
| C3-C4 | 1.391(3) | C9-F3 | 1.346(2) | C11-C12 | 1.389(3) |
| C3-C8 | 1.392(3) | C9-F1A | 1.346(3) | | |

Symmetry transformation to generate equivalent atoms: -x+3/2, +y, -z+1.

**Table S11**. Selected dihedral angles (°).

| code | substituent | Plane 1 defined by atoms | Plane 2 defined by atoms | Angle |
|---|---|---|---|---|
| **3a_1*** | o-F | N1 C1 N2 C2 C3 | C4..C9 | 56.67(5) |
| **3a_1*** | o-F | N1 C1 N2 C2 C3 | C10..C15 | 63.02(5) |
| **3a_2*** | o-F | N1A C1A N2A C2A C3A | C4A..C9A | 59.19(6) |
| **3a_2*** | o-F | N1A C1A N2A C2A C3A | C10A..C15A | 52.38(7) |
| **3a_2*** | o-F | N1B C1B N2B C2B C3B | C4B..C9B | 50.55(7) |
| **3a_2*** | o-F | N1B C1B N2B C2B C3B | C10B..C15B | 54.14(7) |
| **3d** | o-Cl | N1 C1 N2 C2 C3 | C4..C9 | 66.37(13) |
| **3d** | o-Cl | N1 C1 N2 C2 C3 | C10..C15 | 64.32(10) |
| **3g** | o-Br | N1 C1 N2 C2 C3 | C4..C9 | 67.53(6) |
| **3g** | o-Br | N1 C1 N2 C2 C3 | C10..C15 | 66.23(5) |
| **3j** | o-CF$_3$ | N1 C1 N1#1 C2 C2#1 | C3..C8 | 67.12(3) |
| **3e** | m-Cl | N1 C1 N1#1 C2 C2#1 | C3..C8 | 39.14(5) |
| **3k** | m-CF$_3$ | N1 C1 N1#2 C2 C2#2 | C3..C8 | 45.60(5) |
| **3i** | p-Br | N1 C1 N1#3 C2 C2#3 | C3..C8 | 43.99(4) |
| **3iA** | p-Br | N1 C1 N1#1 C2 C2#1 | C3..C8 | 44.07(5) |
| **3l** | m-CF$_3$ | N1 C1 N1#4 C2 C2#4 | C3..C8 | 42.72(6) |
| **3** | - | N1 C1 N2 C2 C3 | C4..C9 | 44.77(5) |
| **3** | - | N1 C1 N2 C2 C3 | C10..C15 | 50.72(5) |
| **3** | - | N4 C21 N5 C22 C23 | C24..C29 | 46.7(4) |
| **3** | - | N4 C21 N5 C22 C23 | C30..C35 | 44.07(15) |
| **3** | - | N4A C21A N5A C22A C23A | C24A..C29A | 25.8(5) |
| **3** | - | N4A C21A N5A C22A C23A | C30A..C35A | 49.3(4) |

*The structures of two polymorph modifications of **3a** (**3a_1** and **3a_2**) were determined earlier.[9] Crystals of **3a_2** contained two non-equivalent molecules.

Symmetry transformations to generate equivalent atoms: #1 -x+1, y, -z+1/2; #2 -x+1/2, -y+3/2, z; #3 -x+1/2, y ,-z+1; #4 -x+3/2, y, -z+1.

**Computational and refinement details**

**Table S12**. Energies and populations of occupied $sp_{LP}$ and vacant $p^*$ orbitals of NHCs with various halogen substituents °

| NHC | Free NHC | | | |
| --- | --- | --- | --- | --- |
| | $sp_{LP}$ | | $p^*$ | |
| | $E^a$ | occ[b] | E | occ |
| **IPh** | -0.28657 | 1.91322 | -0.05392 | 0.63994 |
| **$o$-F-IPh** | -0.29195 | 1.91466 | -0.05886 | 0.64313 |
| **$m$-F-IPh** | -0.29612 | 1.91276 | -0.06323 | 0.63586 |
| **$p$-F-IPh** | -0.29351 | 1.91302 | -0.06091 | 0.64506 |
| **$o$-Cl-IPh** | -0.29088 | 1.9153 | -0.05629 | 0.63635 |
| **$m$-Cl-IPh** | -0.29879 | 1.91229 | -0.06594 | 0.63607 |
| **$p$-Cl-IPh** | -0.29879 | 1.91287 | -0.06602 | 0.64058 |
| **$o$-Br-IPh** | -0.28951 | 1.91543 | -0.05471 | 0.63564 |
| **$m$-Br-IPh** | -0.29844 | 1.91218 | -0.06563 | 0.6362 |
| **$p$-Br-IPh** | -0.29901 | 1.91276 | -0.0662 | 0.63991 |
| **$o$-CF$_3$-IPh** | -0.29423 | 1.91556 | -0.05955 | 0.6368 |
| **$m$-CF$_3$-IPh** | -0.30297 | 1.91214 | -0.0701 | 0.63499 |
| **$p$-CF$_3$-IPh** | -0.30654 | 1.91314 | -0.0734 | 0.63314 |

[a] Energy in Hartree; [b] occupancy.

**Table S13**. Stabilization energies associated with donor-acceptor interactions of NBOs involved in the Pd-NHC bond formation

| Pd/NHC | $E^{(2)}\sigma\,(sp_{LP}\rightarrow 5s_{Pd}*)$ | $E^{(2)}\pi\,(4d_{yz}\rightarrow p^*)$ | $E^{(2)}\sigma + E^{(2)}\pi$ |
| --- | --- | --- | --- |
| **IPh-3** | 157.7 | 43.8 | 201.5 |
| **$o$-F-3a** | 157.6 | 44.0 | 201.6 |
| **$m$-F-3b** | 156.2 | 45.2 | 201.4 |
| **$p$-F-3c** | 157.9 | 43.7 | 201.6 |
| **$o$-Cl-3d** | 160.0 | 45.9 | 206.0 |
| **$m$-Cl-3e** | 156.0 | 45.1 | 201.1 |
| **$p$-Cl-3f** | 156.5 | 44.5 | 201.0 |
| **$o$-Br-3g** | 160.6 | 46.1 | 206.6 |

| | | | |
|---|---|---|---|
| **m-Br-3h** | 156.0 | 45.0 | 201.1 |
| **p-Br-3i** | 156.3 | 44.5 | 200.8 |
| **o-CF₃-3j** | 160.1 | 45.9 | 206.0 |
| **m-CF₃-3k** | 155.6 | 44.6 | 200.2 |
| **p-CF₃-3l** | 155.0 | 45.9 | 200.9 |

**Table S14**. Geometric parameters of complexes Pd(NHC)

| Pd/NHC | $d^a$ | $\varphi^b$ |
|---|---|---|
| **IPh-3** | 1.94133 | 43.8 |
| **o-F-3a** | 1.94031 | 44.4 |
| **m-F-3b** | 1.93992 | 42.9 |
| **p-F-3c** | 1.94076 | 44.6 |
| **o-Cl-3d** | 1.93226 | 55.6 |
| **m-Cl-3e** | 1.93993 | 43.1 |
| **p-Cl-3f** | 1.94042 | 43.3 |
| **o-Br-3g** | 1.93120 | 58.0 |
| **m-Br-3h** | 1.94000 | 43.2 |
| **p-Br-3i** | 1.94045 | 43.1 |
| **o-CF₃-3j** | 1.93167 | 58.9 |
| **m-CF₃-3k** | 1.94066 | 42.6 |
| **p-CF₃-3l** | 1.93929 | 42.4 |

[a] Pd-NHC bond length; [b] dihedral angel between heterocyclic and phenyl rings.

**Table S15**. Dependence of the energies of donor-acceptor interaction of NBOs on the dihedral angle between the heterocyclic and phenyl rings ($\varphi$) in the complex **3**

| $\varphi$, degrees | $\Delta E$ | $E^{(2)}\sigma$ ($sp_{LP} \rightarrow 5s_{Pd}*$) | $E^{(2)}\pi$ ($4d_{yz} \rightarrow p*$) | $E^{(2)}\sigma + E^{(2)}\pi$ |
|---|---|---|---|---|
| 0 | 6.5 | 141.95 | 39.31 | 181.26 |
| 10 | 5.0 | 145.68 | 40.18 | 185.86 |
| 20 | 2.7 | 150.37 | 41.12 | 191.49 |
| 30 | 0.9 | 153.66 | 42.2 | 195.86 |
| 40 | 0.1 | 156.61 | 43.29 | 199.9 |
| 43.8 | 0.0 | 157.7 | 43.8 | 201.5 |
| 50 | 0.2 | 159.8 | 44.6 | 204.46 |

| 60 | 1.0 | 163.0 | 45.8 | 208.79 |
|-----|-----|--------|-------|--------|
| 70 | 2.3 | 165.7 | 46.6 | 212.29 |
| 80 | 3.4 | 167.4 | 47.1 | 214.4 |
| 90 | 3.9 | 167.9 | 47.2 | 215.11 |
| 100 | 3.5 | 166.9 | 47.1 | 214.01 |
| 110 | 2.3 | 164.66 | 46.58 | 211.24 |
| 120 | 1.1 | 162.13 | 45.68 | 207.81 |
| 130 | 0.2 | 159.57 | 44.58 | 204.15 |
| 140 | 0.0 | 156.96 | 43.42 | 200.38 |
| 150 | 0.8 | 154.1 | 42.3 | 196.39 |
| 160 | 2.7 | 150.37 | 41.12 | 191.49 |
| 170 | 5.0 | 145.67 | 40.17 | 185.84 |
| 180 | 6.5 | 141.95 | 39.31 | 181.26 |

**Table S16**. Energies and populations of of NBOs involved in the Pd-NHC bond formation

| Pd/NHC | NHC fragment | | | | Pd fragment | | | |
|---|---|---|---|---|---|---|---|---|
| | $sp_{LP}$ | | $p^*$ | | $4d_{yz}$ | | $5s$ | |
| | $E^a$ | occ[b] | E | occ | E | occ | E | occ |
| **IPh-3** | -0.32363 | 1.60784 | -0.09982 | 0.78755 | -0.19559 | 1.85797 | 0.10853 | 0.35323 |
| **o-F-3a** | -0.32918 | 1.6091 | -0.10438 | 0.78641 | -0.20032 | 1.8572 | 0.10515 | 0.35236 |
| **m-F-3b** | -0.33242 | 1.61507 | -0.10812 | 0.78472 | -0.20289 | 1.85151 | 0.11201 | 0.34482 |
| **p-F-3c** | -0.33059 | 1.60709 | -0.10683 | 0.78943 | -0.20263 | 1.85932 | 0.10245 | 0.35315 |
| **o-Cl-3d** | -0.32975 | 1.60602 | -0.10354 | 0.78137 | -0.19835 | 1.85544 | 0.09657 | 0.35709 |
| **m-Cl-3e** | -0.33559 | 1.61675 | -0.1109 | 0.78479 | -0.20522 | 1.85061 | 0.11313 | 0.34131 |
| **p-Cl-3f** | -0.33535 | 1.6106 | -0.11133 | 0.78738 | -0.20659 | 1.8554 | 0.10356 | 0.349 |
| **o-Br-3g** | -0.32872 | 1.60503 | -0.10235 | 0.78069 | -0.19713 | 1.85567 | 0.0953 | 0.35846 |
| **m-Br-3h** | -0.33548 | 1.61724 | -0.11068 | 0.78485 | -0.20495 | 1.85069 | 0.11331 | 0.3405 |
| **p-Br-3i** | -0.3355 | 1.61099 | -0.11145 | 0.78706 | -0.2067 | 1.85497 | 0.10423 | 0.34844 |
| **o-CF₃-3j** | -0.33207 | 1.6065 | -0.10549 | 0.78064 | -0.20041 | 1.85525 | 0.09397 | 0.35692 |
| **m-CF₃-3k** | -0.33989 | 1.62023 | -0.11484 | 0.78405 | -0.20869 | 1.84927 | 0.11464 | 0.33616 |
| **p-CF₃-3l** | -0.34241 | 1.61554 | -0.11791 | 0.78377 | -0.21216 | 1.84932 | 0.10345 | 0.34368 |

[a] Energy in Hartree; [b] occupancy.

**Table S17**. Changes in occupations of NBOs on passing from an isolated Pd atom and NHC ligand to Pd(NHC) complex

| Pd/NHC | NHC fragment | | Pd fragment | |
|---|---|---|---|---|
| | $sp_{LP}$ | $p^*$ | $4d_{yz}$ | $5s$ |
| **IPh-3** | -0.30538 | 0.14761 | -0.14203 | 0.35323 |
| ***o*-F-3a** | -0.30556 | 0.14328 | -0.1428 | 0.35236 |
| ***m*-F-3b** | -0.29769 | 0.14886 | -0.14849 | 0.34482 |
| ***p*-F-3c** | -0.30593 | 0.14437 | -0.14068 | 0.35315 |
| ***o*-Cl-3d** | -0.30928 | 0.14502 | -0.14456 | 0.35709 |
| ***m*-Cl-3e** | -0.29554 | 0.14872 | -0.14939 | 0.34131 |
| ***p*-Cl-3f** | -0.30227 | 0.1468 | -0.1446 | 0.349 |
| ***o*-Br-3g** | -0.3104 | 0.14505 | -0.14433 | 0.35846 |
| ***m*-Br-3h** | -0.29494 | 0.14865 | -0.14931 | 0.3405 |
| ***p*-Br-3i** | -0.30177 | 0.14715 | -0.14503 | 0.34844 |
| ***o*-CF₃-3j** | -0.30906 | 0.14384 | -0.14475 | 0.35692 |
| ***m*-CF₃-3k** | -0.29191 | 0.14906 | -0.15073 | 0.33616 |
| ***p*-CF₃-3l** | -0.2976 | 0.15063 | -0.15068 | 0.34368 |

**Table S18**. Charge decomposition analysis (CDA) of Pd(NHC) complexes

| Pd/NHC | $d^a$ | $b^b$ | $r^c$ |
|---|---|---|---|
| **IPh-3** | 0.153457 | 0.129527 | -0.238228 |
| ***o*-F-3a** | 0.146067 | 0.13022 | -0.238752 |
| ***m*-F-3b** | 0.151781 | 0.131173 | -0.240521 |
| ***p*-F-3c** | 0.151527 | 0.130673 | -0.236573 |
| ***o*-Cl-3d** | 0.132448 | 0.128735 | -0.222571 |
| ***m*-Cl-3e** | 0.151581 | 0.132046 | -0.241462 |
| ***p*-Cl-3f** | 0.151924 | 0.132338 | -0.239966 |
| ***o*-Br-3g** | 0.1347 | 0.128017 | -0.219563 |
| ***m*-Br-3h** | 0.151486 | 0.132061 | -0.24136 |
| ***p*-Br-3i** | 0.152089 | 0.132537 | -0.240707 |
| ***o*-CF₃-3j** | 0.133158 | 0.127928 | -0.226303 |

| | | | |
|---|---|---|---|
| **m-CF₃-3k** | 0.15186 | 0.133199 | -0.242993 |
| **p-CF₃-3l** | 0.150448 | 0.134034 | -0.243415 |

[a] The amount of electrons donated from NHC fragment to Pd atom; [b] the amount of electrons back donated from Pd atom to NHC fragment; [c] Closed-shell interaction between occupied orbitals of NHC fragment and Pd atom (electron repulsive effect).

**Table S19**. Estimation of relative σ- and π–contributions to the charge transfer (CT) from NHC to Pd atom and to the Pd-NHC bond energy

| Pd/NHC | CT NBO[a] | | CT CDA[b] | | E$^{(2)}$ SOPT[c] | |
|---|---|---|---|---|---|---|
| | σ-donation, % | π-back-donation, % | σ-donation, % | π-back-donation, % | E$^{(2)}$σ, % | E$^{(2)}$π, % |
| **IPh-3** | 68.3 | 31.7 | 54.2 | 45.8 | 78.3 | 21.7 |
| **o-F-3a** | 68.2 | 31.8 | 52.9 | 47.1 | 78.2 | 21.8 |
| **m-F-3b** | 66.7 | 33.3 | 53.6 | 46.4 | 77.5 | 22.5 |
| **p-F-3c** | 68.5 | 31.5 | 53.7 | 46.3 | 78.3 | 21.7 |
| **o-Cl-3d** | 68.1 | 31.9 | 50.7 | 49.3 | 77.7 | 22.3 |
| **m-Cl-3e** | 66.4 | 33.6 | 53.4 | 46.6 | 77.6 | 22.4 |
| **p-Cl-3f** | 67.6 | 32.4 | 53.4 | 46.6 | 77.9 | 22.1 |
| **o-Br-3g** | 68.3 | 31.7 | 51.3 | 48.7 | 77.7 | 22.3 |
| **m-Br-3h** | 66.4 | 33.6 | 53.4 | 46.6 | 77.6 | 22.4 |
| **p-Br-3i** | 67.5 | 32.5 | 53.4 | 46.6 | 77.8 | 22.2 |
| **o-CF₃-3j** | 68.1 | 31.9 | 51.0 | 49.0 | 77.7 | 22.3 |
| **m-CF₃-3k** | 65.9 | 34.1 | 53.3 | 46.7 | 77.7 | 22.3 |
| **p-CF₃-3l** | 66.4 | 33.6 | 52.9 | 47.1 | 77.2 | 22.8 |

[a] Percentage of charge transfer by σ-donation and π-backdonation, calculated from the difference in populations of the occupied $sp_{LP}$ and $p^*$ orbitals in the Pd(NHC) complex and in the isolated NHC ligand and Pd atom (see table S13); [b] Percentage of charge transfer by σ-donation and π-backdonation, calculated in the framework of charge decomposition analysis (CDA, see table S14); [c] Percentage of stabilization energies E$^{(2)}$σ and E$^{(2)}$π, calculated in the framework of second order perturbation theory analysis of fock matrix in NBO basis (SOPT).

## References

1. Bruker. APEX-III. *Bruker AXS Inc.*, Madison, Wisconsin, USA, **2020**.

2. L. Krause, R. Herbst-Irmer, G. Sheldrick and D. Stalke, Comparison of silver and molybdenum microfocus X-ray sources for single-crystal structure determination. *J. Appl. Cryst.* **2015**, 48, 3–10.

3. CrysAlisPro. Version 1.171.42. *Rigaku Oxford Diffraction*, **2021**.

4. G. Sheldrick, A short history of SHELX. *Acta Cryst.* 2008, **A64**, 112-122.

5. O. Dolomanov, L. Bourhis, R. Gildea, J. Howard and H. Puschmann, OLEX2: a complete structure solution, refinement and analysis program. *J. Appl. Cryst.* 2009, **42**, 229-341.

6. G. Sheldrick, SHELXT - Integrated space-group and crystal-structure determination. *Acta Cryst.* 2015, **A71**, 3-8.

7. G. Sheldrick, Crystal structure refinement with SHELXL. *Acta Cryst.* 2015, **C71**, 3-8.

8. C. Macrae, I. Sovago, S. Cottrell, P. Galek, P. McCabe, E. Pidcock, M. Platings, G. Shields, J. Stevens, M. Towler and P. Wood, Mercury 4.0: from visualization to analysis, design and prediction. *J. Appl. Cryst.* 2020, **53**, 226-235.

9. D. Prima, R. Pankov, A. Kostyukovich, M. Minyaev, J. Burykina, V. Ananikov, Synthesis and characterization of Pd/NHC$_F$ complexes with fluorinated aryl groups, *Dalton Trans.*, 2022, **51**, 9843-9856.